

THE UNIVERSITY OF CALGARY

HYDRODYNAMIC FLOW ASSOCIATED WITH LEDUC REEFS

BY

Ken J. Hugo

A THESIS

SUBMITTED TO THE FACULTY OF GRADUATE STUDIES  
IN PARTIAL FULFILLMENT OF THE REQUIREMENTS FOR THE  
DEGREE OF MASTER OF SCIENCE

DEPARTMENT OF GEOLOGY AND GEOPHYSICS

CALGARY, ALBERTA

MAY, 1985

© K.J. HUGO 1985

## THE UNIVERSITY OF CALGARY

## FACULTY OF GRADUATE STUDIES

The undersigned certify that they have read, and recommend to the Faculty of Graduate Studies for acceptance, a thesis entitled, "Hydrodynamic Flow Associated with Leduc Reefs," submitted by Ken J. Hugo in partial fulfillment of the requirements for the degree of Master of Science.



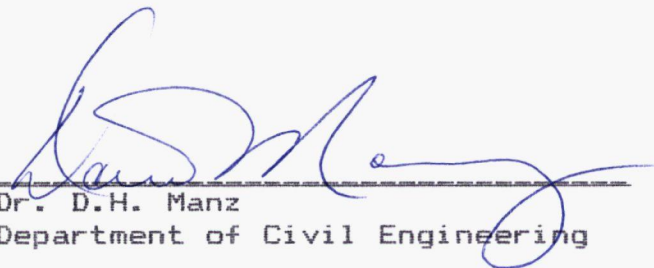
Supervisor, Dr. F.E. Gretener  
Department of Geology and Geophysics



Dr. I.E. Hutcheon  
Department of Geology and Geophysics



Dr. A.A. Levinson  
Department of Geology and Geophysics



Dr. D.H. Manz  
Department of Civil Engineering

Date 85-05-10

## Abstract

The Devonian Rimbey-Meadowbrook reef trend, located in central Alberta, consists of a series of high permeability reefs encased in low permeability shales. This permeability contrast significantly influences the regional hydrodynamic flow patterns as they currently exist. Groundwater flow patterns during the Paleozoic and Mesozoic eras were also likely to have been influenced by the presence of this high permeability reef trend.

Significant volumes of fluid were expelled from the off-reef Ireton, Duvernay and Majeau Lake shales as a result of compaction. Theoretical modelling of the compaction-driven fluid flow during the Paleozoic Era, based on the finite element method, suggests that direct horizontal flow from the shales into the reefs was minimal. Flow from the shales was largely vertical, either upwards or downwards into overlying or underlying units. Some of the fluids expelled into the underlying units were eventually channelled through the reefs into overlying strata. Flow was channelled along these underlying units through the reef from a maximum distance of 16 km beyond the reef margin. Beyond this distance the presence of the reef did not influence the fluid flow migration pathways within the lower units. The shales expelled most of their connate water early in the burial history of the shales and reefs, largely before the reefs were buried by 500 m of

sediments, roughly corresponding to 30 Ma after deposition of the Ireton shales.

Compaction flow after the Paleozoic Era was insignificant. Current groundwater flow patterns can be examined with either the finite element method or from drill stem tests. The observed flow patterns are almost entirely the result of the large scale topographic gradient across Alberta leading to the establishment of regional groundwater flow systems at the depth of the reefs. The Rimbey-Meadowbrook trend serves as a horizontal fluid conduit for the southwest to northeast moving groundwaters. Groundwater is collected at the southern end of the reef trend, and dispersed (to some extent) in the vicinity of the Acheson reef. The Golden Spike reef serves as a vertical fluid conduit between the overlying Upper Devonian and Mesozoic units to the underlying Middle Devonian and Cambrian units. The source of energy to drive the fluids through the Golden Spike reef is attributed to osmosis.

The fluid flow patterns can be related to diagenetic patterns in the vicinity of the Rimbey-Meadowbrook trend. Sulfate-poor waters expelled from the Duvernay shales into the Cooking Lake carbonates during compaction may have provided the fluids necessary for dolomitization. The distribution of oil and gas within the reef trend can also be related to the inferred pathways of groundwater movement that existed when hydrocarbon migration was taking place.

## Acknowledgements

Great appreciation is accorded to my advisor, Dr. P.E. Gretener, who allowed me to pursue this somewhat unorthodox thesis. His advice, encouragement and assistance made much of this thesis considerably easier than it otherwise might have been.

Dr. K.U. Weyer, of the Inland Waters Branch of Environment Canada, allowed me the use of the CAPFEA computer program, on which part of this thesis is based.

Bruce Smith and Kim Wagstaff of the Academic Computing Services of the University of Calgary went to great effort to initialize the CAPFEA program on the Honeywell Multics computer system. My fellow grad students, Kevin Coflin and Kelly Russell, spent considerable time explaining to me the myriad workings of the Multics system. Dr. Ian Hutcheon assisted with the thermodynamics segment of this thesis.

Dr. A.A. Levinson, S. Hugo and Dr. R.S. Woodward reviewed an initial draft of this thesis and corrected several of the all too numerous typographical and grammatical errors.

Texaco Canada Resources kindly awarded a research grant for this thesis. The work was also supported through the awarding of several GA(T)s' and a GA(R) to the author.

Lastly, I would like to thank my wife, Brenda Austin, for her constant advice and encouragement. As always, I got my best advice from my best friend.

## Contents

	Page
Title page .....	i
Approval page .....	ii
Abstract .....	iii
Acknowledgements .....	v
Table of contents .....	vi
List of figures .....	viii
List of tables .....	x
Chapter 1 Introduction .....	1
1.1 Aim of Thesis .....	1
1.2 Stratigraphy of the Study Area .....	4
Chapter 2 Theory of Groundwater Motion .....	11
2.1 Concept of Potential .....	11
2.2 Darcy's Law and Continuity Equations .....	15
2.3 Finite Element Method .....	18
2.4 Hydraulic Head and Abnormal Pressures .....	21
2.5 Sources of Groundwater Energy .....	25
2.6 Permeability .....	30
Chapter 3 Compaction .....	35
3.1 Compaction of Shales .....	35
3.2 Ireton Compaction .....	37

3.3 Interpretation of Compaction Curve .....	50
Chapter 4 Directions of Fluid Migration	
During Compaction .....	58
4.1 Method of Investigation .....	58
4.2 Development of Method .....	59
4.3 Results of Models .....	62
Chapter 5 Flow due to Local Topography .....	80
Chapter 6 Potentiometric Maps .....	92
6.1 Development of Potentiometric Maps .....	92
6.2 Interpretation of Potentiometric Maps .....	100
Chapter 7 Hydrocarbon Migration .....	114
7.1 Source of Hydrocarbons .....	114
7.2 Flow Systems During Hydrocarbon Migration .....	117
7.3 Effect of Hydrodynamics on Secondary Migration .....	121
7.4 Primary Migration .....	124
Chapter 8 Summary and Conclusions .....	129
References .....	134
Appendix 1 .....	141

## List of Figures

	Page
1.1 Location map of the study area.....	3
1.2 Stratigraphic column .....	6
2.1 Relationship between total head, elevation and pressure .....	13
2.2 Graph illustrating fluid pressure, hydraulic head and flow direction relationships .....	24
3.1 Depth versus porosity plot for various sediments .....	39
3.2 Schematic illustration showing developments of discontinuities due to reef collapse .....	45
3.3 Unrestored compaction curve for shales surrounding Golden Spike reef .....	46
3.4 Compaction curve for various Leduc reefs .....	47
3.5 Average porosity versus depth for the Ireton/Duvernay .....	51
4.1 Geology, scale and head distribution of finite element simulation .....	63
4.2 Flow directions for reference model .....	66
4.3a Decrease in geopressure scenario .....	68
4.3b Increase in geopressure scenario .....	68
4.4a Hydrostatic head along boundary .....	71
4.4b Extreme geopressure along boundary .....	71
4.5a Shale permeability of 100:1 .....	74
4.5b Isotropic shale permeability .....	74
4.6a Increase in reef permeability .....	75
4.6b Increase in basal layer permeability .....	75
5.1 Location map for finite element cross section .....	82
5.2 Finite element model for through Acheson reef illustrating flow due to local	

	topography .....	87
5.3	Finite element model illustrating flow due removal of the Acheson reef .....	90
6.1	Hydraulic head distribution within the Ellerslie Formation .....	97
6.2	Hydraulic head distribution within the Wabamun Formation .....	98
6.3	Hydraulic head distribution within the Nisku Formation .....	99
6.4	Location map of Leduc reefs and the Cooking Lake aquifer .....	103
6.5a	Equipotential pattern in region of complex topography .....	104
6.5b	Effect of introducing high permeability lens into flow system .....	104
7.1	Distribution of oil, gas and water in the Leduc reefs .....	115
7.2	Vector diagram of forces acting upon oil in a hydrodynamic environment .....	123
7.3	Vector diagram of forces illustrating divergent flow patterns of water, oil and gas .....	123
A1	Groundwater flow in a small drainage basin ....	143
A2	86 node mesh for finite element simulation ....	144
A3	Basin flow based on 86 node simulation .....	145
A4	68 node mesh for finite element simulation ....	147
A5	Basin flow based on 68 node simulation .....	148

## List of Tables

	Page
3.1 Porosity and per cent shale for the Ireton and Duvernay formations from 16-12-54-26W4 ...	40
3.2 Volume of fluid released during compaction ...	55
3.3 Rate of porosity loss in Ireton/Duvernay sequence with burial .....	55
4.1 Permeabilities of formations for compaction flow scenarios .....	64
4.2 Summary of scenarios .....	78
5.1 Hydraulic conductivity values used for finite element simulation .....	86
6.1 Formation resistivities and brine concentrations .....	96
6.2 Molalities and formation fluid activities .....	110

## Chapter 1 Introduction

### 1.1 Aim of Thesis

A basic premise of geology states that strata within the subsurface exist within a dynamic framework: mineralogies, textures, and compositions of rocks that were present when the rocks were originally deposited are constantly subjected to processes which result in the alteration of the original rocks. Mobile fluids found within the pore spaces play a significant role in determining the type and extent of this alteration. Conversely, the type of rocks can exert a significant influence on the chemistry and flow patterns of these mobile fluids.

The interplay between rock and water has considerable ramifications from both a theoretical and a practical viewpoint. Some geologic events, such as dolomitization of limestones, are generally believed to be possible only if large volumes of fluids are channelled through the system. Stratabound ore deposits, such as lead and zinc deposits within carbonate formations, or uranium deposits within ancient fluvial channels, are formed when water gleans dispersed metal as the water flows through large volumes of strata. These ore bearing fluids subsequently deposit these same metals within the fluid conduits represented by

the fluvial channel or carbonate host rocks. Hydrocarbon migration and accumulation are influenced by the flow direction of water. Effervescence of sodium sulfate salts, common in eastern Alberta and Saskatchewan, requires extensive movement of water through rock to dissolve and remove the salt. Groundwater in itself is a valuable commodity serving as a major source of potable water.

This thesis will attempt to determine mechanisms of fluid flow within a specific study area, and it will also attempt to relate the observed and theoretical groundwater flow to various geologic events. The study area is the Rimbey-Meadowbrook Leduc reef trend in central Alberta (figure 1.1), a 300 km long reef complex of Devonian age. To achieve the aims of this thesis, it will be necessary to examine both the present and the former fluid flow patterns along this trend in order to:

1. illustrate mechanisms of fluid flow, such as the sources of energy to drive fluid flow, and physical concepts of groundwater motion;
2. determine the flow pathways of subsurface water in the vicinity of the Rimbey-Meadowbrook trend that existed when the off reef shales were being compacted and expelling fluids. A detailed study illustrating the effect of the reef on the flow patterns of these fluids, as well as an estimate of the timing and amounts of fluid released from

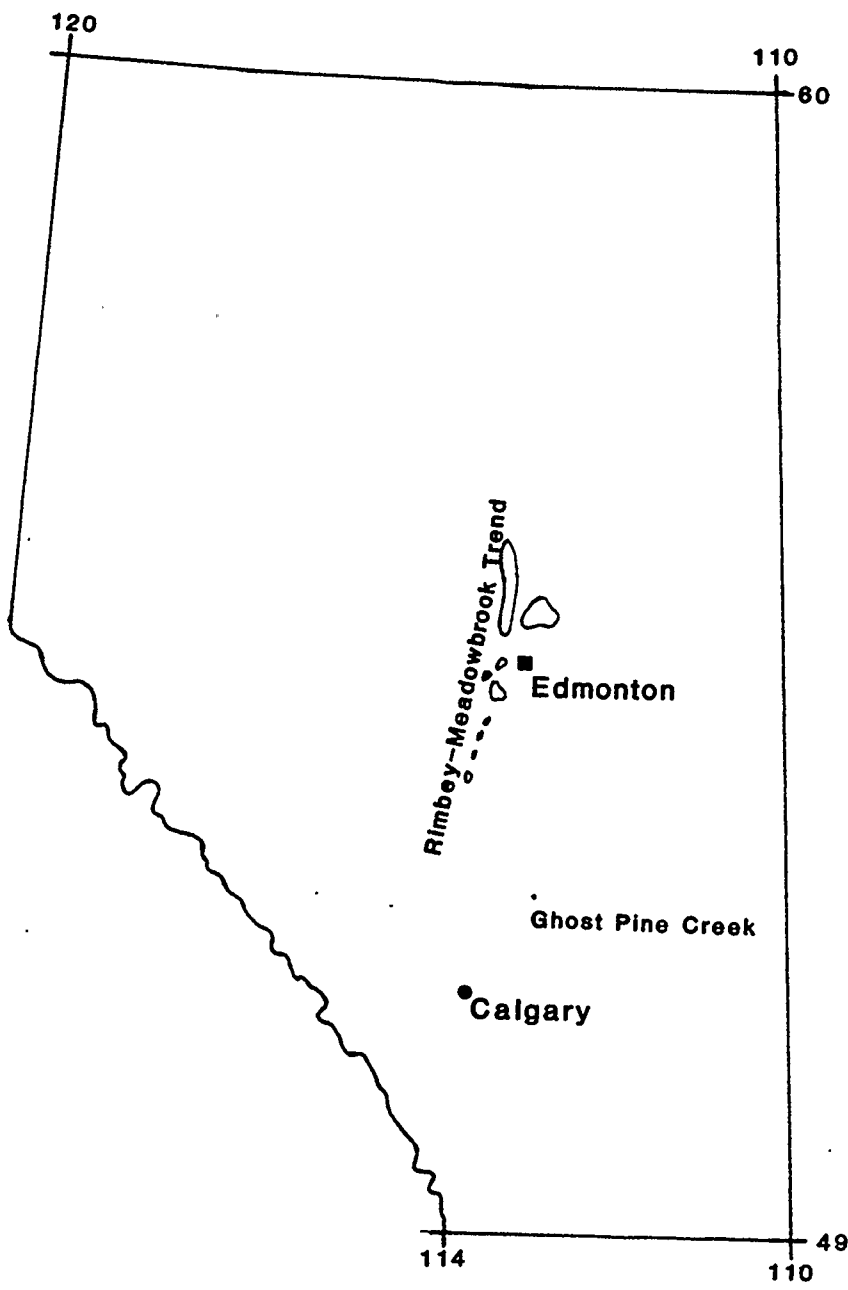


Figure 1.1 Location map of the study area

the compacting shales, will be presented;

3. examine the effect of the reef trend upon current groundwater flow and determine the sources of energy for flow around the Leduc reefs; and,
4. attempt to relate the observed and probable fluid flow patterns to various geologic phenomena such as dolomitization and oil migration.

The Rimbey-Meadowbrook reef trend, situated in the plains of central Alberta, consists of a linear series of Devonian platform reefs. Together with the underlying Cooking Lake aquifer this trend forms a permeable fluid conduit that had significant effects on the groundwater flow patterns in the past, and has similar effects in the present. The reasons for choosing this particular reef trend to illustrate the effect of a conduit on flow patterns are:

1. the geology of the area is well understood;
2. data in the form of well logs and drill stem tests are readily available as a result of hydrocarbon exploration; and,
3. previous work on compaction by O'Connor (1972) greatly facilitated the part of the study dealing with the fluid flow during compaction of the off reef shales.

## 1.2 Stratigraphy of the Study Area

The geology underlying the study area is well known as a result of extensive hydrocarbon exploration. The following brief synthesis of the local stratigraphy is largely taken from The Geological History of Western Canada (McCrossan and Glaister, editors, 1964), Future Petroleum Provinces of Canada, Canadian Society of Petroleum Geologists Memoir #1 (McCrossan, editor, 1973), and from Ceroici (1979).

Regionally, the study area is located within the Western Canada Sedimentary Basin, a broad belt of Middle Cambrian and younger sediments thickening towards the southwest. Within the study area, the maximum thickness of sediments is over 2700 m. These Phanerozoic sediments overlie a crystalline basement of Archean age. Two broad major lithologic divisions can be recognized in the sedimentary package based on time divisions within the Phanerozoic. Paleozoic sediments are largely represented by carbonates, evaporites, and shales, with rare coarse clastics. Evaporites and carbonates are almost unknown within rocks of Mesozoic and Cenozoic age, which are composed of clastic rocks ranging in grain size from fine clays to large cobbles. The geology is summarized in the stratigraphic column of Figure 1.2.

The lowermost sedimentary package consists of an unnamed basal quartzite unit of Middle Cambrian age overlain by glauconitic fine grained sandstones, siltstones

Average Depth (m)	Formation	Period
0	Glacial and fluvial deposits	Quaternary
	Saskatchewan Paskapoo	Tertiary
500	Wapiti	Upper
	Colorado Group First White Specks Cardium Second White Specks Fish Scale Viking Joli Fou	Cretaceous
1000	Mannville Group Glaucouitic Sandstone Ostracod Ellaerslie	Lower Cretaceous
	Wabamun Graminia Calmar Nisku	Upper
1500	Woodbend Group Ireton Majeau Lake Leduc Duvernay Cooking Lake	Devonian
	Beaverhill Lake	
2000	Elk Point Group Upper Elk Point Lower Elk Point	Middle Devonian
2500	Finnegan Deadwood Earlie Basal Quartzite	Middle Cambrian
	Crystalline Basement	Aphebian

Figure 1.2 Stratigraphic Column.

and shales of the Earlie Formation, which are in turn overlain by siltstone and shale lithologies of the Deadwood Formation (Pugh 1971). Deposited upon an unconformity above the Deadwood Formation are the glauconitic siltstones, shales and limestones of the Finnegan Formation. A significant erosional hiatus during the Silurian Period removed Ordovician and Upper Cambrian strata throughout much of Alberta, and produced significant topographic relief on the top of the Finnegan Formation.

Deposited in lows resulting from this period of erosion are the Lower Elk Point shales and carbonates. A gradual transgression above the Lower Elk Point Subgroup led to the deposition of anhydritic dolomites and evaporites of the Upper Elk Point Subgroup. Overlying the Upper Elk Point Subgroup are the limestone and shale interbeds of the Beaverhill Lake Formation. North of the study area, the Beaverhill Lake Formation contains oil producing patch reefs (Swan Hills); within the study area porous limestones are absent, and the facies are characterized by basinal and interreef sediments.

The Woodbend Group, which is the principal concern of this study, is composed of a series of platform carbonates, patch reefs, and interreef shales and fine carbonates. The lowermost Cooking Lake Formation consists of a dense skeletal framework of stromatoporoid and amphipora limestones which form a 60 m thick carbonate platform.

Deposited penecontemporaneously with the Cooking Lake Formation is the Majeau Lake Formation, composed of shales that were deposited in a deeper water environment west of the Cooking Lake Formation. Built upon the seaward margin of the Cooking Lake Formation are the porous stromatoporoid reef mounds of the Leduc Formation, which form a discontinuous chain of reefs of varying extent. Filling in the interreef areas, and formed from a westward prograding wedge of sediments, are the organic rich shales of the Duvernay Formation and the calcite rich shales of the Ireton Formation. These shales, gradually building out from an eastern source, eventually surrounded and capped the Leduc reefs, terminating their growth (Stoakes 1980).

A major transgression over the Ireton shales led to the establishment of the Winterburn Group. The lowermost Nisku Formation, consisting of a porous dolomite, gradually grades into the argillaceous siltstones and dolomites of the overlying Calmar and Graminia formations.

The youngest Paleozoic formations present in the study area comprise the Wabamun Group, the base of which is represented by a shale and anhydritic unit. This is in turn overlain by more porous and permeable units consisting of interbedded limestone and dolomite.

Units deposited above the Wabamun Group during the Paleozoic Era were eroded away on a great Pre-Cretaceous unconformity that saw perhaps as much as 500 m of sediment

removed including the uppermost formations of the Wabamun Group.

Not until early Cretaceous time was significant deposition resumed within the study area. Strata of the Lower Cretaceous Mannville Group consist largely of non-marine sandstones and siltstones deposited in response to the rising Cordillera west of the study area. The overlying Colorado Group is composed of somewhat finer marine clastics, deposited during a more quiescent orogenic period in the Cordillera. Together the two groups represent a large facies wedge cycle, consisting of individual formations with varying grain sizes, from clay to sand, and with minor conglomerate.

Uppermost Cretaceous strata consist of shallow marine and fluvial deltaic beds with a few coal beds. Within southern Alberta, the Upper Cretaceous formations comprise the Lea Park, Belly River and Bearpaw formations. Further north, the boundaries between these formations become indistinct, and the three formations are grouped together as the Wapiti Formation, a thick (300 m) interbedded marine sandstone and shale sequence passing upwards into a more sandy fluvial-deltaic sequence.

Considerable erosion on Upper Cretaceous strata above the Wapiti Formation was followed by Tertiary gravels and sands (Saskatchewan and Paskapoo formations) infilling valleys left on the erosional surface. Overlying these

Tertiary sediments are Quaternary glacial tills of varying thickness composed of clay, silt, sand and gravel. As well as glacial till, glacial-fluvial and glacial-lacustrine deposits are also recognized, illustrating the variable lithology associated with this uppermost unit.

## Chapter 2 Theory of Groundwater Motion

### 2.1 Concept of Potential

Water flows through the subsurface driven not only by pressure differentials, but by a variety of forces. Hubbert's (1940) classic work showed that the total potential energy of a particle of water must be considered in order to determine the fluid movement. Hubbert (1953, p. 193) terms the potential energy that a unit mass of fluid has as potential, and he defines it as "the amount of work required to transport a unit mass of fluid from an arbitrarily chosen datum and state to the position and state of the point considered." The following brief derivation of potential is from Hubbert (1953). A more extensive derivation appears in Hubbert (1940).

Consider a fluid in a closed chamber initially at elevation  $z_0$ , and pressure  $p_0$ . In order to transport the fluid to a new state at elevation  $z$  and pressure  $p$ , work will have to be done in order to lift the mass of fluid from  $z_0$  to  $z$ , and work will be required to increase the pressure on the fluid from  $p_0$  to  $p$ . The sum of these two work terms is the potential which is given by:

$$\phi = g(z - z_0) + \frac{p - p_0}{\rho} \quad (1)$$

where  $\phi$  is the potential,  $g$  is the gravitational

acceleration constant, and  $\rho$  is the fluid density.

Since the initial state is arbitrary, it will be convenient to choose sea level and atmospheric pressure as our reference state, and to set:

$$z_0 = 0; \quad p_0 = 1 \text{ atmosphere}$$

If we work in terms of gauge pressure (absolute pressure less the atmospheric pressure), equation (1) reduces to:

$$\phi = gz + p/\rho \quad (2)$$

For high velocity flow, a kinetic energy term would be required. However, subsurface flows are of such low velocity that this term can be neglected.

The fluid potential may be represented in a manner more easily comprehended if we imagine a manometer open to the atmosphere and measuring the fluid pressure only at some point in the subsurface where the value of the potential is desired. Let  $z$  be the elevation of this point and  $p$  the pressure of the fluid. In response to the pressure  $p$ , the fluid will rise statically in the tube to some height  $h$  above the standard datum, or  $(h - z)$  above the point of measurement (Figure 2.1). The relationship between this rise and the pressure will be given by the hydrostatic equation:

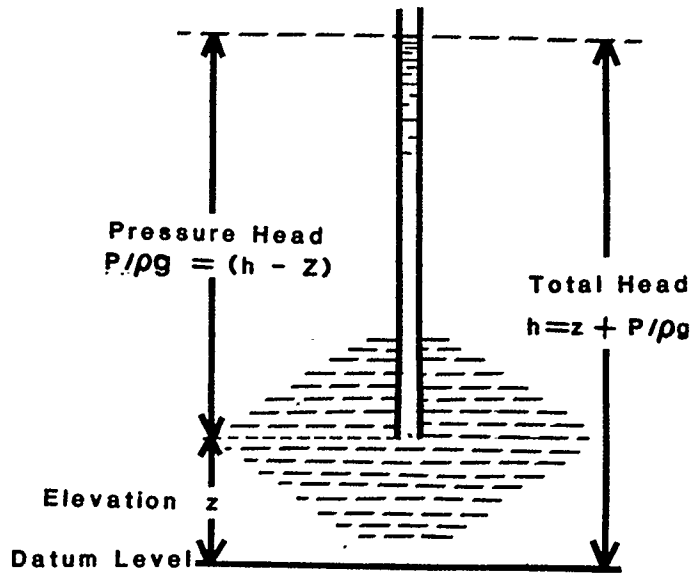


Figure 2.1 Relationship between total head, elevation, and pressure (from Hubbert, 1953).

$$p = \rho g ( h - z ) \quad (3)$$

When this expression for the pressure is substituted into equation (2) we obtain the value for the fluid potential:

$$\phi = gz + p/\rho = gz + g( h - z ) = gh \quad (4)$$

which gives rise to the simple equation relating potential with hydraulic head:

$$\phi = gh \quad (5)$$

where  $h$  is the hydraulic head, and is the height to which fluid would rise above some datum from a point in the subsurface.

In addition to elevation and pressure potential, van Everdingen (1968) has pointed out that a variety of potentials can exist in the subsurface. Included with the elevation and pressure potentials would be:

1) Thermal Potential. Since the density of a fluid is a function of the temperature as well as the pressure, thermal gradients may account for a change in the density term in equation 1, and hence the potential may be influenced. The isobaric thermal expansion of water is

slight, and the geothermal gradient in Western Canada is sufficiently small ( $30^{\circ}\text{C}/\text{km}$ ) such that the thermal potential effect can be considered negligible. Hitchon (1984) has shown that elevation and pressure potentials dominate subsurface fluid movement in western Canada to such an extent that not only is the temperature potential overshadowed, but the temperature gradients themselves are noticeably affected by the fluid movement.

2) Electro-osmotic Potential. Little is known about the nature of the electro-osmotic potential which exists due to the presence of telluric currents. The potential gradient developed due to the effects of these currents is thought to be negligible.

3) Chemico-osmotic Potential. Two formation waters, separated by a semi-permeable membrane, such as a shale bed, will have different potentials if the chemical activities of the water on either side of the membrane are sufficiently different such that a pressure differential can be set up through the process of osmosis. Hanshaw and Zen (1965) have shown that across an ideal membrane, pressure differentials on the order of 100 bars (10 MPa) can be established using two saline solutions of densities 1.07 and 1.12  $\text{g}/\text{cm}^3$ .

## 2.2 Darcy's Law and Continuity Equations

The distribution of potentials through space defines a

field of force. Independent of energy considerations, we may enquire into the field of flow through the subsurface. This field of flow may be represented by the specific discharge vector  $q$ , which is a flux vector. This flux is the discharge of fluids normal to the area of discharge, i.e. the flow across a surface. This flux vector can be related to the potential distribution through Darcy's Law:

$$q = Q/A = -K \text{ grad } h \quad (6)$$

where  $Q$  is the discharge (volume/time),  $A$  is the area normal to the flow direction, and  $K$  is the hydraulic conductivity (length per time). Darcy's Law can thus be seen to express a relationship between the field of flow and the field of force, where the flow occurs in the direction of maximum decrease in the potential field. The coupling mechanism between the two fields is the hydraulic conductivity,  $K$ , which can be written in the following terms:

$$K = \frac{k \rho g}{\mu} \quad (7)$$

where  $k$  is the permeability (in units of length squared),  $\rho$  is the fluid density, and  $\mu$  is the viscosity of the fluid. The hydraulic conductivity can then be thought of as both a

function of the rock medium and of the nature of the fluid that flows through it.

Once the hydraulic conductivities in the subsurface are known, and if the appropriate boundary and initial conditions for the problem of interest can be determined, the hydraulic head distribution and the flow directions can be calculated from the solutions to continuity equations which are described below.

Groundwater flow is mathematically described using continuity equations which rely on the conservation of mass principle. This principle states that within an arbitrary volume of rock, the input into the mass minus the output is equal to the time rate of accumulation within that volume, or:

$$\text{Input} - \text{output} = \text{rate of accumulation} \quad (8)$$

Equation (8) can be expressed in mathematical terms if we consider the change in flow across a volume, expressed by the term  $dq/dx$ , to be equal to the rate of accumulation within the volume due to mineral and fluid compressibilities resulting from a change in hydraulic head within the system. This rate of accumulation is described as the storativity,  $S_s$ , multiplied by the time derivative of hydraulic head,  $dh/dt$ . Equation 8 can then be expressed in mathematical terms as:

$$\frac{\partial q}{\partial l} = S_s \frac{\partial h}{\partial t} \quad (9)$$

The flow rate,  $q$ , can be expressed in terms of the hydraulic conductivity and the head gradient (Darcy's Law, equation 6). Substituting this new expression ( $K \times dh/dl$ ) into equation 9, and rewriting this equation in three dimensions, the continuity equation becomes:

$$-\frac{\partial^2 h}{\partial x^2} - \frac{\partial^2 h}{\partial y^2} - \frac{\partial^2 h}{\partial z^2} = S_s \frac{\partial h}{\partial t} \quad (10)$$

The solution of this equation describes transient saturated flow. For steady state flow, the hydraulic head is not a function of time, and equation (10) reduces to:

$$-\frac{\partial^2 h}{\partial x^2} - \frac{\partial^2 h}{\partial y^2} - \frac{\partial^2 h}{\partial z^2} = 0 \quad (11)$$

The solution of equation (10) or (11) describes the distribution of the hydraulic head at any point in a three dimensional flow field. The hydraulic head distribution determines the direction and magnitude of flow. From the solutions to equations (10) and (11), an equipotential map or flow net can be made which illustrates this flow.

### 2.3 Finite Element Method

Except for simple permeability distributions and

mathematically well defined boundaries within a study area, equations (10) and (11) present complicated boundary value problems which are not amenable to exact mathematical solutions to determine the head distribution. Modelling of the head distribution by electrical resistance analog models is sometimes employed, but two mathematical techniques called the finite difference and the finite element methods are the most commonly used techniques. The finite element method may be described as a process of numerical approximation to the continuity equation in which the unknown function (the hydraulic head) is replaced by an approximate set of functions. The continuously varying hydraulic head distribution is subdivided into separate domains or elements within the section to be examined. The solution of the complete system as the assembly of its elements can then be found by applying the same rules as those applicable to standard discrete problems. The elements take the form of triangular domains which form an irregular mesh covering the section of interest. Each domain or element is characterized by a single specified hydraulic conductivity. The hydraulic potential is solved for each node of the element, or alternately, it may be specified for certain nodes within the mesh given the particular boundary conditions of the problem of interest. The text by Zienkiewicz (1977) is the standard reference for the finite element method, and it gives specific

attention to the solution of the continuity equations for groundwater motion.

Due to the extensive computation required in using the finite element method, this method is specifically developed for large mainframe computers. A version of this method, developed by K.U. Weyer and H.K. Pearse of the Inland Waters Branch of Environment Canada was used in this thesis. This computer program, entitled CAPFEA (calculating and plotting of finite element arrays), is written in Fortran IV for the Honeywell Multics system at the University of Calgary. This program has been modified by B. Smith (formerly of the Academic Computing Services of the University of Calgary) and the author to handle a maximum of 700 nodes and 1500 elements.

The CAPFEA program is a versatile program containing a set of routines to calculate and plot finite element arrays which model groundwater flow systems. This program can be used to solve two dimensional problems in either the horizontal or vertical plane. The flow region (i.e. mesh) may have any complex shape and consist of different elements arranged in arbitrary patterns. Each element may exhibit an arbitrary degree of local anisotropy, and may contain two, three, or four corner nodes. Each node is specified according to whether the head value is to be solved at that node or is included within the boundary conditions of the problem being studied.

Appendix 1 gives a more complete summary of the finite element method, and the CAPFEA program. Included in the appendix is a comparison of the finite element solution with an exact mathematical solution of a theoretical flow system. Also included is a sensitivity analysis of the effect of the form of the mesh (spacing and number of nodes) to the solution of a flow problem.

Computing and plotting time for each individual model is a function of the complexity and size of the model. For the models run in Chapter 4 of this thesis, computing time on the central processing unit was approximately 200 computing time units per run.

#### 2.4 Hydraulic Head and Abnormal Pressures

Abnormal pressures is a term used to describe subsurface fluid pressures that are different from hydrostatic pressures. If these abnormal pressures are greater than hydrostatic pressure, they are termed geopressures. Extreme geopressures are associated with low permeability rocks. The low permeability of the rocks allows for the establishment of high overpressures by preventing the release of the fluids. Highly porous and permeable lenses encased in low permeability lithologies may also be overpressured. Since abnormal pressures deal with fluid pressures, a direct relationship can be shown between geopressures and hydraulic head.

Consider a column of water situated above some datum level open to the atmosphere. Under hydrostatic conditions, where no geopressures exist, the water column at any point will be subject to a fluid pressure given by the term  $\rho g z$ , where  $\rho$  is the fluid density,  $g$  is the gravitational acceleration constant, and  $z$  is the depth from the surface of the water to the point of interest. If this point is some height  $e$  above the datum, the total head will be given by:

$$\text{Total head} = \text{elevation head} + \text{pressure head} \quad (12)$$

where the pressure head is simply:

$$\text{Pressure head} = P/\rho g \quad (13)$$

and the total head is:

$$h = e + P/\rho g = e + \rho g z / \rho g = e + z \quad (14)$$

Consider another point above the first point at a distance  $m$ . The elevation head is increased by an amount  $m$ , such that the elevation head is equal to  $e + m$ . The depth from the top of the water column to the new point is reduced by an amount  $m$ , so that the pressure in the water at the point is equal to  $(z - m)\rho g$ . Adding the pressure

head with the elevation head gives the total head at this point:

$$h = (e + m) + (z - m) \rho g / \rho g = e + m + z - m = e + z \quad (15)$$

This leads to the conclusion that in an open column of water the total head remains constant regardless of the depth of the column. This is the expected result: under hydrostatic conditions, although there is a change in pressure within the system, there is constant head throughout the system, and water does not flow anywhere within the column.

Abnormal pressures are an expression of the deviation in fluid pressures from the hydrostatic condition. Figure 2.2 shows a pressure versus depth plot illustrating abnormal pressures that may be encountered in a theoretical bore hole where there is no change in fluid density with depth. The straight line shows the pressure that would be expected under hydrostatic conditions, whereas the curved line shows the observed pressures due to abnormal pressures. The pressure difference between the two curves at any depth is the extent of the abnormal pressure. The hydraulic head at this depth can now be thought of as consisting of three terms:

Total head = elevation head + static pressure head +

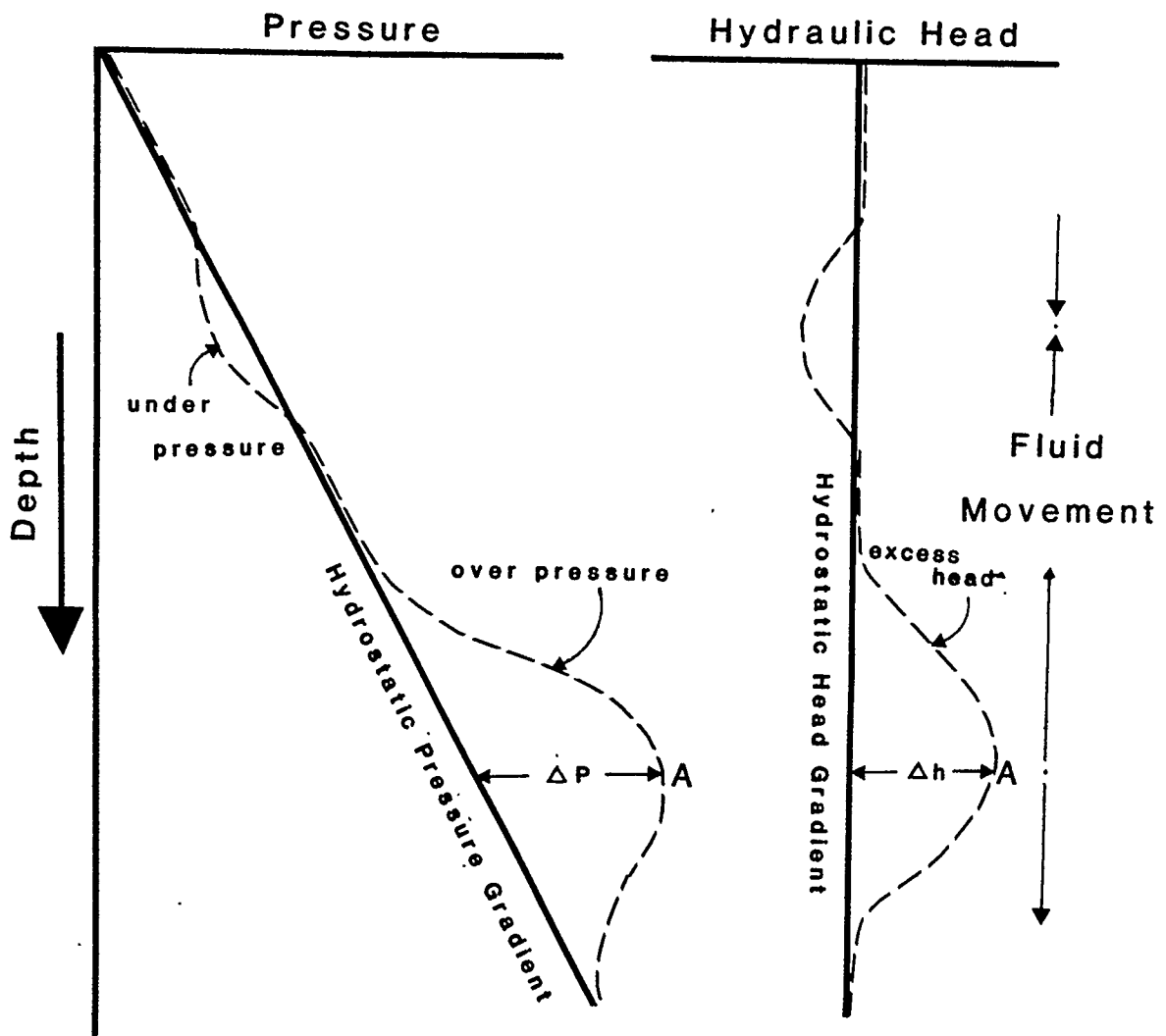


Figure 2.2 Graph illustrating fluid pressure, hydraulic head, and flow direction relationships.

abnormal pressure head. (16)

In practice, however, it is not possible to differentiate between the static pressure head and the abnormal pressure head.

Due to differences in the abnormal pressure head, the total head can vary, with the result that a dynamic situation may exist in which water flows from areas of excess pressure to areas of deficient pressure. The pressure versus depth curve in Figure 2.2 can be directly related to a hydraulic head versus depth curve by considering that any pressure deviation (abnormal pressure) from the hydrostatic curve results in a corresponding deviation from a line of constant head. Since fluid flows in a direction of decreasing hydraulic head, fluid will also flow in a direction of decreasing geopressure. Point A on Figure 2.2 represents a point which has the highest geopressure. Fluid flows both upwards and downwards from this point of maximum geopressure, which also corresponds to a point of maximum hydraulic head. As well as flowing vertically, fluid may also flow horizontally, or in any direction away from the point of maximum hydraulic head.

## 2.5 Sources of Groundwater Energy

In the subsurface where water is continuously moving, there must be a mechanism to continuously provide energy to

the system. Darcy's Law states that in order for fluid to flow, a potential gradient must be set up where water will flow from regions of high potential to regions of low potential. Under geologic conditions, some of the mechanisms that provide for this hydraulic potential gradient are considered below.

Within an area that shows aeriually exposed topographic relief, a potential gradient exists which is a function of the topographic gradient. Water enters the hydrogeologic cycle through precipitation. The initial potential of a particle of water that enters the groundwater cycle is a function of the elevation of the water table where the particle of water enters the system. In higher elevation areas, the water table will be found at a higher elevation, and the water here will have a higher potential than water found at the water table in lower elevation areas. The higher elevations will serve as recharge areas into the groundwater system, water will flow through the subsurface, and will discharge at the lower potential areas found in the lower elevation areas. Within this flow system the maximum potential occurs at the highest surface elevation, and the minimum potential occurs at the lowest surface elevation.

The complexity of groundwater flow patterns due to topographic variations was first illustrated by Toth (1963). He was able to analytically solve the continuity

equation for steady state flow given isotropic, homogenous conditions, and relatively simple boundaries of the flow system. Toth (1963) found that three different flow systems could be found in his models. A local system has its recharge area at a topographic high and its discharge area at a topographic low located immediately adjacent to the recharge area. An intermediate system is one in which although the recharge and discharge systems do not occupy the highest and lowest points in the basin, one or more topographic highs and lows are located between them. A regional system occurs for flow regimes in which the recharge area occupies the highest elevation in the basin, and the discharge area lies at the lowest elevation in the basin. Toth (1963) found that by varying the average gradient throughout the basin, and by changing the heights of the hills and valleys along the section, he was able to increase or decrease the extent to which the various flow regimes extend into the subsurface.

Although Toth (1963) described groundwater flow in small drainage basins, where flow occurs along the flanks of a valley, his results can be generalized to include large areas such as the Alberta and Saskatchewan drainage basins. Local systems of flow would include drainage associated with small rivers and creeks. Intermediate flow would occur for major drainage systems, such as the Athabasca or Bow rivers. Regional flow would have its

recharge area within the Rocky Mountain Foothills and Cypress Hills, and would discharge in areas of low elevation of northeastern Alberta and Saskatchewan (Hitchon 1969b). As Toth (1963) showed, except in areas of accentuated local topography, such as the Rocky Mountains, fluid flow in the deeper subsurface is dominated by the regional flow systems. Occasionally intermediate flow systems may extend to moderate depths; only rarely do local flow systems extend beyond the shallowest horizons.

During the geological history of a basin, extended periods of time occurred when there was no significant topographic variation in the area. Such periods of time have been associated with submergence of the basin and deposition of marine strata. We may enquire whether any fluid movement was occurring for these extended periods, and what might cause these fluids to move. One of the more prevalent mechanisms for fluid movement is the process of compaction. With the addition of more sediments into the basin, the pore fluids in the mechanically weaker sediments take on some of the effective stress that the grains themselves would normally carry. The result is that the fluid pressure is raised within these weaker sediments. This increase in pore fluid pressure (geopressure) can be expressed as an increase in the hydraulic head of the fluids within this overpressured sequence, with the result that a potential gradient is set up from the geopressured

to the normally pressured sequences. Due to the inherent low permeabilities in shales, high overpressures can develop, achieving as much as 90% of the total overburden weight (Fertl 1976). As fluid is expelled from the shale unit, the bed compacts as a result of the porosity decrease. Rocks will also compact due to the mineral and fluid compressibilities, but these effects are minor compared to the porosity decrease due to compaction.

The high initial porosity of shales (approximately 70%), coupled with the high potential gradient, allows for a significant volume of water to move out of the the shale. Within the Western Canada Sedimentary Basin, the Devonian Ireton/Duvernay/Majeau Lake shale sequence and various Cretaceous shale sequences are often cited by various Alberta hydrogeologists as significant units involved in fluid movement during times of deposition. Van Everdingen (1968, p. 528) stated that "during periods of transgression and marine sedimentation, normal hydrodynamic circulation may have stopped altogether leaving only compaction caused movement and possibly osmotic movement of pore waters." Toth (1978, p. 837) in his study on the hydrogeology of the Red Earth region of northern Alberta reported that: "During the first 100 m.y. (-400 to -300 m.y.) of continuous marine sedimentation, compaction of shales and other argillaceous clastics was the main energy generating mechanism," and "Vertical compressive forces generated by

compaction and resulting in lateral but chiefly ascending flows are assumed to characterize the phase of sedimentation." Hitchon (1980, p. 112), in his study on the relationship between hydrodynamics and hydrochemistry, suggested that "in many onshore coastal basins and certainly in offshore basins, compaction phenomena and other processes dominate the regional hydrodynamic patterns."

The process of compaction and the effect of topography both provide sources of energy for subsurface water flow. Besides these two sources for generating fluid flow, several other sources are known which can increase the fluid potential within a rock unit. As a sequence of rocks is buried, the increase in temperature with depth results in mineralogical and density changes of the clay particles and an increase in pore fluid pressure. Aquathermal pressuring, smectite to illite conversion, and kerogen transformation, are among the various mechanisms also suggested for the development of high geopressures. These mechanisms require low formation permeabilities, and only a very limited amount of water is expelled. The somewhat local nature of these mechanisms also leads to a small total volume of fluids being expelled.

## 2.6 Permeability

Whereas the physics of groundwater flow is well

understood, the application of the theory to fluid flow that actually exists in the subsurface is complicated by the incomplete knowledge of the hydrogeologic characteristics of the strata within the subsurface. Permeability is one of the most important factors needed to describe the groundwater flow but, unfortunately, it is also one of the factors whose spatial distribution is the most difficult to assess.

Permeability is a tensor, the value of which varies from place to place, and in direction. Tight shales may show permeabilities as low as  $10^{-9}$  milliDarcies, whereas good reservoir rocks may have permeabilities on the order of several Darcies. This difference of nine orders of magnitude in permeabilities which may be found in a sedimentary sequence suggests that within the realm of groundwater studies only general approximations can be made for any formation permeability.

Measurements of individual cores have revealed an approximate logarithmic relationship between porosity and permeability. There are several other factors that influence the permeability besides the amount of open space in the rock. The geometry of the pore space and the extent to which the pores are interconnected have a great influence on the permeability. Factors such as grain size (permeability varies as the square of the grain diameter), surface roughness, sphericity, and pore to throat ratio all

influence the value of the permeability. The presence of authigenic clays often serves to restrict the pore throats and increase the surface roughness, leading to a decrease in permeability.

Measurement of permeability on individual core samples is probably not a reliable estimate of the permeability of the formation as a whole, as the volume of the core plugs represents but a minute fraction of the total formation volume. Extrapolating the results of core tests from the relatively homogenous cores to the heterogenous formation itself (up to fifteen orders of magnitude) may not be a statistically valid procedure for determining the absolute permeability. It may serve to illustrate relative permeabilities between depositional facies or mineralogic variations within a formation. The effect of open fractures, which can significantly influence permeabilities, is nearly impossible to assess from core tests. Drill stem tests, which determine the permeability by measuring in-situ flow within the formation, are better able to detect the influence of fractures. This method is also somewhat limited by the proximity of the drill hole to the open fracture.

Large rock masses often show high anisotropy and large variations in permeability due to the layered nature of many rocks. This anisotropy has principle directions parallel and normal to the bedding planes. Since some

layers can be several orders of magnitude more permeable than other layers, the permeability across the layers (in series) will be lower than permeability along the layers (in parallel). The ratio between in parallel permeability to in series permeability can be up to three orders of magnitude. Virtually every lithology shows some degree of anisotropy. Reitzel and Callow (1977) report that within the Golden Spike reef the horizontal permeability is fifty times greater than the vertical permeability. Freeze (1969) reports that for near surface unconsolidated gravel deposits the ratio of horizontal to vertical permeability ranges from ten to one hundred. He states that permeability anisotropy is a dominant characteristic of the sediments of western Canada.

The presence of open fractures has a significant effect on permeability values. Reiss (1980) has shown that a one millimetre wide fracture on a one meter spacing will contribute eighty Darcies to the permeability of a rock, while increasing the porosity an insignificant 0.1%. Since fractures are not infinite in extent, the actual influence of a fracture over a large rock mass will be lower. Nevertheless, the presence of vertically orientated fractures can serve to significantly alter the permeability of a rock. They will also enhance vertical permeability and thus decrease the anisotropy of the sediments.

The preceding brief discussion of factors that

influence permeability suggests that a specific permeability need not be exclusively confined to a specific rock type, nor may one formation be restricted to one permeability throughout its entire extent. Because geologic units are often defined on the basis of lithologic, paleontologic, or other criteria, satisfactory definitions of aquifers and aquitards need not correspond with defined geologic intervals. Maxey (1964, p. 126) has proposed the term "hydrostratigraphic unit" which he defined as "bodies of rock with considerable lateral extent that compose a geological framework for a reasonably distinct hydrologic system." As such, two formations may belong to the same hydrostratigraphic unit. Conversely, one formation may be split into more than one hydrostratigraphic unit. Examples from the study area would be the Ireton, Duvernay, and Majeau Lake shale formations, which are grouped together as one hydrostratigraphic unit; and the dolomitized western margin of the Cooking Lake Formation which is considered a separate hydrostratigraphic unit from the Cooking Lake limestone.

## Chapter 3 Compaction

### 3.1 Compaction of Shales

Several authors have suggested that fluid expulsion from shales during compaction is a primary mechanism for dolomitization, oil migration and salt dissolution (i.e. Mattes and Mountjoy 1980; Bonham 1980). The purpose of this chapter is to estimate the timing and amount of fluids derived from the Ireton, Duvernay and Majeau Lake shales during compaction. In order to do this, a brief summary of the mechanisms of shale compaction is in order. The following is not meant to be a review of the literature on compaction, but rather a brief summary of the pertinent information.

Compaction of muds to form shales is a complex process involving mechanical and chemical changes. Athy (1930) was one of the first to try to quantify a porosity-depth relationship for shales. He found that within the Permo-Pennsylvanian shales of Oklahoma there is an exponential relationship between porosity and depth. Hedberg (1936) further studied compaction for various shale sequences in Venezuela and observed that these shale sequences compact less rapidly than the shale sequence observed by Athy (1930). Bishop (1979) noted that there are several variables that influence shale compaction other than depth. Compaction is also a function of pore pressure

dissipation, sedimentation rate, overburden density, age, shale thickness, clay mineralogy and clay content. Powers (1967) examined the effects of clay mineralogy on shale dewatering. For Gulf Coast clays he noted that most of the free water is mechanically squeezed out by the time the sediment is buried to 500 - 1000 m. In montmorillonite clays, however, mineralogical transformations begin at about 2000 m, and the montmorillonite to illite conversion releases water from the hydrated layers of the clay particles.

Hinch (1980), in a thorough review on shale compaction, pointed out some of the fundamental differences between shale compaction and compaction of other types of sediments. The extremely large surface area per volume (up to 5 orders of magnitude larger than sand grains), and the hydrated nature of the clay surfaces result in a complex process of dewatering. He defined four different stages of shale compaction, with shale porosity decreasing with depth in the initial two stages, and increasing with depth in the latter two stages. These latter stages involve mineral transformations and mineral growth, and occur below 3500 m, which is a depth considerably below the maximum burial of the Ireton, Duvernay and Majeau Lake shales. It is important to realize that the empirically derived curves of Hinch (1980) do not show the history of porosity reduction with burial of a specific bed. Instead they show the

porosity changes with depth in a specific basin at the present time. The effects of temperature and time are not specifically noted in these curves. Further, thick sedimentary sequences are unlikely to maintain a constant lithology and chemical composition throughout the sequence. For these reasons direct observation of change in porosity with burial of an individual package is perhaps not represented by depth versus porosity curves from a particular sedimentary basin. Indirect means may have to be found to evaluate the change in porosity with time.

### 3.2 Ireton Compaction

As has been stated previously, several variables influence the compaction of shales. In an examination of the Ireton, Duvernay and Majeau Lake shales, some of these effects, such as temperature and time, are no longer visible. In order to obtain a valid porosity versus depth curve which traces the history of the porosity reduction in the shales as they were being buried, several questions have to be considered:

1. Does the present porosity of the Ireton, Duvernay and Majeau Lake shales at the present depth fall on any observed porosity versus depth curve?
2. If it does, can we be sure that the shales compacted in the same way as the published curve?
3. Can the effects of erosion (both on the

Pre-Cretaceous unconformity and in the Late Tertiary) be accounted for?

4. Do these shales show any change in porosity from the top of the unit to the base, or has the entire shale package reached its maximum compaction?
5. Is there an indirect means of obtaining porosity versus depth other than from core measurements or well logs?

Figure 3.1, modified from Hinch (1980), shows a compilation of porosity versus depth for various shale sequences. There is no unique curve which describes shale compaction. The other variables that influence compaction (such as clay content and mineralogy, rates of burial and initial thickness) are significant. If the shale package showed any systematic change in porosity from the top to the base of the unit, the form of the curve may help in understanding the porosity versus depth relationship, or perhaps allow us to quantify fluid movement to some extent (Magara 1968, 1973, 1976). Unfortunately, the Ireton, Duvernay and Majeau Lake shales are too thin (240 m) and too deeply buried (>2000 m) to permit any conclusion to be made with respect to a systematic change in porosity from the top the Ireton to the base of the Duvernay. Table 3.1 shows porosity at ten meter intervals of the Ireton and Duvernay formations in well 16-12-54-26-W4, based on sonic logs, revealing little systematic change in porosity with

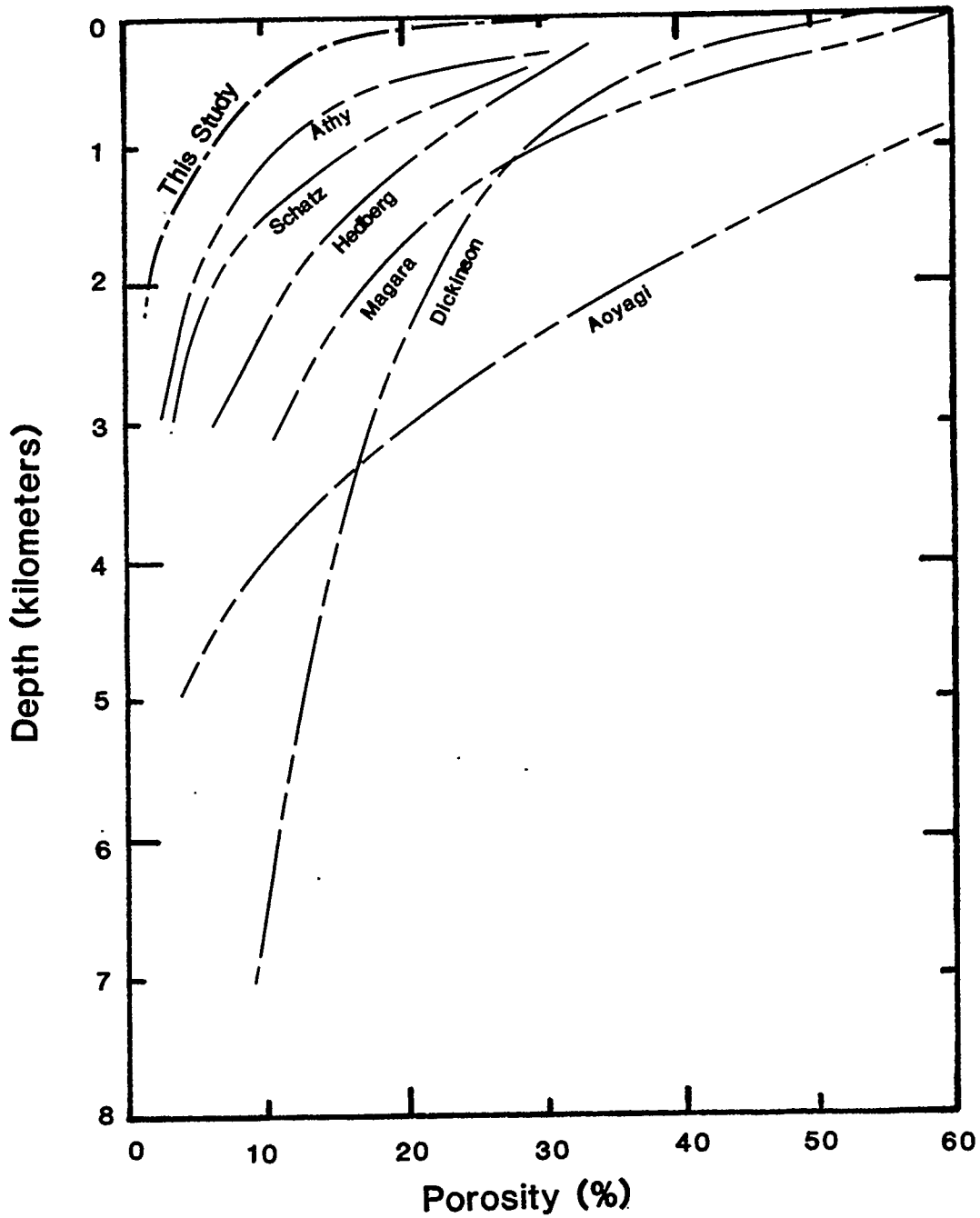


Figure 3.1 Depth versus porosity plot for various sediments (after Hinch, 1980)

Depth m subsea	Sonic velocity us/ft	Volume of Shale %	Porosity %
-750	61	35	0
-760	61.5	35	0
-770	67.5	60	2
-780	74	64	2
-790	80	80	1
-800	83	77	4
-810	80.5	75	3
-820	77	65	4
-830	73	59	2
-840	76	65	0
-850	79	84	1
-860	76	70	5
-870	86	83	4
-880	83	80	3
-890	81	78	5
-900	84	78	2
-910	79	75	2
-920	79	75	0
-930	69	57	2
-940	72.5	60	1
-950	60	35	0
-960	56	25	0

Table 3.1 Porosity and per cent shale for the Ireton and Duvernay formations from well 16-12-54-26W4.

depth.

Table 3.1 also list the per cent volume of shale within the Ireton and Duvernay formations, based on gamma ray logs. The amount of shale within these formation varies from about 25% to over 80%, the remainder consisting largely of fine quartz and calcite. Shales are a poorly defined rock type, usually taken to mean a fine grained fissile rock with varying clay content. Because the clay content can vary from shale package to shale package, or even within the same package, the processes and timing of compaction of one individual shale sequence can differ from the processes and timing of compaction of another shale sequence.

The previous discussion suggests that no direct comparison of the Ireton, Duvernay and Majeau Lake shale compaction can be made with other shale sequences. In order to find the compaction history of these shales an indirect approach was taken which used the drape of Post-Ireton lithologies over a Leduc reef. This approach utilizes the concept of differential compaction. It is based on the fact that during burial the reef compacts less than the surrounding shales, and a drape structure develops in the beds overlying the reef.

Labute and Gretener (1969) and O'Connor and Gretener (1974) examined differential compaction along the Rimbey-Meadowbrook reef trend. They concluded that a large amount

of the drape occurred during the Paleozoic Era, and that there was significant erosion on the Pre-Cretaceous unconformity. They also found that the overburden stress that was applied during the Paleozoic and eroded during the Pre-Cretaceous unconformity was not exceeded until the Late Cretaceous, and compaction was delayed during much of the Cretaceous.

O'Connor (1972) evaluated shale compaction by plotting the amount of drape in several marker horizons above the Ireton versus the thickness of the shale package. He was able to calculate the amount of drape by subtracting a trend surface projection of where the unit would have been had there been no compaction from the actual depth of the unit. On these plots he was able to show that the amount of drape decreased as a linear function of the increase in thickness of the shales, i.e., there is a negative linear relationship between the drape and the thickness of the shale unit.

In order to calculate the total shale compaction, the amount of drape that would have developed if the Leduc reef had completely penetrated through the Ireton Formation must be known. This amount of drape corresponds to the intercept in the drape versus shale thickness graph of O'Connor (1972). The intercept shows the drape that would have developed if there was zero thickness of the Ireton shales over the reef. Calculation of the compaction

follows from the intercept of the drape values. Consider the deposition of the "ith" marker followed by the "jth" marker. Drape on the ith marker is due to compaction in the shale resulting from the additional stress introduced by the weight of the sediments above the ith marker. Similarly, drape on the jth marker is due to the stress of all the sediments above this interval. Since the lower unit has more weight on it than the upper interval, the drape on the ith marker is greater than the drape on the jth marker. The difference in drape is due to the deposition between the ith and jth marker. The compaction that occurred during deposition of sediments between the ith and jth marker can be calculated by subtracting the drape on the jth interval from the drape on the ith interval, or:

$$\text{Compaction}(i,j) = \text{Drape}(i) - \text{Drape}(j) \quad (1)$$

Approximately nineteen different marker horizons were picked by O'Connor (1972) over nine different reefs or portions of reefs along the Rimbey-Meadowbrook trend (Acheson, Golden Spike, Bonnie Glen North, Bonnie Glen South, Bonnie Glen Central, Redwater, Wizard Lake North, Wizard Lake South, Wizard Lake Central, Wizard Lake All). Using his data, compaction was calculated for these intervals in each reef area.

An unexpected observation was that a few of the Paleozoic intervals showed negative compaction, that is, there was less drupe in a lower interval than on a succeeding higher interval. The most likely explanation for this is that the reef itself is not a rigid framework, but that the reef itself undergoes some compaction. Mossop (1972) documented reef compaction through stylolitization in the Redwater reef. A schematic representation on how reef collapse can lead to negative compaction is presented in Figure 3.2.

A graph showing compaction versus depth of burial is presented in Figure 3.3 for the Golden Spike reef. The discontinuities in the curve are caused by compaction of the reef itself. These discontinuities suggest rapid reef compaction early in the burial history of the reef. The discontinuities can be corrected by estimating the offset between the curves and adding this offset to all points before the discontinuity to produce a continuous curve.

The Wizard Lake compaction curve revealed significant offsets between every data point of the Paleozoic markers. Due to the high degree of error that would be associated with the numerous corrections this reef was excluded from the study leaving six compaction curves to be analyzed. These compensated compaction curves are presented in Figure 3.4. The position of the horizontal part of the curves is only a function of the depth of erosion on the

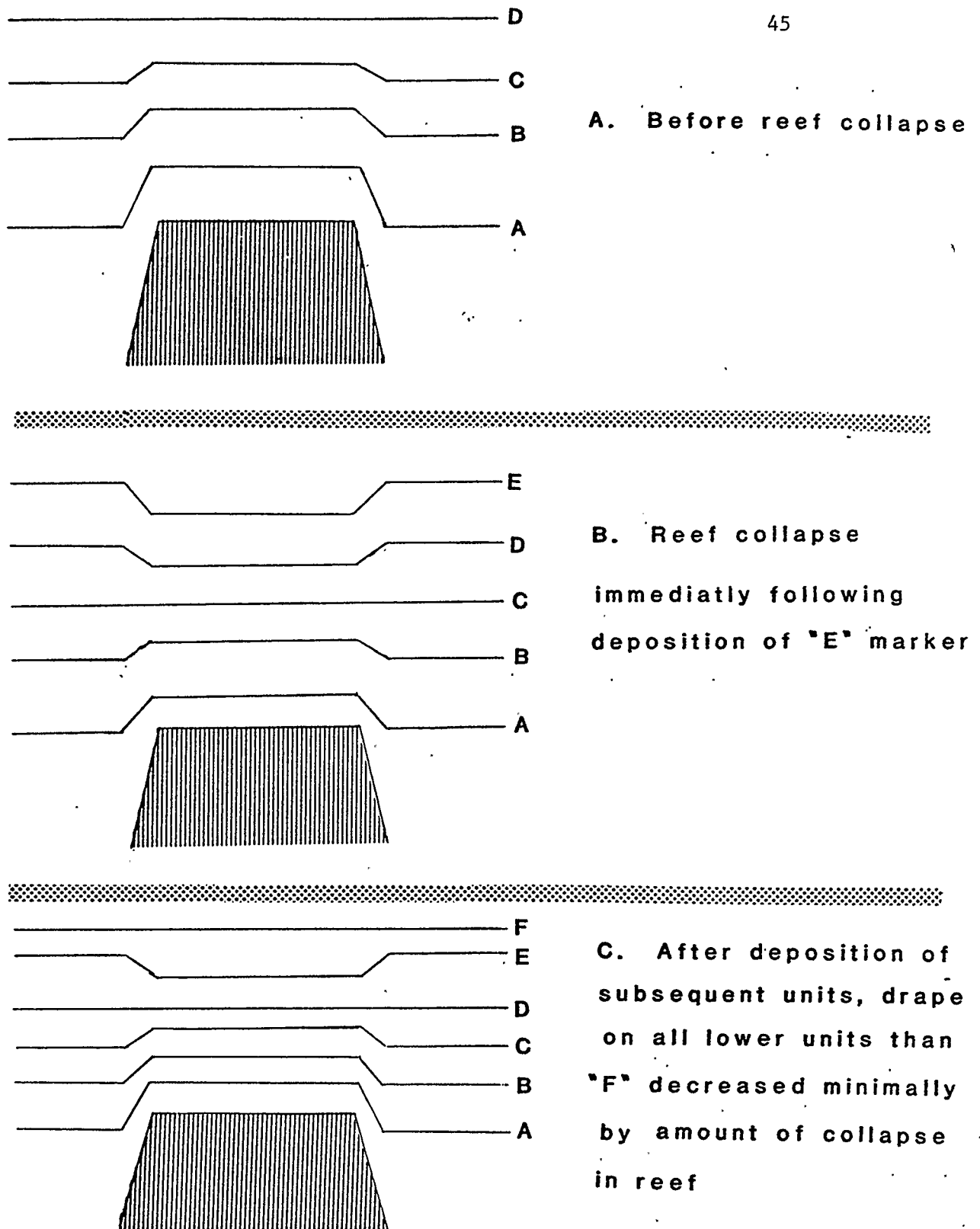


**Figure 3.2 Schematic illustration showing development of discontinuities in compaction due to collapse of Leduc Reef**

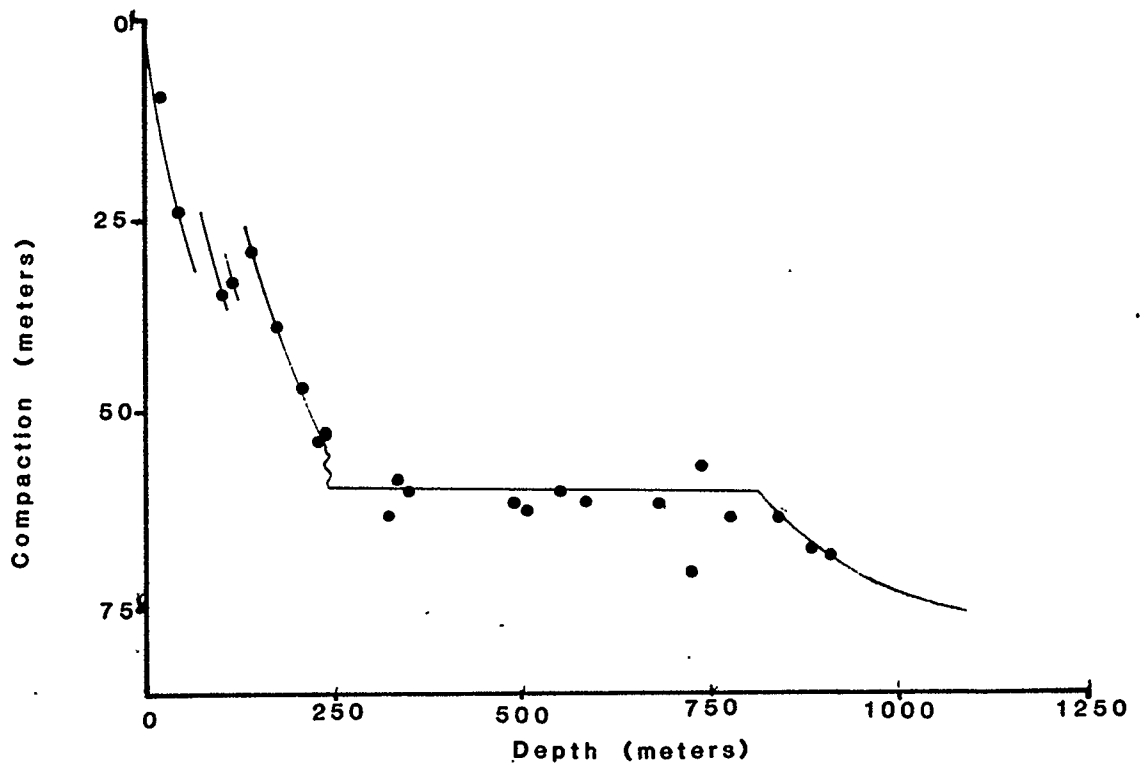


Figure 3.3 Unrestored compaction curve for shales surrounding Golden Spike Reef

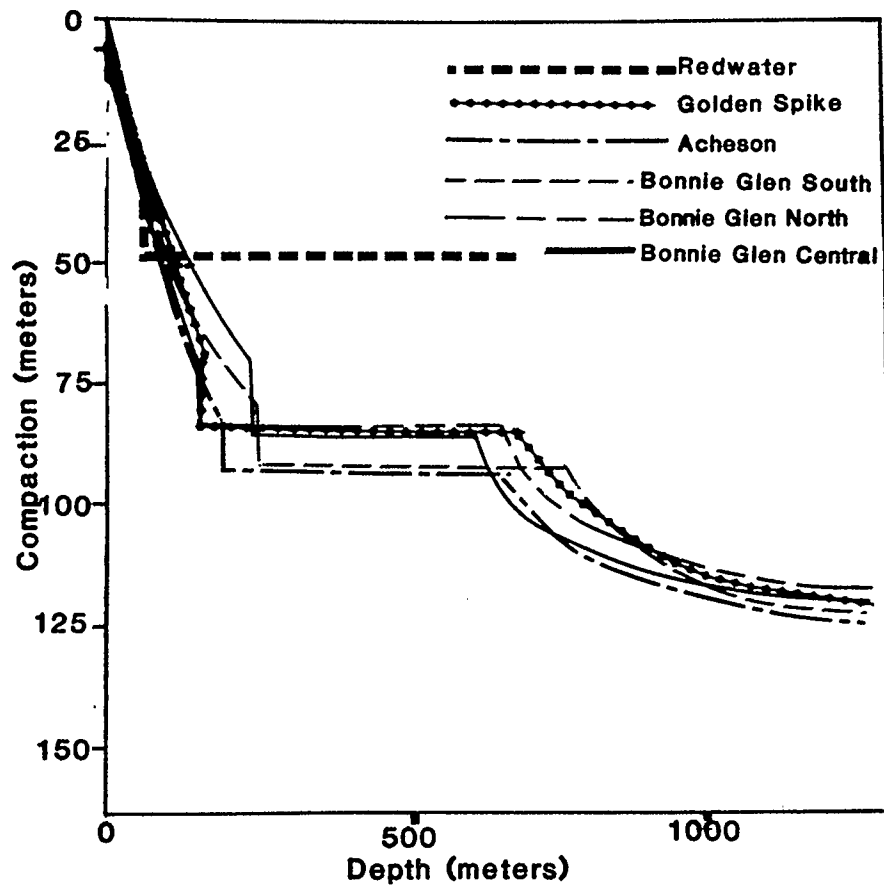


Figure 3.4 Compaction curves for various Leduc reefs.

Pre-Cretaceous unconformity, and is not a function of the shale compaction. The tight clustering of the curves to each other before the Pre-Cretaceous unconformity suggests that, to a large extent, the shales compacted in a similar manner throughout the study area.

Gretener and Labute (1972) pointed out that the total shale compaction is equal to the drape plus the reef compaction. Some reef collapse may have occurred in the late Paleozoic and the record of this collapse within the Upper Paleozoic markers would have been eroded away. The total amount of compaction (120 m), indicated from Figure 3.4, is only a minimum value. It is thought that this unknown compaction is not very extensive, perhaps only a few tens of meters.

At 2000 m of burial, the Ireton and Duvernay formations are about 240 m thick. Adding the 120 m of compaction gives an original thickness of the shale package of 360 m. Westoll (1962) introduced the term "own load thickness" to describe a sequence of substantial thickness which already shows some compaction due to its own weight at the time of deposition. The 360 m original thickness of the Ireton and Duvernay formations is sufficient to compact to some extent due to its own weight. The calculated value of original thickness of 360 m compares favourably with estimates compiled by Perrier and Quiblier (1974). They estimate that a shale now 240 m thick buried to a depth of

about 3000 m should have had an original thickness of 370 m. The 10 meters difference between value of Perrier and Quiblier (1974) and the value calculated here is insignificant in view of the many variables involved.

Calculation of porosity versus depth follows from the compaction versus depth relationship. If the compaction was solely a result of shrinkage of the pore volume, it is possible to calculate the porosity at any depth of burial. If we assume that the sediments compacted in the vertical direction only, the thinning of the shale formations by compaction can be directly related to the pore volume loss. From the present thickness of the shale and its present porosity, the total amount of solid matter within the shale section can be found. This thickness of total solids is thought to remain relatively constant throughout the burial history. Phase transformations, mineral dissolutions, and cementation were probably minor in these low permeability rocks and these effects probably did not cause much change in the total solid thickness. The current porosity of 3% contributes a certain amount of thickness to a column of shale of unit area. The amount of compaction at any point in the depositional history represents the pore space that was lost due to compaction. Adding the current pore "thickness" to the amount of compaction "thickness" gives the porosity as a ratio of the total thickness of the shale at any point in the depositional history. By examining

subsequent points in the compaction history, a continuous curve can be constructed which illustrates the porosity reduction with depth (Figure 3.5). For comparative purposes with other shale compaction curves, this curve is also plotted on Figure 3.1.

As Stoakes (1979), and Oliver and Cowper (1965) have pointed out, the Ireton and Duvernay formations actually consist of three major facies with varying lithologies. Hence, this curve does not represent the change in porosity with depth of any single unit within the Ireton and Duvernay formations, but rather an average porosity of the formations as a whole.

### 3.3 Interpretation of Compaction Curve

The porosity versus depth curve determined in this study is situated to the left of the other published curves in Figure 3.1. This indicates that the shales within the study area compacted to a greater extent when they were buried to a certain depth compared to other shale units. Part of the reason for this is due to the nature of the porosity measurements. Most other curves in Figure 3.1 show the porosity of a particular sample at a particular depth, however, the Ireton/Duvernay/Majeau Lake curve is based on the average porosity throughout the shale sequence. Since the porosity most likely decreased from the top to the bottom of the shale section (especially

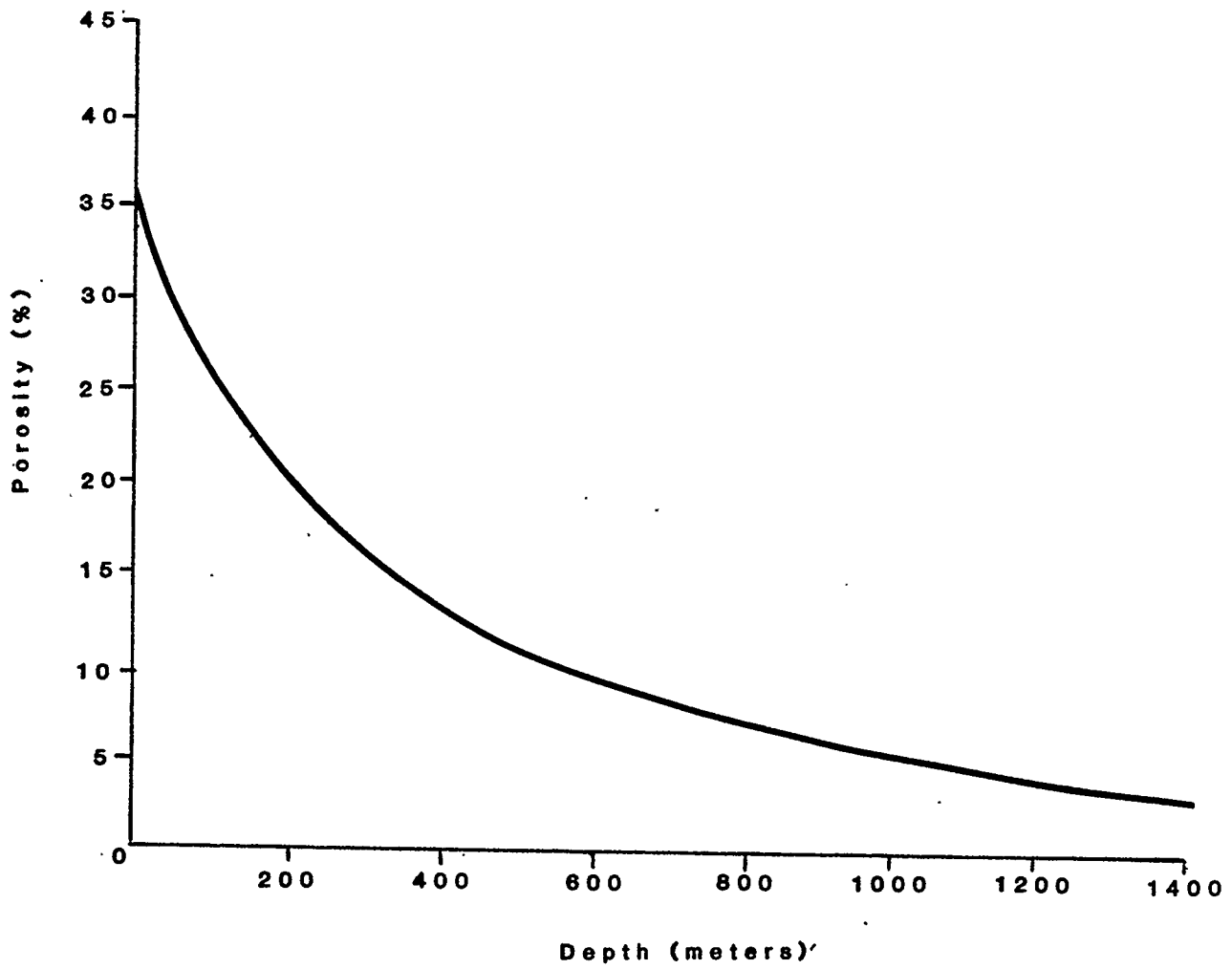


**Figure 3.5** Average porosity versus depth for the Ireton/Duvernay

during the early stages of burial), the porosity of an individual sample at a particular depth would have been higher than the average porosity throughout the sequence. A more proper comparison of the Ireton/Duvernay curve with other porosity versus depth curves would have the Ireton/Duvernay curve shifted downward approximately 200 m, which places it in close proximity to the Athy (1930) curve.

A more important factor relating the position of the Ireton/Duvernay/Majeau Lake porosity versus depth curve with the position of other porosity versus depth curves in Figure 3.1 is the initial thickness of the shale sequence. The other published curves in Figure 3.1 deal with very thick shale sequences. As Ferrier and Quiblier (1974, p. 514) pointed out: "thick layers are not so reduced by compaction as are thin layers." This in effect means that a thick shale sequence is able to maintain a higher porosity to greater depths of burial than a thin layer. The effect of shale thickness on extent of compaction was first noted by Weller (1959). He plotted compaction curves for various shale thicknesses, illustrating that thinner units reach a given amount of compaction at shallower depths than thicker units.

Athy (1930) has been able to fit a curve of the porosity versus depth plot to an equation of the form:

$$\phi_z = \phi_0 e^{-bz} \quad (2)$$

where  $\phi_z$  is the porosity at depth  $z$ ,  $\phi_0$  is the initial porosity, and  $b$  is some empirically determined constant. No single curve of this type could be found that completely describes the change in porosity with depth of the Ireton, Duvernay and Majeau Lake shales. A change in the porosity versus depth curve occurs at about 12% porosity, or 450 m burial depth, from an exponential decrease to a linear decrease. The change in curve form may be due to different mechanisms of compaction above 450 m compared to the mechanisms below 450 m. Hedberg (1936), Weller (1959), Hoshino and Inam (1977), and Aoyagi and Asakawa (1977) (last two references are cited in Aoyagi and Asakawa 1984; original papers in Japanese) describe a change in compaction processes at about 10% porosity, from a mechanical deformation process to a grain recrystallization and crushing process. Since these two different processes would likely result in different responses to overburden stress, the change in curve form noted at 12% porosity is likely due to a change in compaction mechanisms.

Because the loss of porosity must be accompanied by an expulsion of water, it is possible to estimate the amount and timing of fluid release from the Devonian shales during compaction. From the compaction versus depth graph (Figure 3.4), the amount of volume loss can be directly calculated.

A direct conversion of volume loss with time is not possible, as deposition of the overlying Paleozoic and Mesozoic strata was almost certainly discontinuous and affected by disconformities and unconformities. Table 3.2 summarizes the results of the amount and timing of fluid release as a function of the deposition of overlying strata. Estimates on the amount of fluid released during the Paleozoic after Wabamun deposition is somewhat speculative, as the total thickness of sediments eroded away is not accurately known. O'Connor (1972) estimated that approximately 400 m of sediments were removed on this unconformity, and it is believed that this estimate provides a reasonable value for the amount of fluid released.

A large portion of the total volume of fluids were expelled during the Paleozoic Era, with more than half the total expelled during the first ten million years. A significant portion (15% of the total fluid released) occurred during the Mesozoic Era. This is a volume of  $17 \times 10^6 \text{ m}^3$  of fluid per  $\text{km}^2$ , and this volume must be considered when examining diagenetic changes and oil migration that may have occurred from within the Ireton, Duvernay, and Majeau Lake formations during the Mesozoic Era. It is unlikely that the fluid released by compaction of these shales during the Mesozoic Era appreciably affected the hydrodynamics within the study area. Although

Depositional Interval	Depth range of top of Ireton	Volume of fluids released	
		m <sup>3</sup> /km <sup>2</sup>	bbls/mile <sup>2</sup>
Nisku	0 - 51 m	24 × 10 <sup>6</sup>	390 × 10 <sup>6</sup>
Calmar	51 - 63 m	6 × 10 <sup>6</sup>	100 × 10 <sup>6</sup>
Graminia	63 - 90 m	9 × 10 <sup>6</sup>	146 × 10 <sup>6</sup>
Wabamun	90 - 273 m	37 × 10 <sup>6</sup>	600 × 10 <sup>6</sup>
Remainder of Paleozoic	273 - 670? m	20 × 10 <sup>6</sup>	325 × 10 <sup>6</sup>
Cretaceous	670 - 1500 m	17 × 10 <sup>6</sup>	275 × 10 <sup>6</sup>

Table 3.2 Volumes of fluid released during Ireton compaction

Depth (meters)	dφ/dz (per meter, × 10 <sup>-3</sup> )
0	-1.13
50	-0.94
100	-0.78
150	-0.64
200	-0.52
300	-0.33
400	-0.21
500	-0.13
600	-0.10
700	-0.09
800	-0.10
1000	-0.14
1200	-0.12
1500	-0.19

Table 3.3 Rate of Ireton porosity loss with depth

the total volume of fluids released was relatively large, it was expelled over a large span of time (approximately thirty million years) and the total fluid flux (volume discharged across a specific surface in a given time) is quite small. The fluid flow driven by variations in topography due to Cordilleran uplift would have been the prevalent source of energy for fluid migration during this time. This flow may have been sluggish, but it still would have played a more substantial part in fluid flow than the fluids derived by compaction of the Devonian shales. Fluid flow due to Ireton, Duvernay, and Majeau Lakes shale compaction must have been the dominant mechanism for flow during the Devonian Period. It would have been less influential during the Upper Paleozoic Era, and would not have had any appreciable influence on regional hydrodynamics during the Mesozoic Era.

In order to determine the rate of porosity loss with depth, the porosity versus depth curve was parameterized to fit a Lagrange Polynomial of fourth order. The porosity versus depth relationship for the shale sequence can be expressed by the formula:

$$\begin{aligned} \bar{\rho}_z = & 0.335 - 1.127 \times 10^{-3} z + 1.942 \times 10^{-6} z^2 - \\ & 1.559 \times 10^{-9} z^3 + 4.460 \times 10^{-13} z^4 \end{aligned} \quad (3)$$

where  $\bar{\rho}_z$  is the porosity at any depth  $z$  (in meters). The

first order derivative of this equation gives the rate of porosity loss at any depth. Values for this derivative are shown in Table 3.3 for the first 1500 m of burial. The slight increase in the rate of porosity change with depth below 700 m indicated in Table 3.3 is probably due to minor fluctuations in the Lagrange approximation, and is not related to any real event. In reality the derivative remains constant below 700 m, or perhaps decreases slightly.

Calculations based on simple integration show that at the initial rate of porosity loss, all the porosity would be lost after only about 300 m of burial if this initial rate were to continue. Between zero and five hundred metres burial, the rate of porosity loss continually decreases. Below the five hundred metre burial depth (12% porosity), the porosity loss per meter occurs at only one tenth the rate of porosity loss at the shallower depths. At greater depths, it is possible that, as a result of mineralogical changes, the porosity increases with depth of burial (Powers 1967), although there is no indication that the Ireton, Duvernay, and Majeau Lake formations have been buried to such an extent.

## Chapter 4 Directions of Fluid Migration During Compaction

### 4.1 Method of Investigation

The process of compaction, with its associated fluid expulsion, results in a directional movement of water. Although the fluid is ultimately directed upwards with respect to a stratigraphic marker, high permeability conduits exist where the fluids may flow laterally before flowing upwards. This lateral movement of fluids is possible only if the pathways of fluid movement through the conduit require less energy than direct vertical migration out of the compacting bed. A highly permeable reef situated within the low permeability compacting shales is a prime geological model of such a fluid conduit. The purpose of this chapter is to examine how the presence of a Leduc reef influences the flow directions of fluids expelled from the Ireton, Duvernay and Majeau Lake shales.

Since direct examination of the fluid flow in this situation is impossible, this study employs the CAPFEA finite element program developed by K.U. Weyer and H.K. Pearse of the Inland Waters Branch of Environment Canada. With this modelling technique, the hydraulic head distribution that existed when the Ireton Formation was buried beneath four hundred meters of carbonates (during the Upper Paleozoic Era) can be found.

#### 4.2 Development of Method

This theoretical model necessitates approximations of the formation permeabilities and the hydraulic head within the compacting shales. Diagenetic reactions in the past may have either increased or decreased the formation permeabilities compared to the present permeabilities of the formations. Lighter sedimentary loads upon the strata than exist now would have meant less compaction (in both the argillaceous and carbonate sediments) and, hence, higher permeability. Since a finite element model relies on relative permeabilities rather than absolute permeabilities, several of the diagenetic or compaction affects would serve to enhance or decrease various formation permeabilities equally. Orders of magnitude estimates can still be made of the various carbonate formational permeabilities. Numerous theoretical estimates of the relationship between shale porosity and permeability have been published. Values from Smith (1971) were used in this model.

The hydraulic head distribution within the compacting shales also relies on theoretical estimates. The head distribution due to compacting shales would be a function of the geopressures developed within these shales. Fluid pressures can range from 45% to 90% of the total overburden weight. The lower limit corresponds to the proportion of fluid pressure to overburden weight in a normally pressured

sequence. The upper limit corresponds to a nearly impermeable sequence where the fluids cannot escape and must support a considerable amount of the sedimentary load. The selection of a value describing the amount of geopressures has considerable ramifications in the head distribution within the shales and hence the direction of fluid flow. Smith (1971, 1973), using continuity equations and a finite difference algorithm, estimated the fluid pressure profile within a 250 m thick shale sequence buried at various depths. His pressure values were taken directly to calculate the hydraulic head found within the compacting Ireton, Duvernay, and Majeau Lake shales. According to Smith (1971), a 250 m thick shale sequence sandwiched between two normally pressured units has its highest overpressure (1200 kPa) at a point slightly below the middle of the shale unit, with flow directed both upwards and downwards from this plane. The ratio of fluid pressure to total overburden stress is about 0.54, which appears reasonable for this relatively thin unit. In terms of hydraulic head, this overpressure translates into 120 m of excess head greater than hydrostatic. Immediately west of the Rimbey-Meadowbrook trend, the Cooking Lake Formation is absent. The laterally equivalent Majeau Lake Formation serves to thicken the shale sequence. This thicker shale sequence would be expected to have a higher overpressure than the thinner shale package east of the Rimbey-

Meadowbrook trend. Although no units of approximately 350 m thickness were studied by Smith (1971), an estimate of the geopressure of this unit was made by extrapolating between thicker and thinner units examined by Smith (1971, 1973). Accordingly, a pressure profile similar to the one developed for the 250 thick shale unit was developed which shows an excess pressure of about 2000 kPa, or a fluid pressure to total overburden stress ratio of 0.58. The excess head for this section of overpressured shales was about 200 m.

Head distribution along the upper boundary was considered to be constant. The study area was submerged during Wabamun deposition and no surface head gradient would have developed on this submerged surface.

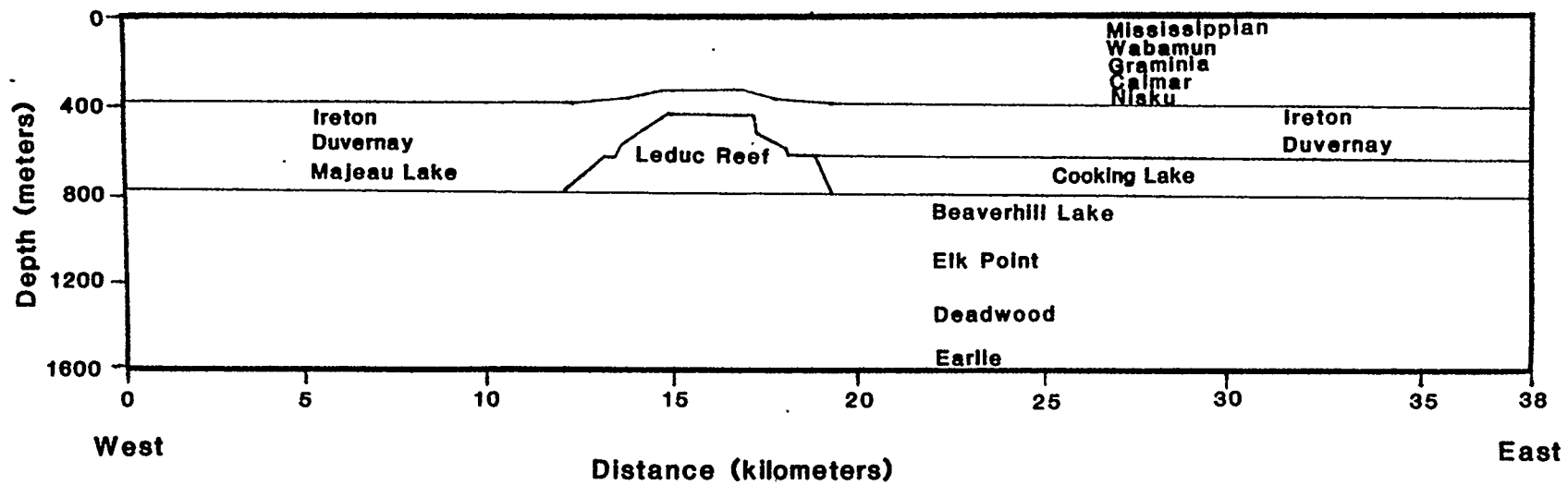
Based on the geology, permeability and head distribution, the finite element model constructed consists of 360 nodes and 638 elements. The dimensions of the model represent a 38 km long west - east transect centered on a 5 km wide Leduc reef. The depth of the section represented by the model (from the base of the Cambrian sequence to 400 m above the top of the Ireton Formation) is 1600 m. Since only broad estimates can be made on some of the formation permeabilities, several formations are grouped together as single hydrostratigraphic units. The lowermost formations, consisting of the Beaverhill Lake, Elk Point, and the Cambrian formations, are grouped together as one unit, as

are the Nisku, Calmar, Graminia, and Lower Wabamun formations. The model constructed has an impermeable base, constant head along the top, and permeable sides, so that water could flow in or out of the edges of the section. With this model, fluid migration pathways can be analyzed by varying the head distribution and permeabilities of various formations, with the result that an analysis can be made of those factors which have the greatest influence on flow.

#### 4.3 Results of Models

Owing to the inherent uncertainties in the permeability and the head distribution of the various formations, nine different scenarios are presented with varying parameters in order to ascertain what effect these parameters have on the overall fluid flow pattern. The form of the reference scenario (Figure 4.1) consists of a geopressure distribution within the shales of the type previously described. The basal unit of the section along both margins is overpressured by 40 m of excess head. Relative permeabilities of the various formations are listed in Table 4.1; only order of magnitude estimates are made of the permeabilities. A horizontal to vertical permeability ratio of 10:1 is applied to all units with the exception of the reef itself, where a 2:1 ratio is applied.

Fluid flow described by this reference scenario is



Vertical Exaggeration - 6x      Head at east and west boundary - 40 meters above hydrostatic

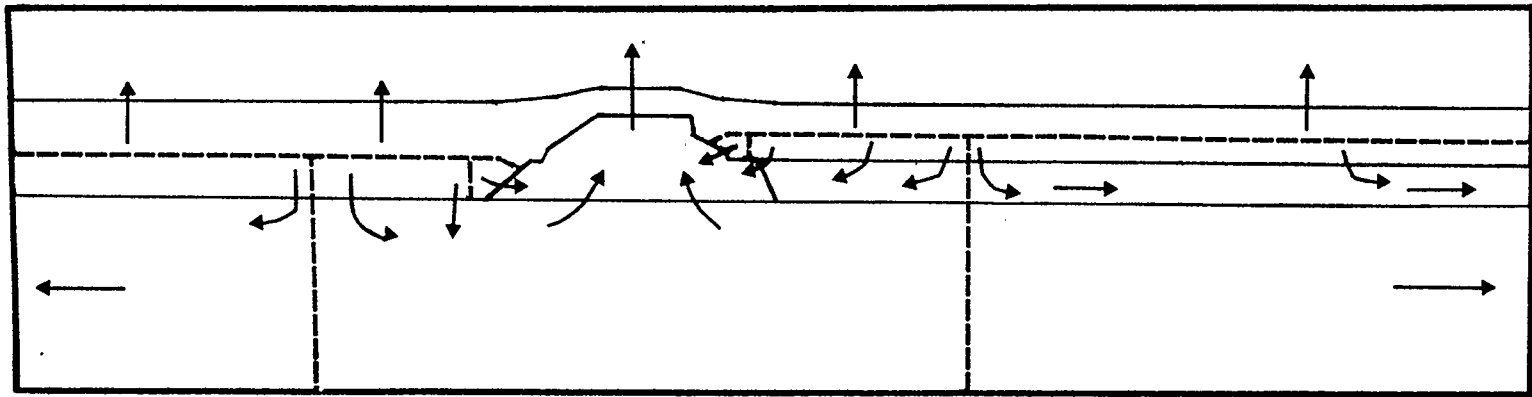
Figure 4.1 Geology, scale, and head distribution of finite element simulation.

Hydrostratigraphic unit	Normalized Permeability	
	Horizontal	Vertical
Upper unit	$1 \times 10^5$	$1 \times 10^4$
Ireton/Duvernay/ Majeau Lake	10	1
Leduc Reef	$1 \times 10^7$	$5 \times 10^6$
Cooking Lake	$1 \times 10^4$	$1 \times 10^3$
Basal unit	$1 \times 10^3$	$1 \times 10^2$

Table 4.1 Relative permeabilities of formations for finite element simulation of compaction flow used in reference scenario.

shown in Figure 4.2. Vertical exaggeration of the section is six times. The asymmetry of the flow is due to the asymmetric geology and head distribution within the area. The Cooking Lake platform east of the Leduc reef provides a layer of higher permeability than do the underlying Beaverhill Lake, Elk Point and Cambrian sections. As well, the shale unit east of the reef is thinner and has a lower fluid pressure than the shales west of the reef. An important concept illustrated by the model is that only a small fraction of the flow occurs directly from the shales into the reef. Much of the flow is channelled vertically downwards into the lower units, then laterally towards the Leduc reef and, finally, upwards through the reef to the sea floor. West of the reef, fluids expelled from the shales are channelled to the reef from a distance of 4320 m west of the western reef margin. East of the Leduc reef, fluid flow is channelled from the shales to the reef from a distance of 6250 m beyond the eastern margin of the reef. Direct flow from the shales into the reef occurs upon the east flank of the reef 160 m west of the eastern edge to approximately 130 m east of the margin. On the western flank, fluid flow directly from the shales to the reef occurs from 800 m east of the west margin of the reef to a point 225 m beyond the western margin of the reef.

An important conceptual aspect of the model is the relatively high head loss of the ascending fluids as they



← Flow arrows

----- Hydraulic divide

Figure 4.2 Flow directions for reference model.

cross the Ireton shales immediately above the Leduc reef. These shales significantly decrease the effectiveness of the reef as a vertical fluid conduit.

Following this reference model, eight variations are presented with one parameter (permeability, head or boundary condition) altered in order to provide various scenarios of flow patterns. These scenarios fall into four categories:

- 1) varying the head (geopressures) within the shales;
- 2) varying the head (geopressures) of the basal units;
- 3) altering the degree of anisotropy within the shale units; and,
- 4) varying the permeability within the basal units and Leduc reef.

The geopressure distribution within the shales was varied because of the uncertainty involved in the geopressure estimates taken from Smith (1971). Since Smith (1971) estimated various parameters in his calculations (such as permeability and burial rates), a model with higher geopressures, and a model with lower geopressures than estimated by Smith (1971) are presented to illustrate the change in flow patterns with varying geopressures.

Figure 4.3a differs from the reference scenario of Figure 4.2 in that the excess pressure within the shales has

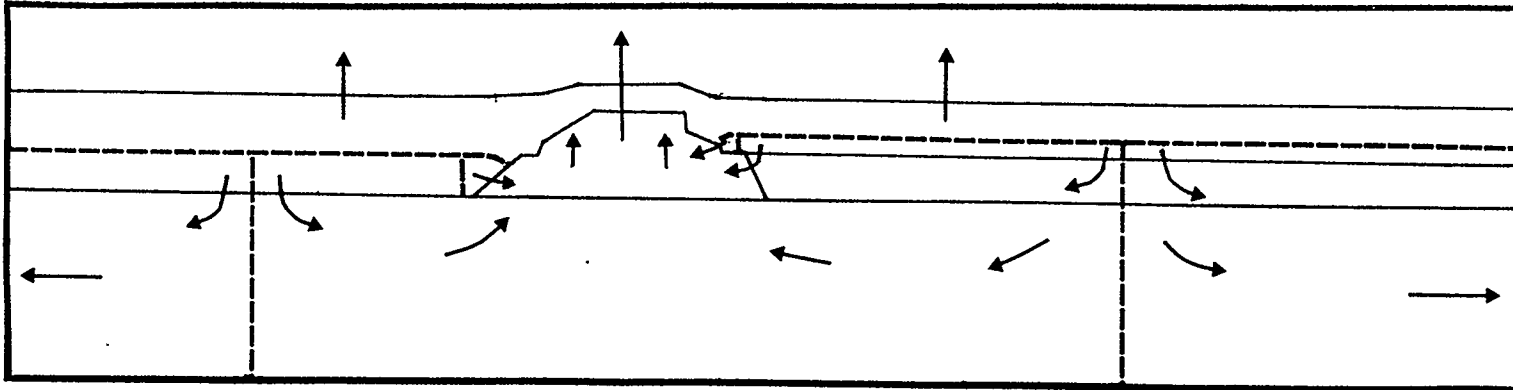


Figure 4.3a Effect on fluid flow resulting from a decrease in geopressures within the shales.

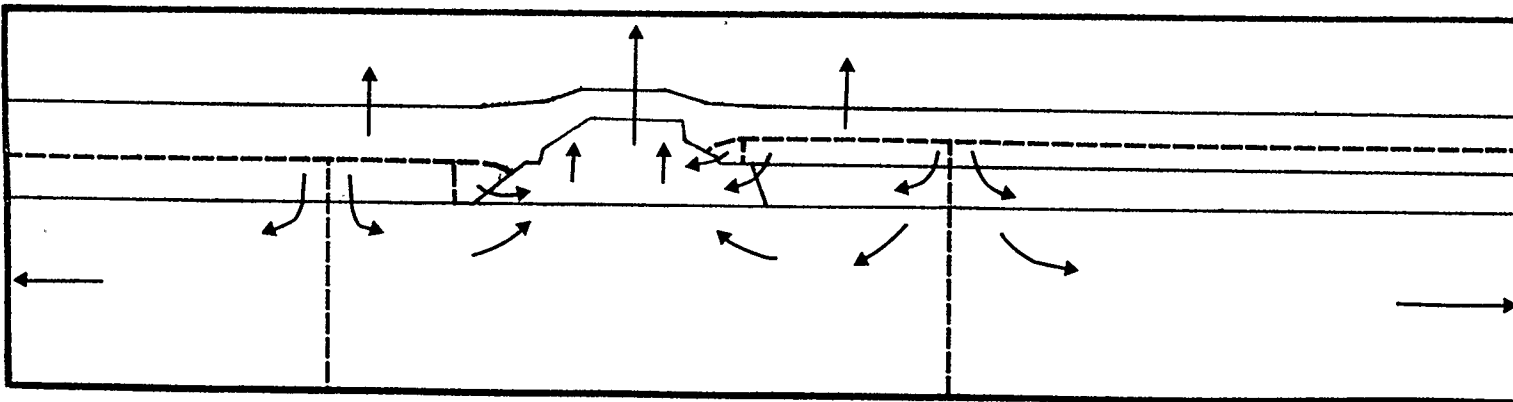


Figure 4.3b Effect on fluid flow resulting from an increase in geopressures within shales.

been reduced (80 m excess head east of the reef, and 150 m excess head west of the reef). Results indicated that the reef now has a larger influence upon flow than in the reference scenario. Fluid flow from a maximum distance of 5750 m west of the reef is channeled through the reef. Flow from a distance of 10,400 m east of the reef is also channelled through the reef. Direct flow from the shales into the reef is perhaps increased only slightly, occurring only about 150 m laterally further up the flank of the reef.

Increasing the geopressures within the shales (240 m excess head west of the reef, 160 m excess head east of the reef) results in a lowering of the area of influence of the reef upon fluid flow (Figure 4.3b) compared to the reference model. One hydraulic divide, which separates water eventually moving through the reef with water moving out towards the boundary, is found 3840 m west of the reef. The other hydraulic divide is found 6200 m east of the reef, which is a decrease of 480 m and 50 m, respectively, compared to the reference scenario. Flow directly into the reef is very similar to flow observed for a lowering of the geopressures (Figure 4.3a)

While it may at first seem anomalous that a raising of the geopressures within the shales results in a lowering of the fluid flow radius of influence of the reef, a probable explanation is that the extra energy in the system introduced from an increase in the amount of geopressuring

is more easily dissipated by having fluid flow bypass the reef and drain out the flanks of the model. The models indicate that the head within the reef itself is increased by about 20 m for every 40 m increase in head within the shale. Since the head within the reef increases and the head along the flank remains constant, fluid is more likely to drain through the flanks than through the reefs.

It is possible that 40 m of excess head is not a proper estimate for the overpressuring within the basal unit along the margins of the model. Therefore two different models are presented in Figure 4.4a and Figure 4.4b which illustrate the effect on fluid flow of no excess head in the basal units at the margins of the model and 80 m of excess head at the margin. As expected, lowering the excess head along the boundary provides a greater impetus for fluid to drain through the boundary, whereas raising the head along the boundary has the opposite effect. Figure 4.4a, which illustrates flow for no excess pressure along the boundary, reveals that the western hydraulic divide lies 3200 m west of the reef margin and the eastern hydraulic divide is 4960 m east of the eastern reef margin, a decrease of 1120 and 1290 m, respectively. In Figure 4.4b, where the boundary is overpressured (by 40 m greater than the reference scenario), the western hydraulic divide is 5760 m west of the western reef margin, and the eastern divide is now 12,320 m east of the eastern reef margin (an

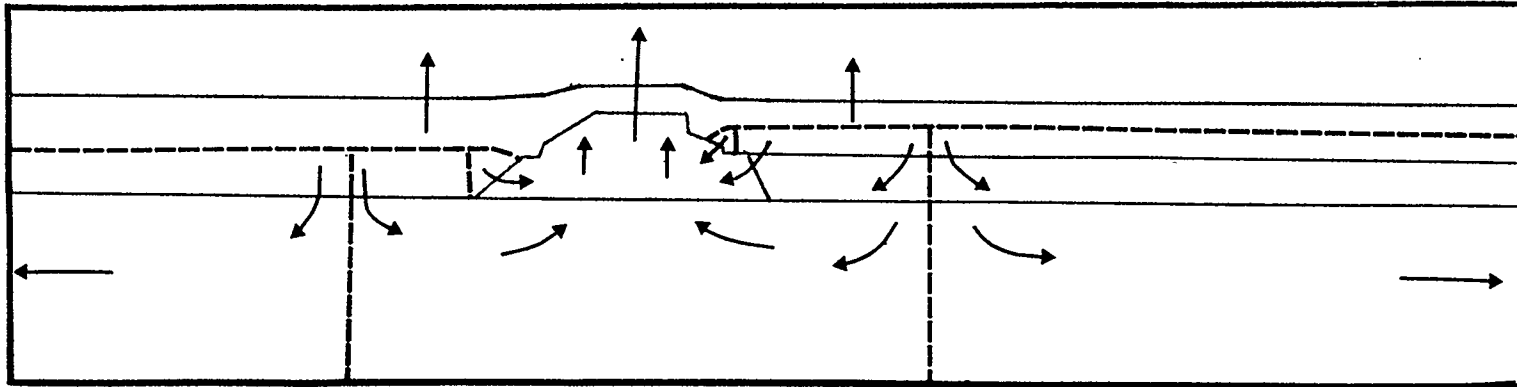


Figure 4.4a Flow pattern with hydrostatic head along basal unit margins.

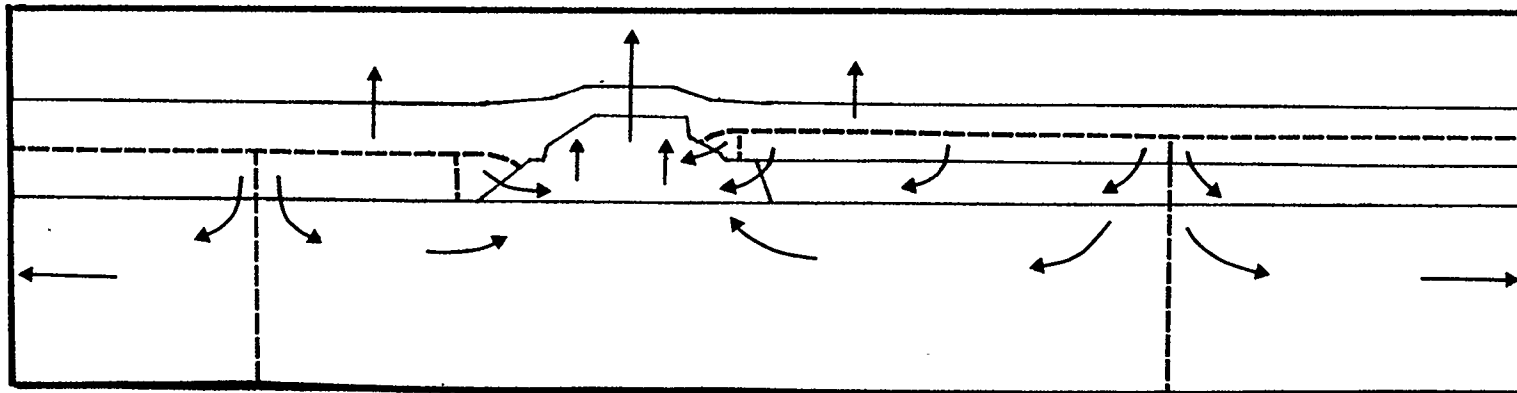


Figure 4.4b Flow pattern with extreme geopressure along basal unit margins.

increase over the reference scenario of 1440 m and 6080 m, respectively).

Although the influence of the head at the boundaries may appear to have a significant effect on the fluid flow patterns, the two scenarios presented here represent "end-member" scenarios. Almost certainly the basal unit is overpressured to some extent, however, the model in Figure 4.4a is based on no overpressuring of the basal unit. Probably realistic values for the head at the boundaries, such as is presented in the reference scenario, would reveal only a moderate to slight change in the position of the hydraulic divide with varying boundary conditions.

The previous four scenarios are presented with singular effects (head values) varied individually. In reality an increase in the head within the shales would likely result in an increase in head within the basal units. The decrease in radius of reef influence due to the shale head increase would be compensated for by an increase in the radius of influence due to the head increase within the basal units. The net effect of a change in the geopressures within the shale package would be to show little change of radius of influence compared to the reference model.

The scenarios with varying geopressure values did not alter the flow directly from the shales into the reef compared to the standard model. The degree of anisotropy within the shales may exert a more significant influence

upon this flow. A high degree of anisotropy, with a horizontal to vertical permeability ratio of 100:1, would allow for easier lateral movement of fluid from the shales to the reef while discouraging flow vertically from the shales to the basal units. This effect is shown in Figure 4.5a where flow directly into the reef is increased by an increase in the horizontal to vertical permeability ratio of ten times the reference model (100:1 versus the previous 10:1). A change in the anisotropic ratio to isotropic conditions, shown in Figure 4.5b, results in a decrease in the amount of fluid flowing directly from the shales to the reef. Isotropic shale permeabilities do not lead to a change in the position of either hydraulic divide west or east of the reef compared to the standard model. An increase in the permeability anisotropic ratio to 100:1 leads to a slight decrease in the radius of influence of the reef upon fluid flow. The hydraulic divide occurs 320 m closer to the reef on the western side than the reference scenario, and 640 m closer to the eastern side than the reference scenario.

The reef, which serves as the conduit across the shale sequence, functions as such because of its higher permeability. Altering this permeability results in a change in the influence of the reef on the flow patterns. Figure 4.6a shows the result of an increase in the reef permeability by one order of magnitude. The result of this

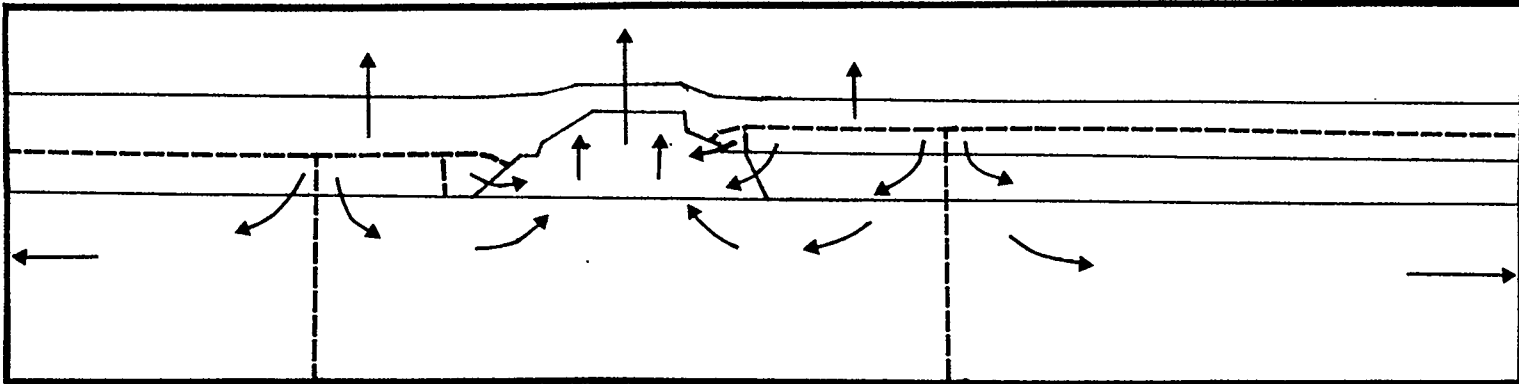


Figure 4.5a Effect on flow patterns due to increase in shale anisotropy to 100:1.

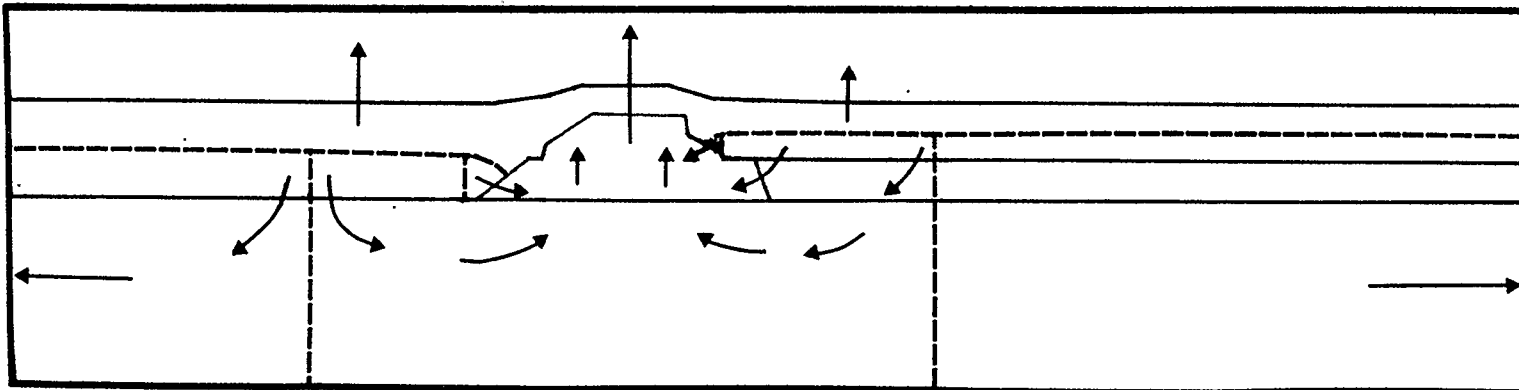


Figure 4.5b Flow patterns with isotropic shale permeabilities.

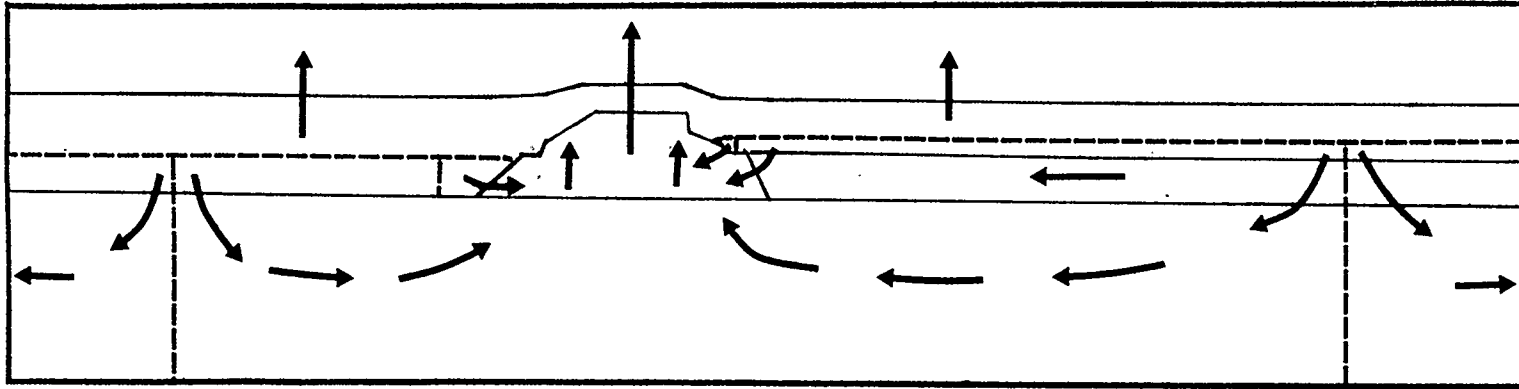


Figure 4.6a Fluid flow pattern established due to ten times increase in reef permeability.

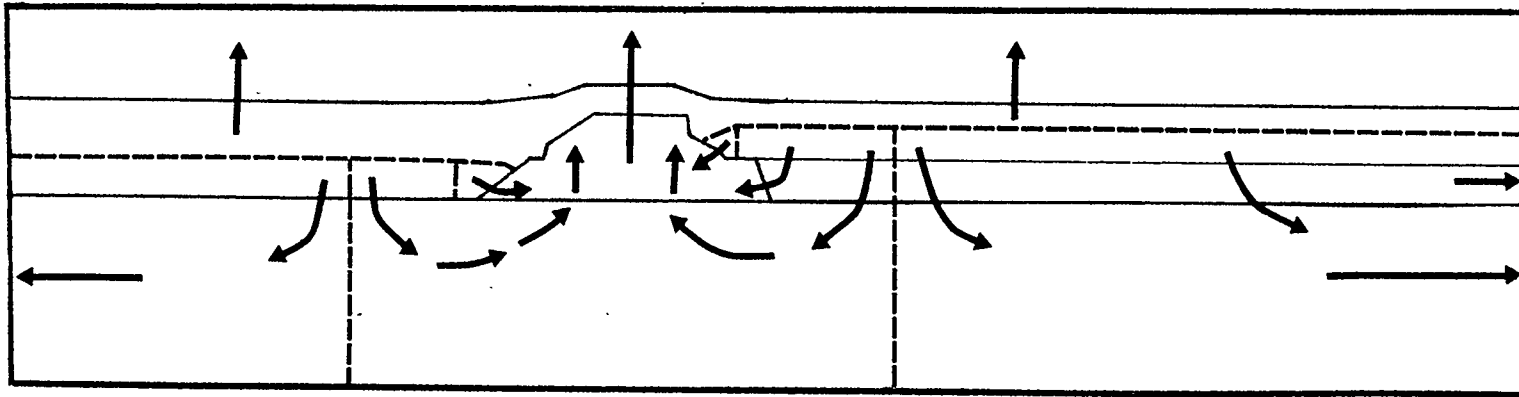


Figure 4.6b Fluid flow pattern established due to ten times increase in permeability of the Cooking Lake and basal formations.

change in reef permeabilites is that the effect of the reef on channelling flow is considerably enhanced. The western hydraulic divide is found 8000 m west of the western reef margin (an increase of 3680 m over the reference section) and the eastern divide has shifted to 16,000 m east of the eastern reef edge (an increase of 9760 m over the reference section). As well, direct fluid flow from the shales into the reef has increased, from 800 m up the western flank of the reef to 1300 m. Along the eastern flank of the reef, this flow into the reef shifts from 160 m up the flank of the reef in the standard section to over 500 m in the reef with the increased permeability.

The very low excess head found within the reef in this scenario (3 m above hydrostatic) indicates that an additional increase in reef permeability would not serve to increase the radius of influence of the reef upon fluid flow. Since some energy would be needed to drive the fluid within the reef across the overlying Ireton shales, the reef has to maintain some amount of excess head, presumably at least a few metres, greater than hydrostatic.

Flow along the basal unit results in a measureable head loss. In order to measure the effect of the head loss a final scenario is presented in Figure 4.6b differing from the reference scenario by a ten fold increase in the permeability along the basal units. Flow directly from the shales into the reef is unaffected compared to the standard

model. Owing to the greater ease for fluid to migrate laterally out of the edges of the section than through the reef with the higher permeability within the basal units, a decrease in the radius of influence of the reef upon fluid flow is noted for this model compared to the reference model. The hydraulic divide on the west side occurs 3200 m west of the western reef margin (a decrease of 1120 m over the standard section) and the eastern hydraulic divide occurs 3840 m east of the eastern reef margin (a decrease of 2400 m over the standard section).

In summary, the scenarios illustrate that there is an asymmetry to the flow pattern due to the presence of the Cooking Lake platform and thinner shales east of the Leduc reef compared to the thicker shales west of the Leduc reef. Most of the flow through the reef is not directly from the shales into the reef, but rather vertically downwards from the shales into the underlying units, laterally along these units to the reef, and then up through the reef to units which maintain open hydrologic communication with the sea. The reef influences fluid flow from a minimum of 3200 m west of the reef and 3840 m east of it, to a maximum of 8000 m west of the reef and 16000 m east of it.

Table 4.2 summarizes the results of these scenarios and shows the extent of the influence of the reef given the particular conditions of the scenario. Factors which influence the flow pathways to the largest extent are the

Scenario	West Divide (m)	Change (m)	East Divide (m)	Change (m)
Reference	4320	--	6240	--
Change in head in lower units				
Decrease by 40m	3200	-1120	4960	-1280
Increase by 40m	5760	+1440	12320	+6080
Change in head within shales				
Decrease by 40m	5760	+1440	10400	+4160
Increase by 40m	3840	- 480	6160	- 80
Change in permeabilities				
Increase reef 10x	7840	+3520	16000	+9760
Increase basal units 10x	3200	-1120	3840	-2400
Change in shale anisotropy				
Isotropic shales	4000	- 320	5440	- 800
$K_H/K_V = 100:1$	4000	- 320	5600	- 640

Table 4.2 Summary of results of compaction scenarios.

reef permeability and the hydraulic head found within the basal units.

The hydraulic divide in flow paths between water flowing into the reef from the Cooking Lake platform versus water flowing away from the reef in the Cooking Lake corresponds roughly to the edge of the Cooking Lake dolomites. Kastner (1984) argued that, through microbial action, organic rich shales remove much of the sulfate ion found within seawater and that these sulfate-free waters are the primary fluid by which limestones are dolomitized. The organic rich Duvernay shales would have expelled fluids into the Cooking Lake and Leduc formations that would have had a chemical composition conducive to the process of dolomitization. The position of the hydraulic divide within the Cooking Lake Formation and the increase in Duvernay thickness and organic content towards the Rimbey-Meadowbrook trend (Stoakes 1980) strongly suggest that the fluids derived from compaction of the Ireton and Duvernay shales could have had an important influence on the dolomitization of the underlying Cooking Lake Formation and the Leduc reefs. This scenario would also suggest that dolomitization took place early in the burial history of the reef trend and carbonate platform.

## Chapter 5 Flow Due to Local Topography

Groundwater studies have shown that the subsurface fluid flow in aerially exposed regions is chiefly driven by variations in the topographic relief. Since the water table is a subdued replica of the surface topography, large variations in topography will result in a large potential difference between water at the highest and lowest elevations in an area. As a result there will be enough energy to drive a significant amount of fluid through the underlying strata. Within the study area, the North Saskatchewan River represents a major drainage system. Due to the variation in topography associated with this drainage system, significant flow may occur in the subsurface that is directly attributable to the presence of the North Saskatchewan River. The purpose of this chapter is to investigate to what extent: 1) fluid flow around the Leduc reefs is influenced by the local topography associated with the North Saskatchewan River; and, 2) to what extent the presence of the reefs themselves influence the groundwater flow pattern established by the North Saskatchewan River.

The North Saskatchewan River originates in the Rocky Mountains west of the study area and generally flows from west to east across Alberta. After crossing the Rimbey-Meadowbrook trend, the river makes a sharp turn to a

northeasterly flow direction, briefly flowing parallel with the Rimbey-Meadowbrook trend in the vicinity of the Acheson reef (Figure 5.1). In order to investigate the fluid flow associated with the presence of the river in this area, a finite element simulation was undertaken along a fifteen kilometer transect perpendicular to the North Saskatchewan River and the Rimbey-Meadowbrook trend through the Acheson Leduc reef.

In order to make a geologic cross section along which a finite element simulation could be made, the topography of the area, the geology, and the permeabilities of the rock units were examined in great detail. The surface topography was taken from a 1:50,000 base map with 25 foot contour intervals. The topography along the transect can be described as having a moderate easterly dipping slope on the western side of the section, flattening out to near level in the middle of the section, and steepening in the last kilometer near the river, forming a 60 m deep river valley.

The geology for the model was constructed from structure contour maps that were made for the study area. Five different intervals were chosen in order to show both thickness and structure (drape and regional tilting) of various formations. Data used in constructing the maps were taken from IPL petrofiche data. Thickness of formations between the intervals chosen for structural

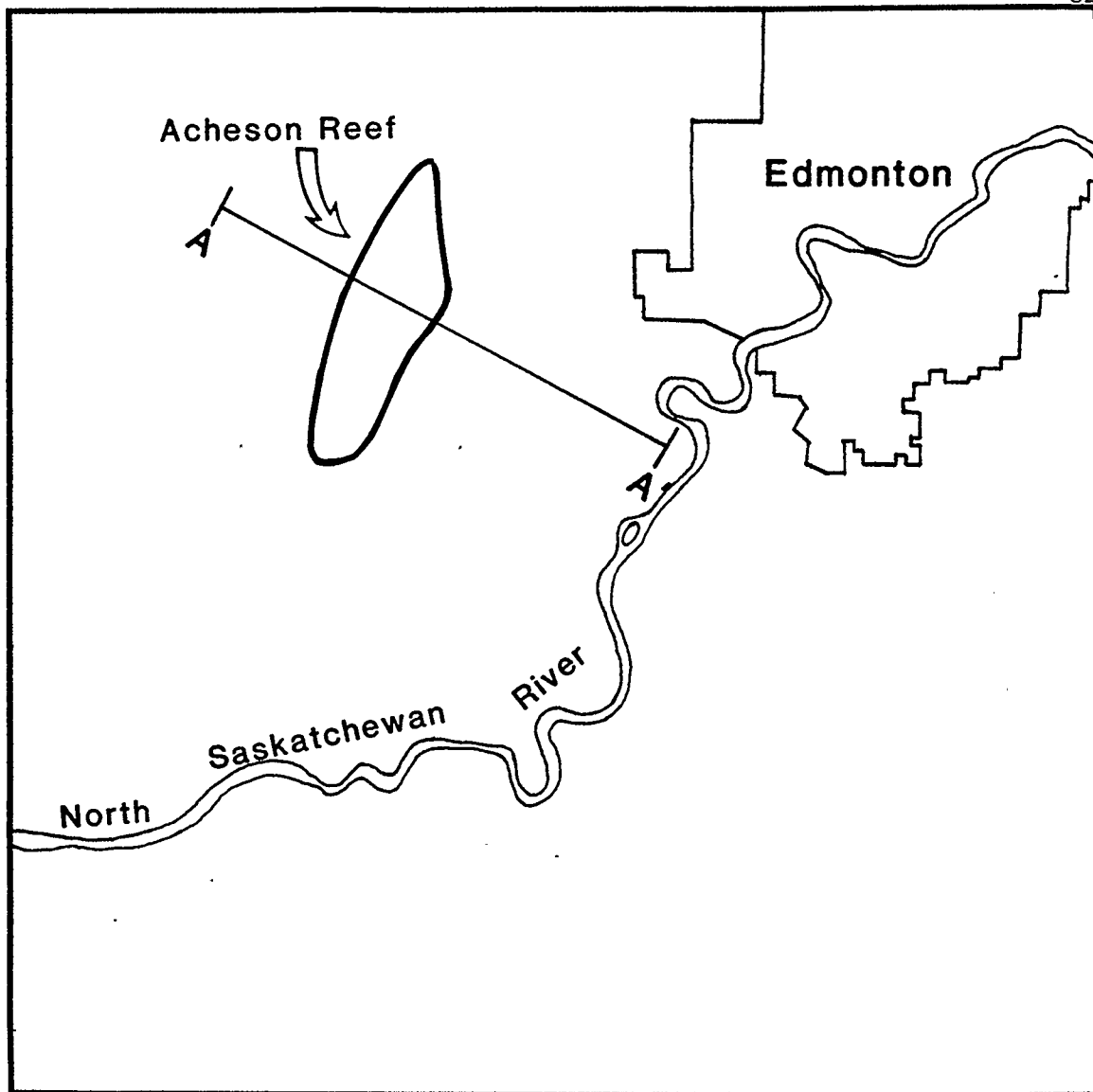


Figure 5.1 Location map for finite element cross-section

contouring were also taken from IPL petrofiche, with the exception of the Wapiti, Tertiary, and Quarternary units which are from Ceroici (1979). Variations in the Tertiary isopach due to the preglacial Stony Valley were also included within the cross section.

Permeabilities of the various units represent the least well known factor in the construction of the model. Permeabilities for the Quarternary, Tertiary, and Wapiti sequences were taken from Ceroici (1979) who studied the hydrogeology of the near surface units in the study area, and from Gabert (1975) who studied the near surface hydrogeology immediately south of the study area. The permeabilities of the Colorado and Mannville hydrostratigraphic units were based on values derived from drill stem tests. The tests were usually only conducted on the more permeable units such as the Viking or Ellerslie formations, so the results were scaled downwards accordingly. No permeability values are available for the Calmar, Graminia and Lower Wabamun formations. Various units within these formations serve as seals for the Nisku oil reservoirs, so they were assigned a low permeability. The Nisku Formation, like the Leduc reefs, represents a high permeability formation. Values for the Acheson reef were taken from Hnatiuk and Martinelli (1967) and a similar value was assigned to the Nisku Formation. No data is available for the Ireton/Duvernay/Majeau Lake shales. Toth

(1978) used a value of  $1 \times 10^{-11}$  cm/sec for the Ireton Formation in the Red Earth region of Alberta. This value was thought to be too low by K. Weyer (pers. comm.) so the permeabilities were increased by one order of magnitude within the study area. Along the margins of the Rimbey-Meadowbrook reef trend, the underlying Cooking Lake Formation has been dolomitized. This dolomitization has served to increase the permeability of the Cooking Lake carbonates such that they serve as a high permeability aquifer. No data are available for the Beaverhill Lake, Elk Point and the Cambrian formations which were grouped together as a single hydrostratigraphic unit. In eastern Alberta the Elk Point evaporites are thought to be totally impermeable (S. Bachu and C. Sauveplane, pers. comm.). From eastern Alberta to the study area, the Elk Point Formation grades from a dolomitic anhydrite to an anhydritic dolomite (Geological History of Western Canada, McCrossan and Glaister, editors, 1964). The Elk Point dolomite, along with the shales and carbonates of the Beaverhill Lake Formation, and the clastics and carbonates of the Cambrian formations, were assigned a moderate permeability. The impermeable base of the section may be within the Elk Point evaporites rather than at the base of the Cambrian succession. It is felt that the choice of the base level should not seriously affect the overall conclusions with respect to the fluid flow in the overlying units. These

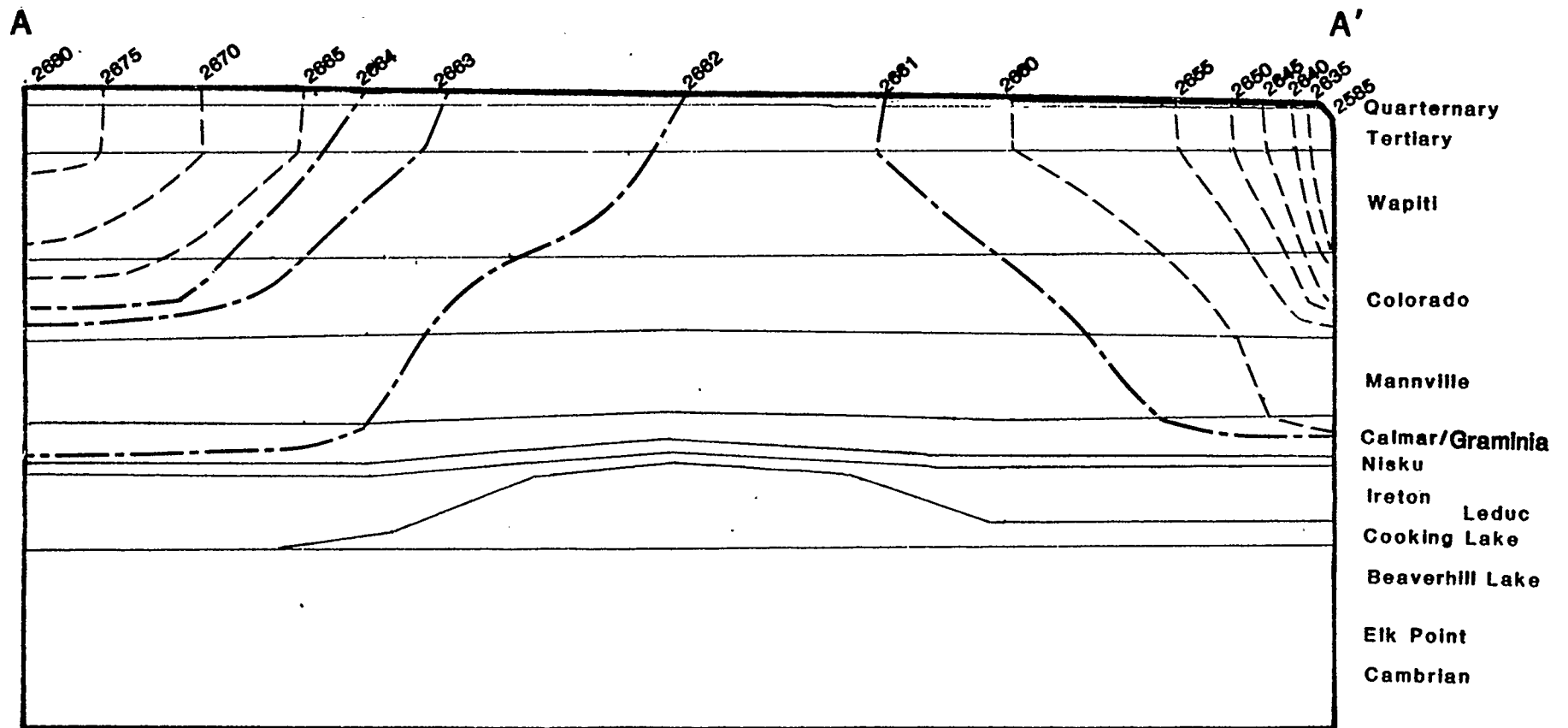
permeability estimates are summarized in Table 5.1. Only order of magnitude estimates are possible for many of the units, nevertheless it is felt that with these estimates a reasonable approximation of the fluid flow in the area can be made.

For the finite element simulation, all the permeabilities were divided by the lowest permeability (the Ireton, Duvernay and Majeau Lake hydrostratigraphic unit) in order to normalize all the permeabilities relative to each other. From these permeability values, the geology and the topography, a finite element model was constructed consisting of 676 nodes and over 1450 elements in which the effects of a high permeability lens (the Acheson reef) on the fluid flow due to local topography could be examined. The base of this section was chosen to be the base of the Cambrian strata. This base represents an impermeable boundary, although it is possible that the crystalline basement below the Cambrian sediments is fractured and may show some permeability. Within the model, the two lateral boundaries are impermeable. In reality, the eastern boundary located at the North Saskatchewan River, and the western boundary, located at a drainage divide, represent hydraulic divides, across which no flow occurs. These boundaries can be treated as impermeable within the confines of the model.

Figure 5.2 shows a reconstruction of this model with

Hydrostratigraphic unit	Hydraulic Conductivity (m/s)
Quaternary	$2 \times 10^{-7}$
Tertiary	$5 \times 10^{-8}$
Wapiti	$5 \times 10^{-11}$
Colorado	$1 \times 10^{-10}$
Mannville	$5 \times 10^{-9}$
Wabamun/Calmar/ Graminia	$2 \times 10^{-10}$
Nisku	$8 \times 10^{-7}$
Leduc	$5.2 \times 10^{-7}$
Ireton/Duvernay/ Majeau Lake	$1 \times 10^{-12}$
Cooking Lake	$5 \times 10^{-8}$
Beaverhill Lake/ Elk Point/Cambrian	$2 \times 10^{-8}$

Table 5.1 Hydraulic conductivity values used in finite element simulation.



Datum: Base of Cambrian

Vertical Exaggeration - 3X

Contour Interval

- 5 meter spacing
- 1 meter spacing

Figure 5.2 Finite Element Model through Acheson Reef illustrating fluid flow due to local topography

three times vertical exaggeration. The contour lines shown represent lines of equal hydraulic head and are spaced at five meter intervals. In the center of the section the lines are spaced at one meter intervals to show greater detail. The hydraulic head lines are discontinued from 2630 m to 2585 m, near the valley of the North Saskatchewan River, where the high slope would have caused an extreme crowding of the contour lines. The contour lines intersect the topographic surface where the value for the hydraulic head equals the elevation of the topographic surface above the Pre-Cambrian datum level. The contour lines terminate perpendicular to the vertical edges and the base of the cross section, such that flow lines are not allowed to cross these boundaries, which is in compliance with the initial assumptions of the model.

The cross section illustrates a typical flow regime: the western side of the section shows recharge into the groundwater flow system, and the eastern side shows groundwater discharge into the North Saskatchewan River. Neither the recharge nor the discharge sub-systems can be seen to penetrate below the Graminia Formation; hydrostatic conditions prevail at depth. The reason for this is twofold: 1) the topography is not sufficiently variable to impart sufficient energy into the system for the flow to penetrate to deep depths; and, 2) the head loss across the Wapiti, Colorado and lower Wabamun formations prevents a

significant energy transfer to underlying formations. The model studies, therefore, indicate that the groundwater flow regime associated with the North Saskatchewan River does not extend to the deeper horizons of the Leduc reefs.

The Acheson reef does appear to affect the hydraulic head contours in that the contours diverge away from the reef in both the recharge and the discharge side of the basin. The presence of the reef, however, is not thought to significantly affect the flow pattern. The concentration of flow lines at either end of the section is typical for most flow regimes. In order to illustrate this point, a second model is presented in which the Acheson reef has been replaced by a continuous section of Ireton shales (Figure 5.3). Comparison of Figures 5.2 and 5.3 reveals that the majority of the contour lines are not significantly affected by the removal of the reef, rather, only the finer detail of the 2660 - 2664 m lines have been affected. Freeze and Witherspoon (1967) have modelled the effect of the introduction of a high permeability lens into a flow system. With the introduction of such a lens, the hydraulic head lines wrap around the edges of the lens and diverge away from the center of the lens, concentrating flow through the lens. This divergence effect extends to the shallower horizons, and an analogy can be drawn between the studies of Freeze and Witherspoon (1967) and the effect observed here. It should be noted that the observed effect

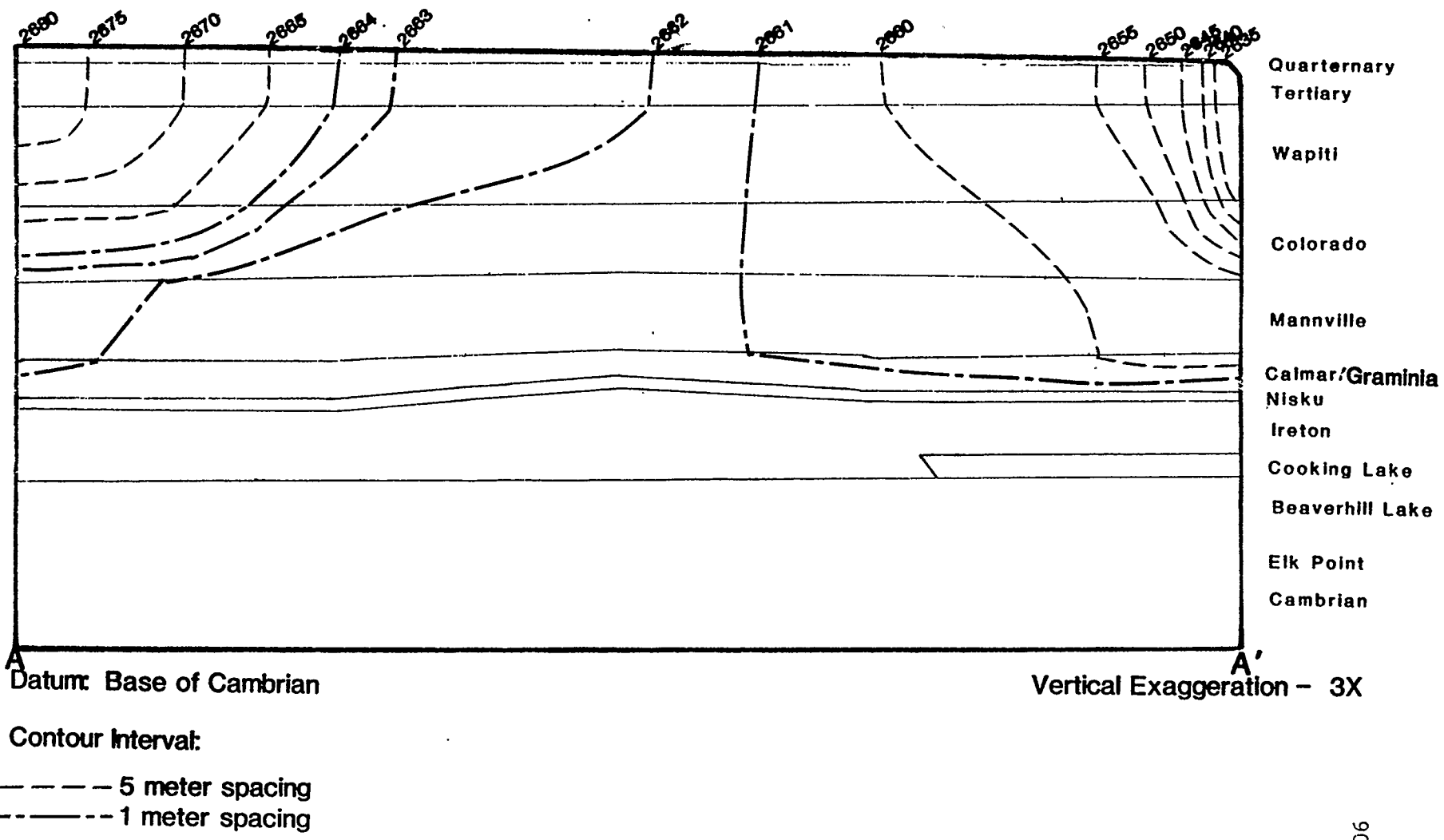


Figure 5.3 Finite Element Model illustrating effect on flow due to removal of the Acheson Reef

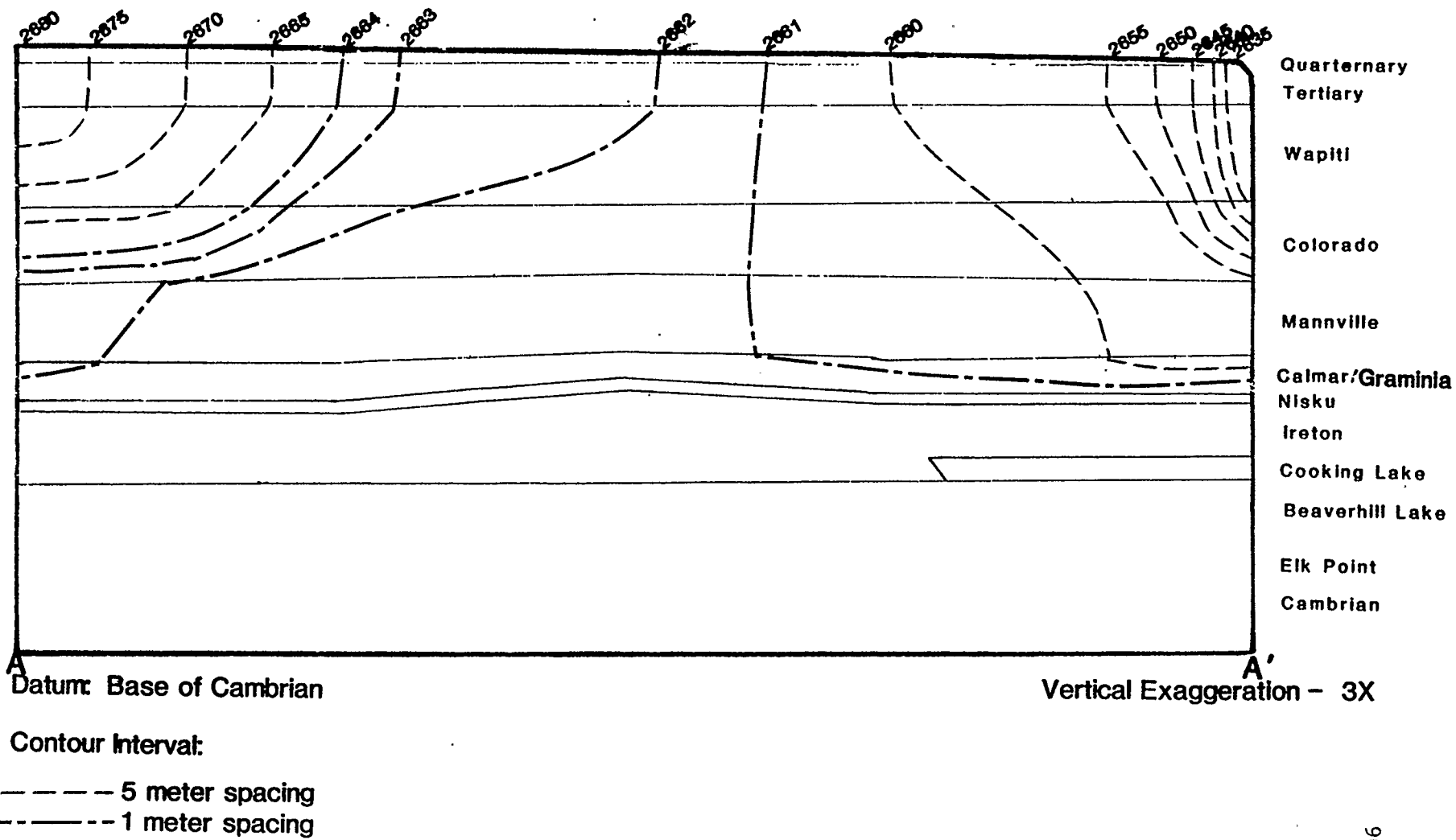


Figure 5.3 Finite Element Model illustrating effect on flow due to removal of the Acheson Reef

over the Acheson reef is minor, altering the head distribution over a relatively small range of four meters. It is quite likely that a change in any one of the permeabilities of the units would significantly affect the positioning of these contours.

In summary, it has been shown that fluid flow due to the local topography associated with the drainage system of the North Saskatchewan River does not penetrate to the Devonian horizons and thus the local drainage does not affect fluid flow around the reefs. Conversely, it has been shown that the presence of the Leduc reefs does not significantly affect the groundwater flow pattern established due to the local topographic conditions. This does not mean that at the present time there is no fluid flow around the Leduc reefs, nor does it mean that the Leduc reefs do not influence the regional hydrodynamic pattern. It simply suggests that there are other mechanisms for fluid flow that are more significant than the effects of the local topography.

## Chapter 6 Potentiometric Maps

### 6.1 Development of Potentiometric maps

In order to determine the current fluid movement, it is not necessary to resort to mathematical models. A direct measurement of the fluid potential will show the hydraulic head distribution and thereby reveal the system of fluid pathways in the subsurface as it currently exists. The advantage of this procedure is that it is no longer a modelling process but, rather, a direct examination of groundwater flow systems within the study area. The most commonly used method for illustrating this potential distribution within a specified area is the potentiometric map.

Potentiometric maps are contour maps of the hydraulic head distribution within a specified geologic or elevation interval. They show the fluid energy distribution within an interval and, from them, the direction of fluid movement can be inferred. In shallow intervals they can be made from piezometer tests and surface phenomena (springs, seeps, etc). In deeper intervals the head distribution is found using pressure readings from drill stem tests.

Drill stem tests are performed on geologic zones as part of the normal procedure for hydrocarbon evaluation. Briefly, the procedure involves sealing off a zone and allowing fluid from the formation to enter the drill

string. After a short period of flow, the zone is shut in, and the pressure within the drill stem is allowed to begin to return to the fluid pressure originally found in the formation. The pressure is continuously recorded as a function of time while the fluid is flowing and as the zone is shut in. Because it would be impractical to shut in the zone for the extended period of time required for the pressure in the drill string to return to the original formation pressure, Horner (1951) devised a method where the shut-in time is extrapolated to infinity and the original formation pressure can be found. This is the basis for the Horner Plots, which are commonly used in formation evaluation. As well as formation pressure, drill stem tests can be used to evaluate permeability, well bore damage (skin effect), and reservoir geometry (Dake 1978).

Drill stem test data for wells in the study area drilled since 1962 were taken from file listings at the Energy Resources Conservation Board. For earlier listings (1954 - 1962), data were obtained from IPL petrofiche reports. The listings from the ERCB consist of the actual formation evaluation sheets reported by the various service companies and, as such, are quite variable in quality. Frequently, the Horner Plots were performed by the service companies, however, often only the raw data were presented, and the Horner Method was applied to the pressure readings. Occasionally, only the initial and final shut-in pressures

were recorded.

Strict quality control was ensured by using only extrapolated pressure values derived from Horner Plots or, where data were not available to perform a Horner Plot, pressure readings were used only when the final pressure readings on the initial and second shut-in were in close agreement. Dahlberg (1983) suggested that the final shut-in pressure is reasonably close to the formation pressure in almost all cases, nonetheless, several cases were observed on the Horner Plots where the final shut-in pressures were 100 - 200 psi less than the extrapolated values. Thus, it was felt that it was improper to indiscriminately choose every recorded drill stem test as this might lead to erroneous interpretations.

The hydraulic head can be calculated from the pressure values from the drill stem test by the formula:

$$h = z + P/\rho g \quad (1)$$

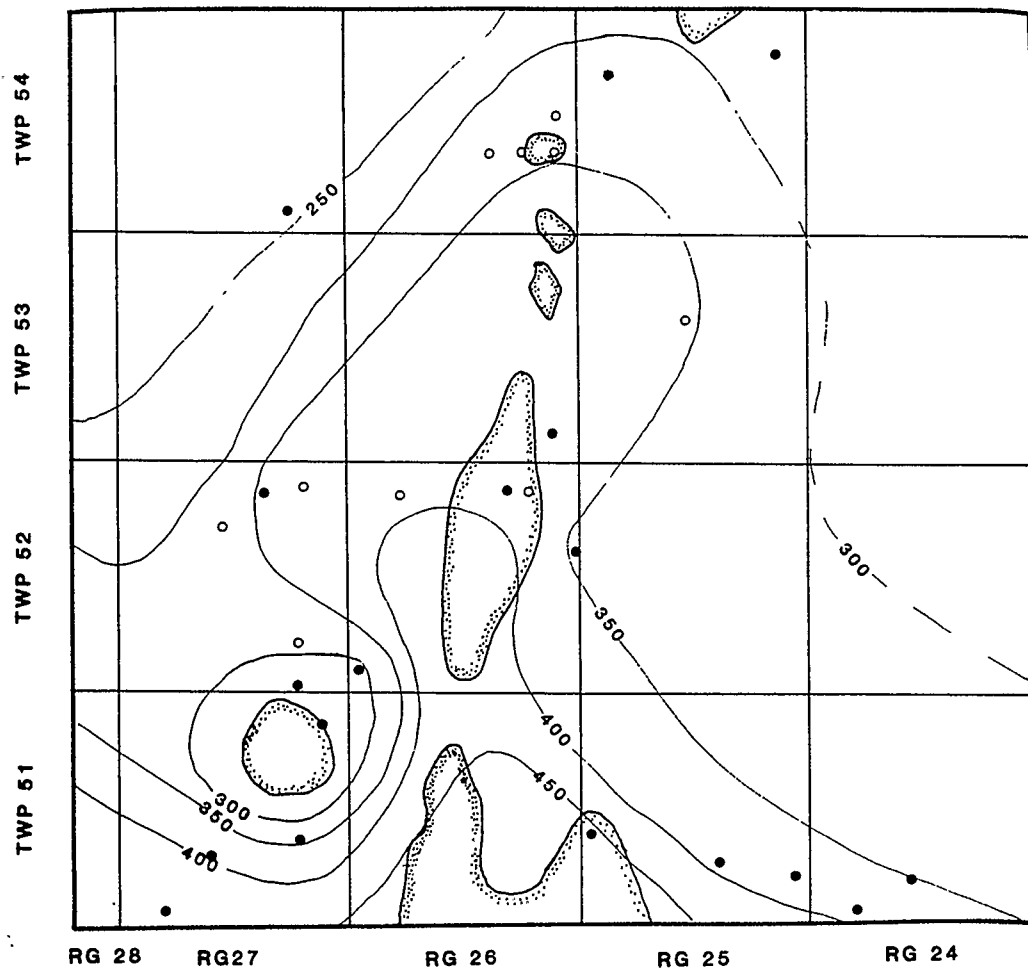
where  $z$  is the vertical distance from a chosen horizontal datum,  $P$  is the formation pressure,  $\rho$  is the average fluid density, and  $g$  is the gravitational constant. Fluid densities were found by using brine concentrations based on water resistivities. These resistivity values were taken from tables prepared by the Canadian Well Logging Society (CWLS) (1978). Resistivity values were examined over the

study area, averaged, and then converted into NaCl concentrations. Fluid densities were then calculated from the brine concentration and corrected for reservoir pressure and temperature. These values are presented in Table 6.1. Since the CWLS attempted to ensure accurate values for the formation water resistivities, the fluid densities are believed to be fairly accurate. Sea level was chosen as the horizontal datum. Based on the pressure, average fluid densities and elevation measurements, hydraulic head was calculated for various intervals.

Three intervals were chosen for potentiometric maps. Figures 6.1, 6.2, and 6.3 show potentiometric maps for the Ellerslie (Lower Mannville), Wabamun (D1) and Nisku (D2) formations, respectively. These formations were chosen for two principal reasons: 1) the chosen formations show well developed homogenous permeabilities, and thus anomalies should not be the result of permeability variations. Tests within the Viking Formation were sufficiently numerous to construct a potentiometric map, however, this formation is characterized by complex lithologies resulting in varying permeabilities within the study area (M. Dean, pers. comm.). Because of this complex lithology, the effects of the reef are masked by the effects of the permeability variations; and, 2) lack of data precluded construction of potentiometric maps for many other intervals, especially for those formations below the Nisku Formation.

Formation	Average Depth (meters)	Resistivity (ohm-meters at 25°C)	NaCl conc. ( ppm )	Brine Density (gm/cc)
Paskapoo	80	9.2	500	0.999
Edmonton	150	5.0	1000	0.999
Wapiti Belly River	500	0.56	9500	0.999
Colorado upper	2300	0.677	80000	1.006
lower	2600	0.140	48000	1.020
Mannville upper	3450	0.080	85000	1.048
middle	3600	0.110	65000	1.028
lower	3950	0.088	78000	1.046
Wabamun	4400	0.077	95000	1.050
Calmar/ Graminia	4480	0.070	100000	1.054
Nisku	4750	0.063	122000	1.070
Ireton/ Duvernay	5250	0.056	150000	1.100
Leduc	5400	0.055	152000	1.101
Cooking Lake	5820	0.056	150000	1.095
Beaverhill Lake	6400	0.047	175000	1.114
Elk Point	7250	0.042	200000	1.124
Cambrian	8050	0.042	200000	1.122

Table 6.1 Formation resistivities and brine concentration.



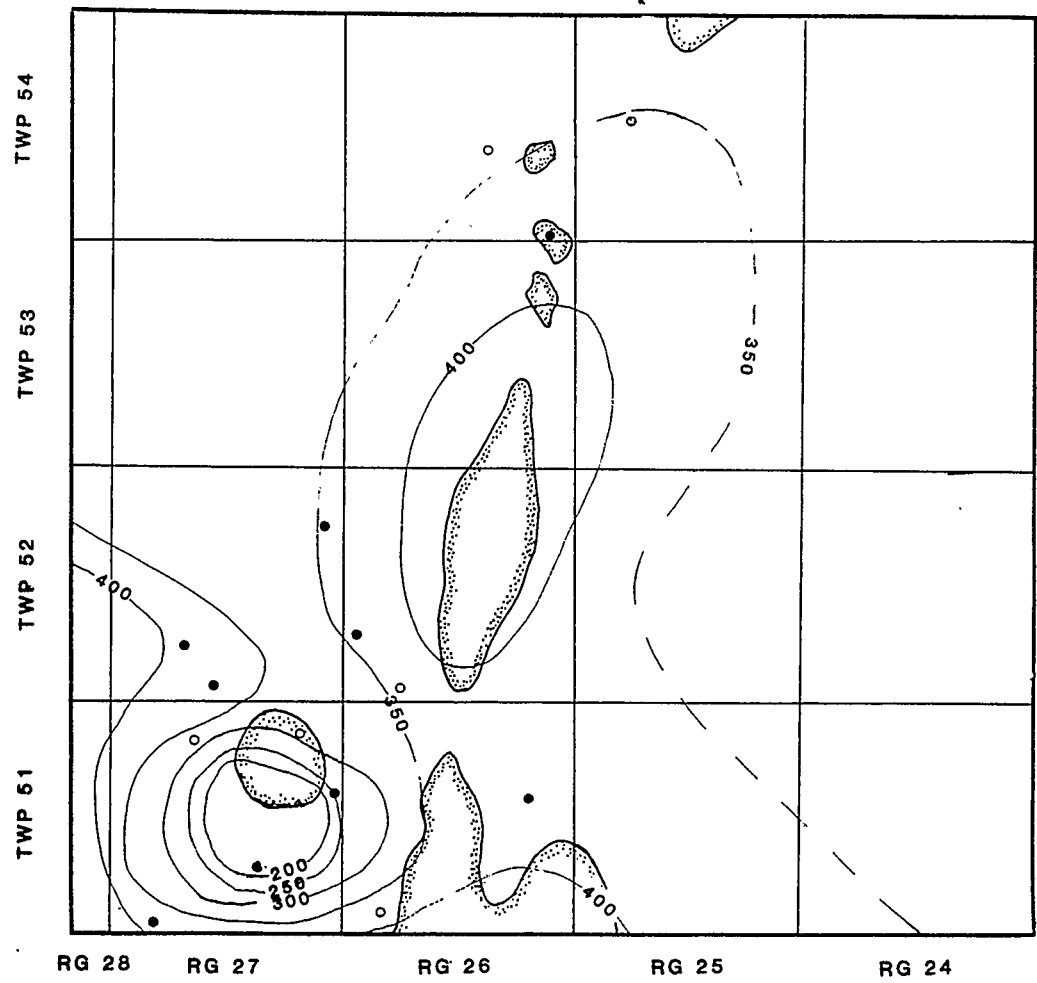
Datum: Sea level

Contour interval: 50 meters

Wellsite locations:

- Pressures derived from Horner Plots
- Pressures derived from final shut in pressures

Figure 6.1 Hydraulic head distribution within the Ellerslie Formation



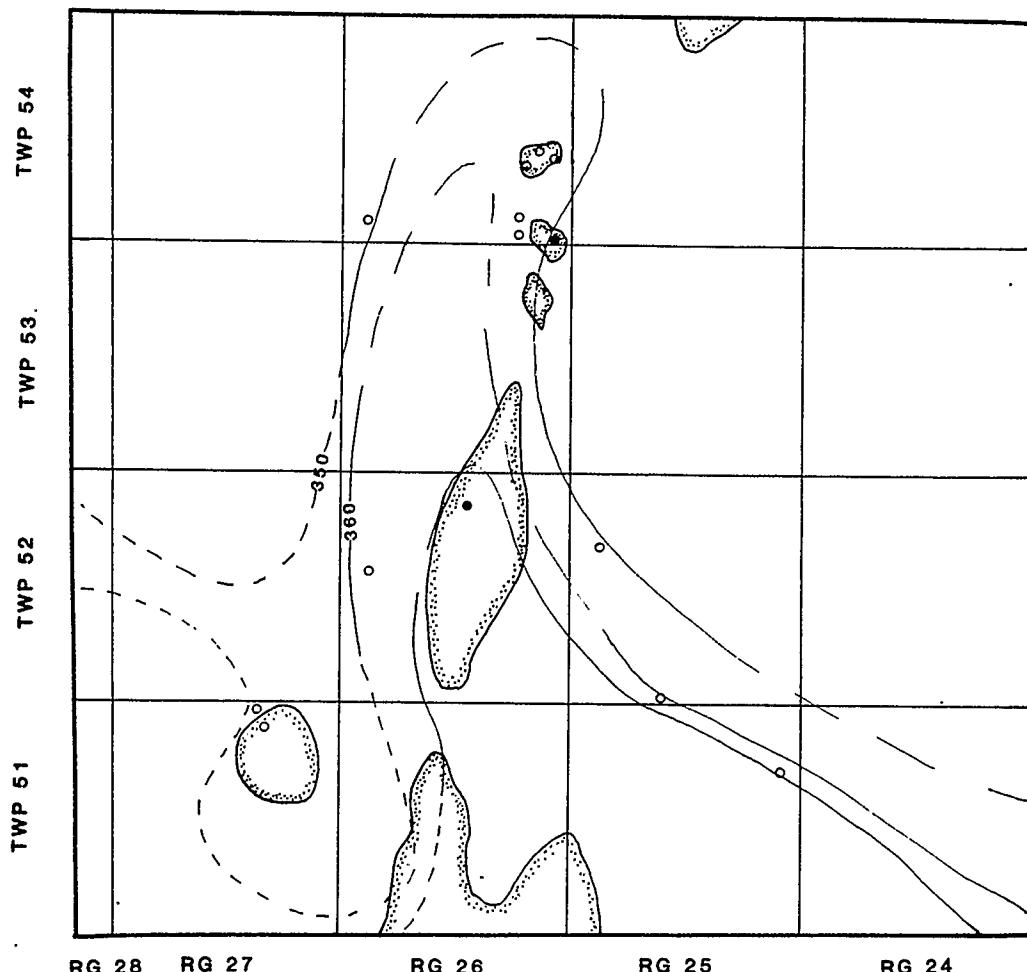
Datum: Sea level

Contour interval: 50 meters

**Well site locations:**

- Pressures derived from Horner Plots
- Pressures derived from final shut in pressures

Figure 6.2 Hydraulic head distribution within the Wabamun Formation



Datum: Sea level

Contour interval 10 meters

Wellsite locations:

- Pressures derived from Horner Plots
- Pressures derived from final shut in pressures

**Figure 6.3** Hydraulic head distribution within the Nisku Formation

Hitchon (1969a) pointed out that in addition to examining the potentiometric data over some geologic interval, information can be derived from potentiometric maps constructed over constant elevation intervals. Because the study area is relatively small, and the dip on the formations is low, measurements within a formation are all at approximately the same elevation and the potentiometric maps can be considered as both formation head maps and horizontal slice maps.

## 6.2 Interpretation of Potentiometric Maps

When the potentiometric maps were contoured, it was found that occasionally certain single points did not fit the local pattern. In most cases these points were values taken from final shut-in pressures and usually they were too low. In such cases, the measurement was discarded as the error is likely due to the tool not being shut in long enough for the pressure in the drill stem to return to the original formation pressure. In rare cases the values were from Horner Plots and the values may have been too low or too high. Causes of such errors could be due to incorrect pressure readings and recordings, or they may be the result of mechanical failure, such as packer seat leakage when the test was run.

Besides showing the hydraulic head distribution within a geologic interval, each map shows the location of the

underlying Leduc reefs. The potentiometric contours show a general decrease from south to north with inflexures and anomalies centered over the Leduc reefs. Hitchon (1969a, 1969b) documented this general decrease in potentiometric head throughout Alberta from south-south west to north-north east. He related the head decrease to a regional flow system, with groundwater recharge occurring in the southern Rocky Mountains and Cypress Hills, lateral flow in the subsurface across much of Alberta, and discharge in northern Alberta and Saskatchewan.

The broad inflexure, illustrating a divergent flow pattern away from the Rimbey-Meadowbrook trend, is the dominant anomaly in the map area. This anomaly is seen in all three potentiometric maps and is roughly of the same magnitude in each. Hitchon (1969b, 1984) suggested that high permeability rock units, such as the Rimbey-Meadowbrook trend, serve as a drain, and form a channel where fluids from the Cretaceous intervals can enter into the Lower Devonian and Cambrian intervals. The potentiometric maps should therefore show a trough like feature, the opposite of that which is observed.

Underlying the Rimbey-Meadowbrook reef trend is a narrow band of dolomitized Cooking Lake carbonates (Andrichuck 1958). The extent of this band, known as the Cooking Lake aquifer, has been documented by Hnatiuk and Martinelli (1967), who noted that it attains maximum width

in the vicinity of the Leduc-Woodbend reef, and thins immediately north of the Acheson reef (Figure 6.4). The effect of the dolomitization on the Cooking Lake carbonates is to create a narrow zone of higher porosity and permeability as compared to the non-dolomitized segments of the Cooking Lake Formation north and east of the Leduc-Woodbend and Acheson reefs.

In order to explain the hydraulic head distribution within the Mesozoic and Upper Devonian units, one can consider the Leduc-Woodbend and Acheson reefs, together with the Cooking Lake aquifer, and possibly other reefs south of the Leduc-Woodbend reef on the Rimbey-Meadowbrook trend, to serve as a high permeability lens. This lens is surrounded by shales with permeabilities of several orders of magnitude less. Where the fluid enters the lens in the southern portion of the reef trend, the equipotential lines wrap around the edge of the lens, forming a pattern where water converges into the lens from nearby strata. Where the fluid leaves the lens, immediately north of the Acheson reef, the equipotential lines also wrap around the edge of the lens, allowing the fluid to diverge from the lens.

The effect of introducing a high permeability lens into a relatively lower permeability system is illustrated in figures 6.5a and 6.5b taken from the theoretical studies of Freeze and Witherspoon (1967). Figure 6.5a shows the hydrodynamic situation that exists with complex topography,

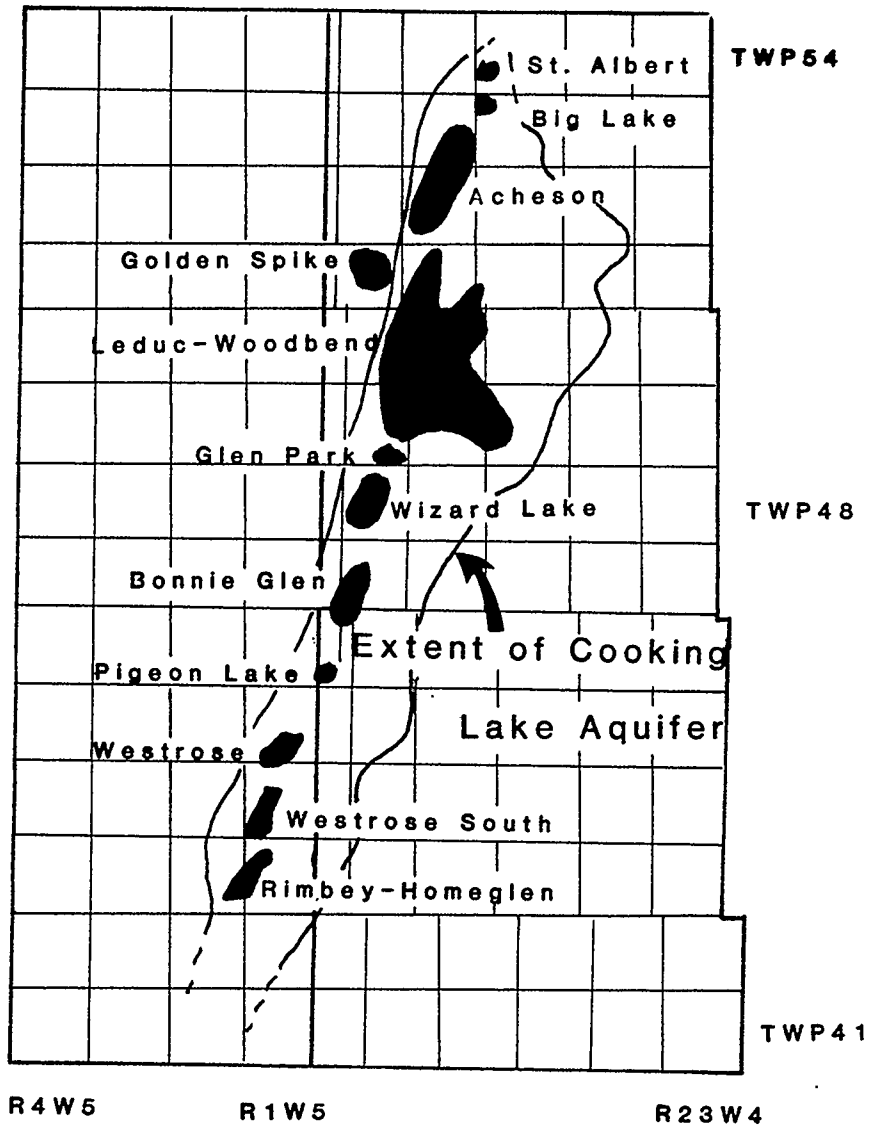
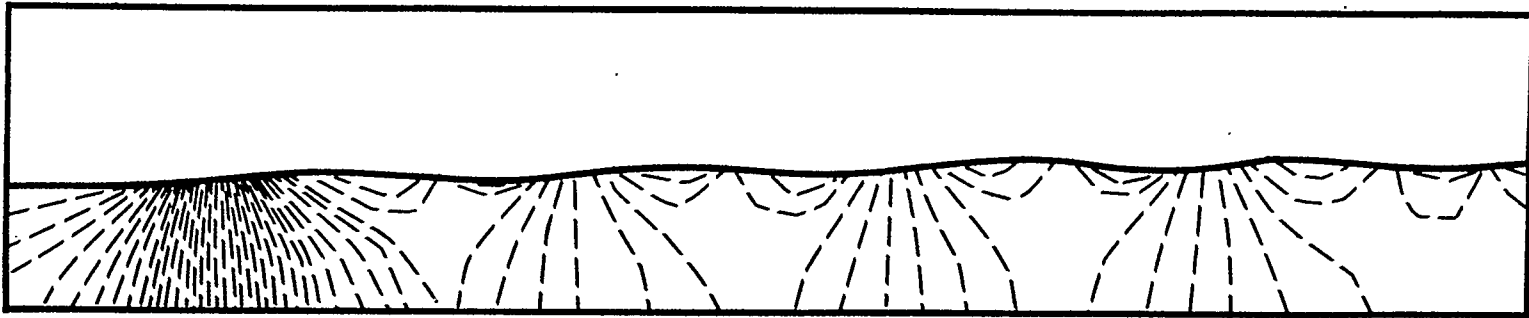
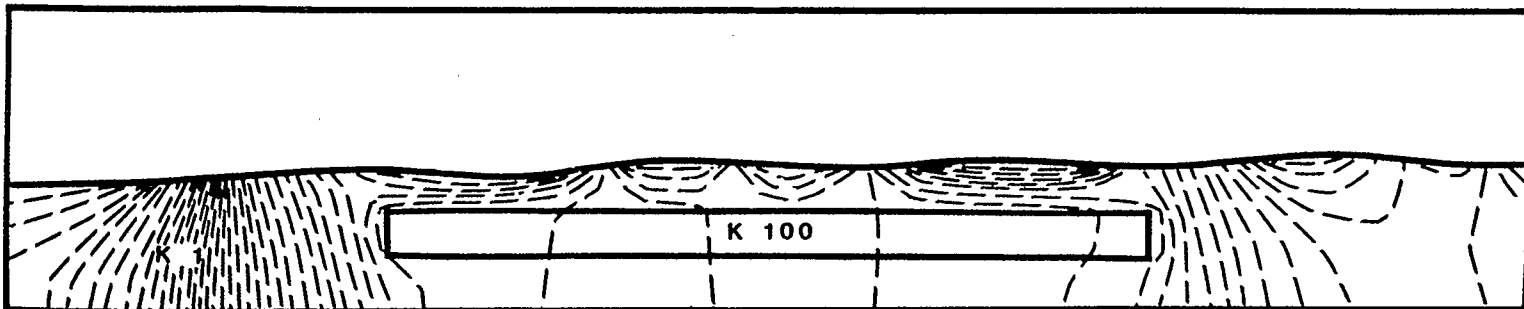


Figure 6.4 Location Map of Leduc Reefs and Cooking Lake Aquifer



**Figure 6.5a Equipotential pattern in region of complex topography and homogenous permeability (from Freeze and Witherspoon, 1967)**



**Figure 6.5b Effect of introducing high permeability lens into flow system (from Freeze and Witherspoon, 1967).**

but with no permeability variations. Figure 6.5b illustrates the effect that a high permeability lens has on the fluid flow. Originally the equipotential lines are all subvertical; with the introduction of the high permeability lens the equipotential lines wrap around the ends of the lens. The effect of the introduction of the lens on the equipotential lines extends beyond the lens itself to quite close to the surface. In map view the effect of the lens would show a concentration of flow lines in the upstream end of the lens, the hydraulic contours forming a "U" shaped pattern, with fluids draining in towards the centre of the "U". The head contours in the map pattern on the downstream end of the lens would resemble an inverted "U", with fluid flowing from the interior of the "U" outwards. It should be kept in mind that the theoretical studies of Freeze and Witherspoon (1967) are somewhat simplified. The geology in the study area is considerably more complex, the permeability variations are more severe, and, most importantly, the Rimbey-Meadowbrook trend may consist of a series of more or less discrete lenses, with varying amounts of converging and diverging flow into and out of the lenses. Nevertheless, the theoretical studies correlate well with the observed phenomena. The pattern of equipotential lines over the Rimbey-Meadowbrook reef trend can, therefore, be explained as the result of the introduction of a lens of high permeability into a

relatively lower permeability system. Fluid flows into the lens at the upstream end, travels along the lens, and diverges away from the lens at the downstream end.

A second anomaly is the low potentiometric drain seen in Township 51, Range 27 in the Ellerslie and Wabamun potentiometric maps. Presumably the same effect is visible in the Nisku potentiometric map but lack of data precludes a unequivocal determination of this. This anomaly is centered over the Golden Spike reef. The Golden Spike reef is somewhat different from other reefs in the study area in that the other Leduc reefs (with the exception of Redwater) have been extensively dolomitized, however, the Golden Spike reef is almost entirely composed of limestone (McGillivray and Mountjoy 1975). The Golden Spike reef is not on the Rimbey-Meadowbrook reef trend itself, but a few kilometres west of it. Unlike the other reefs, which sit on the permeable Cooking Lake aquifer, Golden Spike sits west of the depositional edge of the Cooking Lake Formation and the strata beneath Golden Spike have very low permeability (Haskett 1951). These three geologic characteristics of the Golden Spike reef set it apart from the other reefs and contribute to the different fluid flow pattern.

The potentiometric contours in each interval form a two dimensional enclosure around Golden Spike. Hubbert (1940) pointed out that three dimensional enclosure is impossible under steady state conditions and, hence, Golden

Spike must be serving as a drain from overlying units through the Golden Spike reef into the underlying units. Davis (1972a, 1972b) inferred similar vertical movement of fluids through various Devonian reefs within Alberta. Specifically, he suggests that selective dolomitization and solutioning of salt associated with the Rainbow reefs could be explained only if the reefs served as loci for vertical fluid movement. He also observed velocity anomalies over the Strachan reef north of the study area and he thought the anomaly was largely due to accentuated vertical brine movement associated with the reef itself. Potentiometric drains have also been noted by Meissner (pers. comm., 1984) in the Mesa Basin, and by Hitchon (1969b) and Harris and Young (1970) in the Viking Formation of southern Alberta. Meissner ascribes the potentiometric drain in the Mesa Basin to hydrocarbon generation. Since hydrocarbon generation is probably not an active process in the study area at present, the pattern of fluid flow over the Golden Spike reef is probably not the result of the same mechanism that Meissner ascribes to the pattern in the Mesa Basin. Harris and Young (1970) and Hitchon (1969b) attribute the closed potentiometric contours in the Viking Formation to an osmotic potential that exists between the Upper and Lower Cretaceous formation waters. In the Viking Formation the potentiometric low is centered over the lenticular high permeability sands of the Joffre-Bentley-Gilbey oil fields

and it is thought that this lateral facies change from low permeability shales to a high permeability unit is analogous with the situation of Golden Spike.

Osmosis occurs when a shale membrane separates two formation waters of different salinities. The difference in salinities results in different chemical activities of the two fluids. The shales separating the two formation waters consist of clays which have negative charges on their surface. As a result, cations are adsorbed onto the surface of the clays resulting in a double layer of negative and positive charges within the pores of the rock. This double layer tends to inhibit passage of cations across the membrane and, in order to maintain electrical neutrality, anions are also restricted from crossing the shale bed. Driven by the chemical potential difference in the two formation waters on either side of the membrane, uncharged water molecules pass from the less saline side to the more saline side of the membrane. This flow will serve to increase the hydraulic head of the more saline water until the chemical activity is the same for the formation waters on either side of the membrane. Presumably highly permeable conduits such as Golden Spike facilitate this flow of water from the relatively fresh waters of the Mesozoic clastics and Upper Devonian carbonates to the more saline waters of the Middle Devonian carbonates and evaporites.

In order to calculate whether the salinity contrast is sufficient to provide for an osmotic pressure of the order of magnitude that is observed, thermodynamic calculations can be performed on available formation water data from either side of the Ireton Formation. Graf (1982) has shown that the chemical osmotic pressure difference between a more saline NaCl solution II and a less saline solution I separated by a semi-permeable membrane is:

$$P(\text{II}) - P(\text{I}) = \frac{RT}{V_w} \ln \left( \frac{a(\text{I})}{a(\text{II})} \right) \quad (2)$$

where  $a$  is the activity of water,  $T$  is the temperature in degrees Kelvin,  $R$  is the gas constant, and  $V_w$  is the molar volume of pure water. In order to determine the activity of the various formation waters, chemical analysis of the formation waters were taken from a study by Hitchon et al. (1971). These values were converted into molality in NaCl equivalents. Since chemical analyses were not available for formation waters from the BeaverHill Lake Formation, the molality was estimated based on NaCl concentrations from Table 6.1. The molality was converted to activity of water using the Pitzer method, the results of which are summarized in Table 6.2. The molar volume of pure water at formation pressure and temperature was calculated to be 18.33 cm<sup>3</sup>/mole based on data from Clark

Geologic Interval	Molality (H <sub>2</sub> O)	Activity	LN Activity
Mannville	1.80	0.9388	-0.06311
Wabamun	2.06	0.9293	-0.07329
Winterburn	3.30	0.8810	-0.12670
Woodbend	4.10	0.8471	-0.16584
Beaverhill Lake	5.30 (estimate)	0.7928	-0.23211

Table 6.2 Molalities and activities of formation waters

(1966). Temperature of the formation was estimated to be about 340K.

These values suggest that an osmotic pressure of about 16 MPa could develop in the system. From the potentiometric maps, the head anomaly would appear to be a maximum of about 300 m, which in terms of pressure is about 3.1 MPa. Marine and Fritz (1981) noted that not all shales behave as perfect membranes; their osmotic efficiencies can vary from 0 to 100%. The Ireton Formation, with its high quartz and carbonate content, is not expected to be a perfect membrane, and the observed osmotic effect would be expected to be lower than the maximum calculated value based on thermodynamic calculations. Denbigh (1968) pointed out that the osmotic pressure indicated from thermodynamic calculations is not the same osmotic pressure difference that would be measured in two fluids separated by a semi-permeable membrane. The osmotic pressure shown from thermodynamic calculations is the pressure that would be required to prevent water from crossing the membrane, whereas the observed osmotic pressure is the excess pressure resulting from an equilibrated system where the water has moved across the membrane in order to equalize the the chemical activities of the two fluids. Nevertheless, the thermodynamic calculations are sufficiently larger than the observed pressure differential to suggest that the observed anomaly over Golden Spike

could be explained by the process of osmosis.

As previously mentioned, Golden Spike is a limestone reef, whereas the other reefs in the Rimbey-Meadowbrook trend have been extensively dolomitized. The exact chemical mechanism for this dolomitization will not be the subject of speculation here, but it is worthwhile to consider that the radically different hydrodynamic pattern over the Golden Spike reef, in contrast to the other reefs along the Rimbey-Meadowbrook trend, may have in some way prevented dolomitization. The present hydrodynamic regime need not be responsible for the diagenetic patterns however. Whatever the flow regime was when the Rimbey-Meadowbrook trend was dolomitized, the flow pattern may have been significantly different around Golden Spike so that this reef escaped being dolomitized.

The final item to be noted from the potentiometric maps is that although the North Saskatchewan River traverses the study area, it does not seem to have any observable effects on the fluid flow at the intervals examined. Presumably the head loss across the Wapiti, Colorado and Upper Mannville formations prohibits the local topographic situation from having any effect on flow at levels below the Mannville Group. This conclusion was independently reached based on the finite element modelling of the flow perpendicular to the North Saskatchewan River across the Acheson Reef (discussed in Chapter 5) in which

a static head distribution was found below the Mannville Group further supporting the conclusion that local topography does not influence flow at depth within the study area.

## Chapter 7 Hydrocarbon Migration

### 7.1 Source of Hydrocarbons

Since 1947, when Leduc #1 was spudded southwest of Edmonton, the Rimbey-Meadowbrook reef trend has been established as a prolific oil and gas producer within Alberta. Although the reefs serve as major traps for hydrocarbons, the reefs themselves were not the original source of hydrocarbons. Stoakes and Creaney (1984) reported that sections of the Duvernay Formation contain up to 17% total organic carbon in anoxic laminated fine-grained (deep basin) beds, and they have suggested that these organic rich shales served as the source rock for the hydrocarbons found within the reefs. The maturation of the kerogen into hydrocarbons within the Duvernay Formation, and the accumulation of the dispersed hydrocarbons within the Leduc reefs, implies that considerable primary and secondary migration must have occurred from the shales into the reefs.

Gussow (1954) attempted to describe the distribution of oil and gas along the Rimbey-Meadowbrook trend as a result of secondary migration along the basal Cooking Lake Formation. He suggested that the predominance of gas at the lowest end of the reef chain and oil at the updip end (Figure 7.1) could be explained by a theory of differential entrapment, or the "spill point theory". According to this

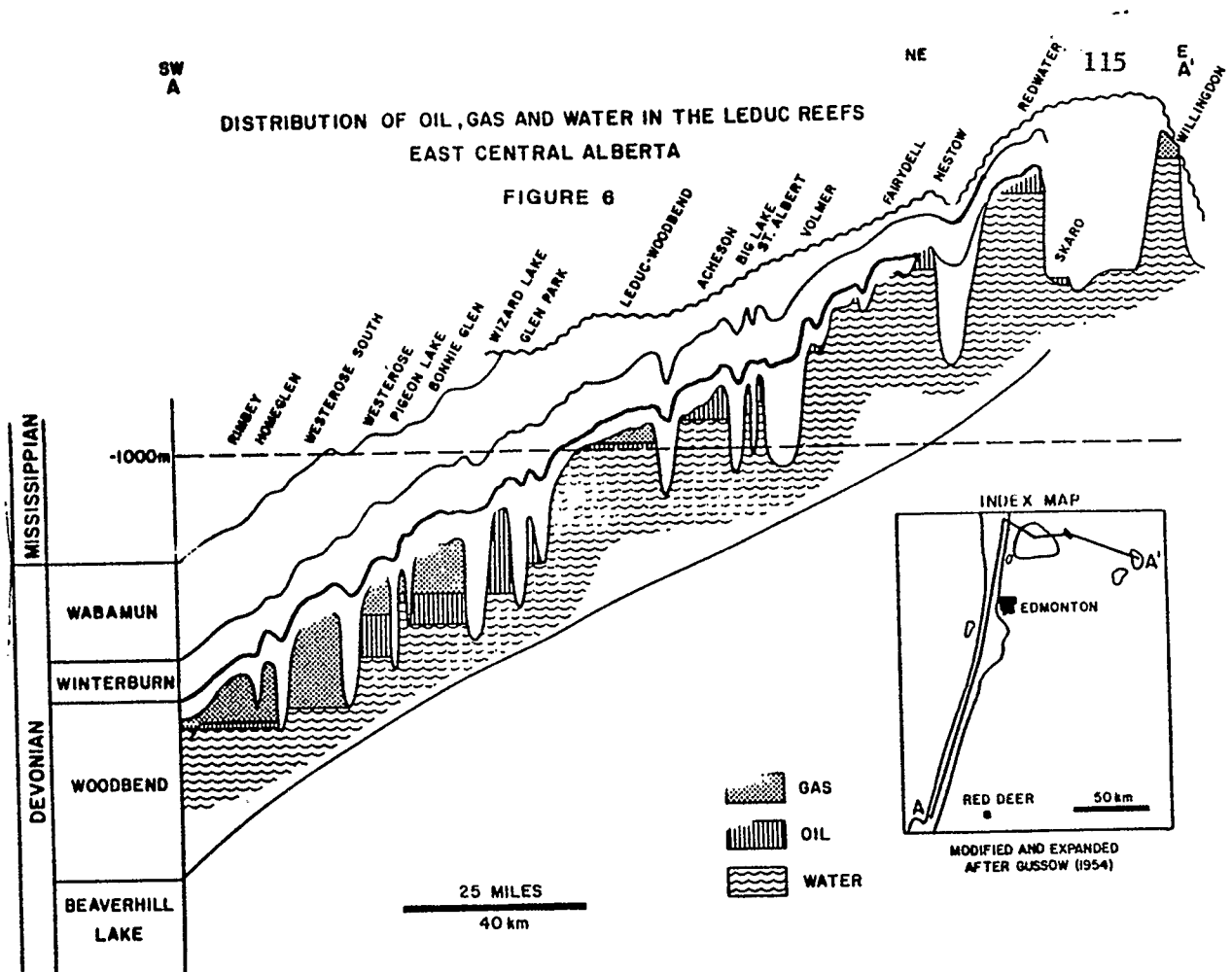


Figure 7.1 Distribution of oil, gas, and water in the Leduc reefs along the Rimbey–Meadowbrook trend (from Stoakes and Creaney 1984)

theory oil migrates into the downdip reefs from adjacent shales, gradually filling the reefs from the top down, until the oil within the reef spills out the base of the trap, at which point it migrates updip in the Cooking Lake Formation to the next reef where the process is repeated. As the sedimentary package is buried more deeply, the Duvernay Formation begins to generate gas, which displaces the oil in the downdip reefs, pushing the oil past the spill point and on to the next reef. Even though this theory explains the general distribution of oil and gas along the Rimbey-Meadowbrook trend, Stoakes and Creaney (1984) noted several discrepancies in the application of the theory to specific reefs. For example: gas is found in some reefs that are structurally higher than oil bearing reefs; and, some oil water contacts are hundreds of feet above the spill point, suggesting that these reefs could not have spilled over. Because of these discrepancies, Stoakes and Creaney (1984) suggested that the distribution of hydrocarbons might be better explained by a "leaky pipeline theory" in which oil was prevented from entering certain reefs due to permeability restrictions that existed along the base of some reefs.

Both Gussow (1954) and Stoakes and Creaney (1984) rely on buoyancy for oil migration; the less dense oil and gas rise vertically through the formation until the hydrocarbons encounter an impermeable boundary, then they

migrate updip along the lower surface of the boundary until the hydrocarbons enter a reef trap. Figure 7.1 is somewhat misleading with respect to this buoyant migration theory. Although the figure indicates a dip of over  $20^\circ$ , the actual dip of the reef trend is less than  $0.5^\circ$ . Resolving a vertical buoyancy vector into components tangential and normal to the bedding planes reveals that the tangential force along the bed is less than 1% of the normal force. This difference between the normal and the tangential force suggests that even a leaky pipeline would likely drain all contained hydrocarbons vertically upwards into a Leduc reef rather than along the top of the Cooking Lake Formation for long distances.

The spill point theory and the leaky pipeline theory treat the migration of oil and gas as essentially driven by buoyancy forces alone. This implies a totally hydrostatic situation within the subsurface. Since much of the preceding chapters were an attempt to show that hydrodynamic situations within the subsurface are the rule, rather than the exception, the purpose of this chapter is to examine how a hydrodynamic situation influences oil and gas migration (both primary and secondary) and the hydrocarbon distribution along the Rimbey-Meadowbrook reef trend.

## 7.2 Flow Systems During Hydrocarbon Migration

In order to ascertain the flow systems that existed during primary and secondary migration, it is first necessary to estimate when oil migration occurred. Based on burial histories, Deroo et al. (1977) felt that hydrocarbon genesis from Devonian source rocks did not occur until the Cretaceous and probably, the Late Cretaceous Era. Deroo et al. (1977) thought that petroleum formation occurs at a depth of 1200 to 2700 m for Upper Devonian sediments, a depth of burial that was probably not reached until sometimes in the Upper Cretaceous Era.

Knowledge of the flow systems that existed during the Cretaceous is, of course, highly speculative, and only broad inferences can be made. Nevertheless, general flow patterns can be suggested based on the regional Cretaceous stratigraphy and knowledge of the tectonic environment of western Canada. Two major mechanisms probably existed to drive the fluid flow. The first mechanism would be due to the topography that existed in the Western Canada Sedimentary Basin, largely in response to the considerable relief imposed upon western Canada due to the rising Cordillera west of the study area. This relief would have been reflected in the deposition of the fluvial-deltaic units across the Western Canada Sedimentary Basin. The second mechanism is due to shale compaction, principally compaction of the numerous shale sequences within the Cretaceous and with a minor component of flow due to

compaction of the Ireton, Duvernay and Majeau Lake shales.

Shale compaction within the Cretaceous units would have generated flow that was occasionally in lateral or descending directions, but chiefly in ascending flow directions. The lowermost Mannville Group consists of a highly permeable formation (Ellerslie Formation) that would likely have served to laterally drain away any descending fluids. Below the Mannville Formation are the poorly permeable units within the lower Wabamun Group which would have retarded flow to the underlying units. The highly permeable drain of the Ellerslie Formation, coupled with the restriction to flow imposed by the Wabamun Group, would have prevented any significant portion of the fluids derived by compaction of the Cretaceous sediments from penetrating to the Woodbend Group. The Ireton, Duvernay and Majeau Lake shales were also undergoing some compaction in the Late Cretaceous. The volume of fluids contributed by these compacting shales is not large enough to significantly influence the regional hydrodynamic patterns within the Devonian aquifers, although it may have had an important effect upon primary hydrocarbon migration.

Fluid flow driven by topography is thought to have had a more important influence within the Paleozoic intervals than did compaction. Similar to today, groundwater would recharge in areas of high topographic elevation, and discharge in areas of low elevation, and thus the

groundwater flow patterns should parallel regional topographic drainage patterns. Reconstruction of paleodrainage patterns in Alberta by Eisbacher et al. (1974) based on sedimentology of the clastic units reveals that during the Early-Middle Cretaceous Period the drainage pattern was largely from south to north. The clastic sources and areas of high topographic relief were slightly west of the present position. This western source of Lower Cretaceous clastics was also reported in a study by Putnam and Pedskalny (1983) on the provenance of clasts from within the Clearwater Formation. The south to north flow directions was also noted by Hopkins et al. (1982) in their study on depositional environments of Lower Cretaceous formations.

During the Upper Cretaceous - Tertiary Eras, deposition shifted to a more west to east direction, with the major rivers draining into a major inland sea in southern Saskatchewan. These paleodrainage studies suggest that throughout the Late Cretaceous Era, large scale topographic gradients extended from southwest to northeast throughout Alberta. Groundwater flow systems would likely have paralleled the topographic drainage system. Groundwater would have entered the system in the rising Cordillera west of the study area and would have flowed laterally updip throughout most of Alberta, discharging on the northeastern edge of the Western Canada Sedimentary

Basin. Local stratigraphy would have complicated a simple potentiometric gradient, similar to the way that the Devonian carbonate trends influence the present flow patterns. Due to the lower topographic gradient in the Cretaceous Era than at present, the fluid flow may have been more sluggish and may have had some quasi-stagnant zones (Hitchon 1984). However, as Jones (1978) pointed out, compaction of the Cretaceous shales, coupled with the meteoric recharge of water, would have ensured a dynamic fluid system throughout much of the Alberta basin that would have had a significant effect on hydrocarbon migration.

### 7.3 Effect of Hydrodynamics on Secondary Migration

Because the groundwater in the strata during the Cretaceous Era likely existed in a dynamic rather than a static environment, one must consider the effect of this moving water on oil and gas migration. Hubbert (1953) has shown how the impelling force that moves the oil (the oil potential gradient) can be related to the impelling force that acts upon the water phase by the equation:

$$E_o = g + \rho_w/\rho_o (E_w - g) \quad (1)$$

where  $E_o$  and  $E_w$  are the oil and water impelling forces,  $\rho_w$  and  $\rho_o$  are the water and oil densities, and  $g$  is the

gravitational vector acting upon a fluid particle. The oil impelling vector,  $E_o$ , is a linear function of two primary vectors: 1) the acceleration of gravity vector,  $g$ , which by definition is directed downwards; and, 2)  $E_w$ , which is the total impelling force per unit mass acting upon a particle of water, and has the direction of water flow. In terms of  $E_o$ ,  $g$  is the force per unit mass exerted by gravity, and  $+(\rho_w/\rho_o)(E_w - g)$  is the force per unit mass exerted by the now suppressed gradient of pressure. A plot of these vectors (Figure 7.2) reveals how the impelling force for oil is influenced by the impelling force for water. The magnitude and direction of the oil impelling force vector is largely influenced by the ratio  $\rho_w/\rho_o$ . If the oil has about the same density as water, the oil would flow in the same direction of the water. The larger the density contrast between the hydrocarbon and water, the larger the impelling vector, and the more vertical the direction of that vector. Figure 7.3 illustrates the impelling vector for water, oil and gas. As would be expected, the gas has the strongest tendency to rise vertically with the most force, water flows horizontally (in this case) and the impelling force for oil is found to be between the gas and water (in both magnitude and direction). The net result is that gas will have a great propensity to rise vertically throughout a sequence, whereas oil will have a greater tendency to be swept along with the water.

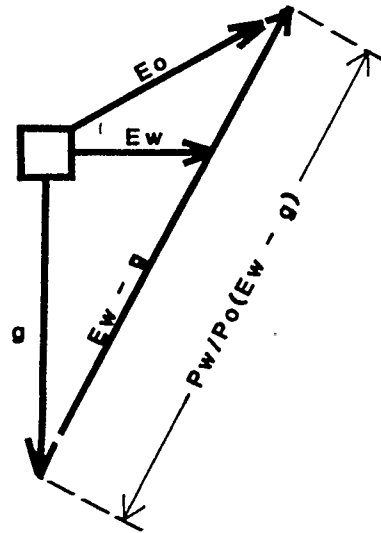


Figure 7.2 Vector diagram of forces acting upon an element of oil in a hydrodynamic environment (from Hubbert, 1953).

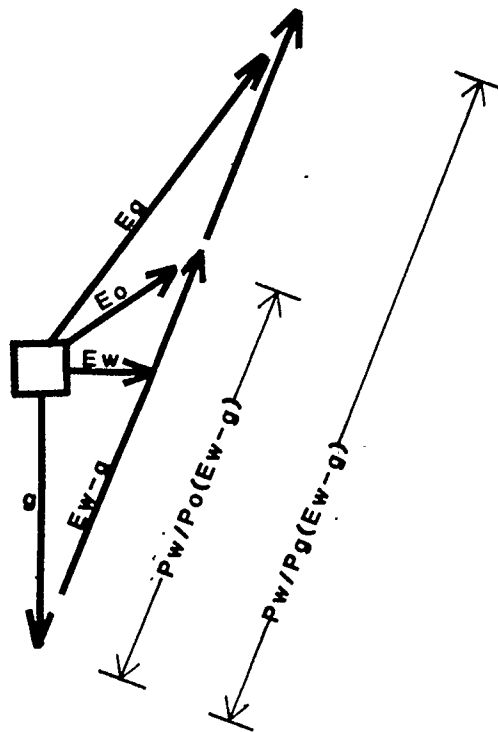


Figure 7.3 Vector diagram of forces illustrating divergent flow patterns of water, oil, and gas (from Hubbert, 1953).

The hydrodynamic condition that existed during the Cretaceous Era would also be expected to have had an effect on oil and gas migration. Because the water potential gradient ran from southwest to northeast, subparallel to the Rimbey-Meadowbrook trend, oil and gas migration may have been partially segregated into two different orders of flow by the water movement. Whereas the oil, gas, and water would tend to flow in the same horizontal direction, the gas would have a greater inclination to rise vertically through the sequence. The oil would be more swept along by the water, with the water moving along the Rimbey-Meadowbrook trend in a northwest direction. Because of the tendency of the gas to rise vertically rather than move horizontally, it would show a large propensity to fill up the traps in the downdip end of the reef trend. Oil would show a stronger tendency to move into the updip traps. The leaky pipeline theory of Stoakes and Creaney (1984) could then be used in conjunction with a hydrodynamic situation. Oil was prevented from moving into certain traps not only by permeability barriers that could only be breached by gas, but also because the horizontal impelling force on the oil was greater than on the gas, which tended to move the oil along to the next updip trap.

#### 7.4 Primary Migration

Mechanisms for primary migration are among the least

well known mechanisms for fluid movement. Hunt (1979, p. 165) states that "the primary cause of the movement of fluids from a source sediment is compaction". An alternative mechanism suggested by du Rouchet (1981) states that the kerogen to hydrocarbon transformation results in a pore pressure increase, and oil is able to migrate as a separate phase out of the high pressured shales. Other mechanisms that have been suggested include: 1) oil migrating as a micelle; 2) along organic matter (kerogen wick theory); 3) in solution; 4) by capillary forces; and, 5) by diffusion (Hunt 1979). Because the volume and timing of fluid expulsion from the Ireton/Duvernay sediments have been derived in a previous chapter, an attempt can be made to explain whether compaction effects alone could account for primary migration.

The volume of water released by compaction during the Cretaceous Era has already been calculated (Chapter 3). Since compaction was delayed during much of the Cretaceous (O'Connor and Gretener 1974), most of the water released due to compaction during the Cretaceous Era would have coincided with the main period of hydrocarbon generation during the Late Cretaceous. This water would have been directed both upwards and downwards from the center of the Ireton/Duvernay sequence. Therefore, about one half of the total volume released during the Cretaceous Era, or about 8,000,000 m<sup>3</sup>/km<sup>2</sup> of fluid, would have passed through the

Duvernay source rocks during periods of hydrocarbon generation.

Since individual beds within the Duvernay vary considerably in total organic content (from less than 0.5% to as much as 17%), an average estimate of total organic carbon is difficult to ascertain. A conservative estimate for the average total organic content (TOC) of the Duvernay shale is 2%. Moshier and Waples (1985) have estimated that only about 10% of the TOC is converted into hydrocarbons as a result of thermal maturation. The Duvernay Formation would therefore contain a minimum of 2000 ppm (0.2%) hydrocarbons as a result of this thermal maturation of its organic matter. From these values the total volume of hydrocarbons generated per square kilometer can be determined. Hunt (1977) has suggested that only about 15% of the total hydrocarbon generated by a source rock is released from that source rock. The Duvernay Formation varies considerably in total thickness in the study area, and assuming an average thickness of 40 m (Stoakes 1980), 12000 cubic metres of oil per square kilometre could be released from the Duvernay source rock during primary migration. Consequently, the minimum ratio of oil to water during primary migration would be about 1500 ppm of oil in water (12000 m<sup>3</sup>/km<sup>2</sup> of oil divided by 8,000,000 m<sup>3</sup>/km<sup>2</sup> of water). For thicker, more kerogen-rich sequences, the minimum amount of oil in the water would be

about 5,600 ppm.

According to Price (1976), whole crude oil solubilities for various oils in water will not exceed 300 ppm at the temperature of generation. Since the minimum ratio of oil expulsion to water expulsion considerably exceeds this value, it is unlikely that oil migrated out of the source beds dissolved in the water that was being expelled due to compaction.

In order to account for the amount of hydrocarbons that migrated out of the source rock, it is necessary to consider other mechanisms to increase the volume of oil leaving the Duvernay. Increasing the flux of water through the Duvernay by means of movement of meteoric water would serve to lower the oil/water ratio to such an extent that significant portions of the oil could be dissolved in the pore waters. However, rather than have water move down through the sedimentary sequence, Hitchon (1984) has indicated that meteoric water was largely ascending rather than descending in the eastern part of the Alberta syncline. Therefore, it is doubtful that the relatively sluggish fluid flow during the Cretaceous Era could have contributed much to the flux across the poorly permeable Ireton and Duvernay sections.

Clearly, mechanisms must exist to increase the concentration of oil in the fluid phase. The several mechanisms suggested by various authors will not be

discussed here, however separate oil phase migration is thought to be one of the more plausible mechanisms (Hunt 1979). It should be noted that the migration pathway from the Duvernay to the Cooking Lake Formation implies a downward flow of fluids; a separate oil phase would be less dense, and would tend to rise rather than descend under hydrostatic conditions. The downward moving pore waters from compaction processes would assist in the downward migration of oil. This downward flow of water, coupled with the possible high geopressures developed from the kerogen to oil transformation, may be able to account for the primary migration of oil out of the Duvernay source rocks.

## Summary and Conclusions

The main points of this thesis can be summarized as follows:

1. The Upper Devonian Ireton and Duvernay shale sequence compacted approximately 120 m during the course of its burial history, from an initial thickness of about 360 m to its present thickness of less than 240 m. 75% of this compaction occurred before the sediment was buried 500 m, or less than 30 million years after deposition. A total of  $110 \times 10^6 \text{ m}^3/\text{km}^2$  of fluid was expelled from these compacting shales. Approximately 85% of the total fluid expelled occurred during the Paleozoic Era. The remaining 15% ( $17 \times 10^6 \text{ m}^3/\text{km}^2$ ) was expelled during the Late Cretaceous Era, at about the same time as when hydrocarbon generation took place.

2. Theoretical studies of fluid flow directions due to compaction during the late Paleozoic, based on the finite element method, reveals that there was limited fluid movement directly from the shales into the reef. Most of the fluid was expelled vertically upwards or downwards from the shales into overlying or underlying units. The upper half of the shale sequence expelled fluid upwards, and this flow was not influenced by the presence of the reef. The

lower half of the shale sequence expelled fluid downwards into the underlying carbonates. This fluid then flowed laterally through the underlying units and was channelled either vertically upwards through the reef into the overlying units or continued to flow laterally through the underlying units out to the margins of the basin. The extent of the influence of the reef upon flow, based on various scenarios, was not less than 3,200 m and probably not greater than 16,000 m.

Direct geologic confirmation of this flow pattern for the Leduc reefs is not possible. A similar geologic setting occurs in northwestern Alberta in the Rainbow area, where Middle Devonian Black Creek salts have been at least partially dissolved for up to 3000 m around Keg River reefs. Davis (1972a) ascribes this salt solutioning to concentrated fluid migration through the Keg River reefs. Barss et al. (1970) noted that much of the solutioning of the salts around the reef occurred early in the burial history of the reefs. The extent and timing of salt solutioning near these high permeability reefs corresponds well with the estimates for compaction fluid flow around the Leduc reefs.

3. The water expelled from the organic rich Duvernay shales into the underlying Cooking Lake Formation may have provided the fluids necessary for dolomitization of the

western margin of the Cooking Lake carbonates and the Leduc reefs.

4. Study of current fluid movement reveals that the source of energy for flow is provided by the large scale topographic relief across the Western Canada Sedimentary Basin. The intermediate flow system imposed by the presence of the North Saskatchewan River does not influence fluid flow at depths below the Upper Cretaceous horizons.

5. The Rimbey-Meadowbrook trend, along with the underlying Cooking Lake aquifer, serves as a high permeability lens surrounded by low permeability shales and carbonates. This lens channels lateral fluid movement along its length, collecting flow at the southern end, and dispersing flow (to some extent) immediately north of the Acheson reef. The location of dispersion of fluid flow from the lens corresponds to a thinning of the reef trend and the underlying Cooking Lake aquifer.

6. The Golden Spike reef, west of the Rimbey-Meadowbrook trend, functions as a drain for the relatively fresh fluids in the Upper Devonian and Cretaceous formations to the more saline fluids within the underlying Middle Devonian and Cambrian formations. The cause for this fluid flow pattern is attributed to osmosis.

The effect on the fluid flow patterns of the Leduc reefs extends upwards to at least the Ellerslie Formation, and possibly higher. Davis (1972b) noted density and velocity variations in the strata overlying the reefs. A correlation may be suggested between the different fluid flow patterns over the reefs and the anomalous density and velocity values of the same strata over the reef.

7. A hydrodynamic situation within the subsurface is believed to have existed during the time of hydrocarbon migration in the Late Cretaceous. The inferred northeasterly flowing subsurface water would have segregated the secondary migration pathways of the oil and gas into two different streams. The less dense gas would have risen more or less vertically throughout the sequence. The oil would have been swept along by the water, with a greater propensity to fill the updip traps.

8. The amount of water expelled due to compaction from the lower Ireton and Duvernay shales during the late Cretaceous era is insufficient to account for primary migration of oil dissolved in the water. The oil must have migrated out of the source beds as a separate phase, although it is possible that the water pathways did assist in the oil movement.

9. The flux of the fluids derived from the compaction of the Ireton, Duvernay and Majeau Lake shales had a significant influence on fluid flow during the Late Devonian, and a lesser influence during the remainder of the Paleozoic Era. The flow due to shale compaction did not influence the hydrodynamic pattern within the aquifers during the Cretaceous, as well as the present, Era.

## References

- Andrichuk, J.M. 1958. Stratigraphy and facies analysis of Upper Devonian reefs in Leduc, Stettler, and Redwater areas, Alberta. Bulletin of the American Association of Petroleum Geologists, vol. 42, pp. 2189-2222.
- Aoyagi, K. and Asakawa, T. 1984. Paleotemperature analysis by authigenic minerals and application to petroleum exploration. Bulletin of the American Association of Petroleum Geologists, vol.68, pp. 903-913.
- Athy, L.F. 1930. Density, porosity, and compaction of sedimentary rocks. Bulletin of the American Association of Petroleum Geologists, Vol. 14, pp. 1-35.
- Barss, D.L., Copland, A.B., and Ritchie, W.D. 1970. Geology of Middle Devonian reefs, Rainbow area, Alberta, Canada. American Association of Petroleum Geologists Memoir 14, Geology of Giant Petroleum Fields, M.T. Halbouty, editor, 575 p.
- Bishop, R.S. 1979. Calculated compaction states of thick abnormally pressured shales. Bulletin of the American Association of Petroleum Geologists, vol.63, pp. 918-933.
- Bonham, L.C. 1980. Migration of hydrocarbons in compacting basins. Bulletin of the American Association of Petroleum Geologists, vol. 64, pp. 549-567.
- Canadian Well Logging Society. 1978. Formation Water Resistivities of Western Canada.
- Ceroici, W. 1979. Hydrogeology of the south-west segment, Edmonton area, Alberta. Alberta Research Council, Earth Sciences Report 78-5, 14 p.
- Clark, S.P. 1966. Solubility. in Handbook of Physical Constants. Geological Society of America Memoir 97, editor S.P. Clark, pp. 415-436.
- Dahlberg, E.H. 1983. Applied Hydrodynamics to Petroleum Exploration. J. Wiley and Sons, New York, 161 p.
- Dake, L.P. 1978. Fundamentals of Reservoir Engineering, Elsevier Scientific Publishing Company, Amsterdam, 443 p.
- Davis, T.L. 1972a. Velocity - density variations around

- Keg River reefs, Alberta. Canadian Society of Exploration Geophysics Journal, vol. 8, pp. 1-13.
- Davis, T.L. 1972b. Velocity variations around Leduc reefs, Alberta. Geophysics, vol. 37, pp. 584-604.
- Denbigh, K. 1968. The Principles of Chemical Equilibrium. Cambridge University Press, London, England, 494 p.
- Deroo, G., Powell, T.G., and Tissot, B. 1977. The origin and migration of petroleum in the Western Canadian Sedimentary Basin, Alberta. Geological Survey of Canada Bulletin 262, 136 p.
- du Rochet, J. 1981. Stress fields, a key to oil migration. Bulletin of the American Association of Petroleum Geologists, vol. 65, pp.74-85.
- Eisbacher, G.H., Carrigy, M.A., and Campbell, R.B. 1974. Paleodrainage pattern of late orogenic basins of the Canadian Cordillera. Society of Economic Paleontologists and Mineralogists Special Publication #22, Tectonics and Sedimentation, editor W.R. Dickinson, pp 143-166.
- Fertl, W.H. 1976. Abnormal Formation Pressures. Elsevier Scientific Publishing Co., Amsterdam, 382 p.
- Freeze, R.A. and Witherspoon, P.A. 1967. Theoretical analysis of regional groundwater flow. 2. Effect of water-table configuration and subsurface permeability variation. Water Resources Research, vol. 3, no. 2, pp. 623-634.
- Freeze, R.A. 1969. Regional groundwater flow - Old Wives Lake Drainage Basin, Saskatchewan. Inland Waters Branch, Department of Energy, Mines, and Resources Scientific Series No. 5, 245 p.
- Freeze, R.A. and Cherry, J.A. 1979. Groundwater. Prentice Hall Publishers, New Jersey, 604p.
- Gabert, G. 1975. Hydrogeology of Red Deer and vicinity, Alberta. Alberta Research Council Bulletin #31, 100 p.
- Graf, D.L. 1982. Chemical osmosis, reverse chemical osmosis, and the origin of subsurface brines. Geochimica et Cosmochimica Acta, vol. 46, pp. 1431-1448.
- Gretener, P.E. and Labute, G.J. 1972 Total Ireton

- compaction - a revision. Bulletin of Canadian Petroleum Geology, vol. 20, pp. 281-285.
- Gussow, W.C. 1954. Differential entrapment of oil and gas: A fundamental principle. Bulletin of the American Association of Petroleum Geologists, vol. 38, pp.816-853.
- Hanshaw, B.B., and Zen, E. 1965. Osmotic equilibrium and overthrust faulting. Bulletin of the Geological Society of America, vol. 76, pp. 1379-1386.
- Harris, D.G. and Young, A. 1970. Formation pressure pattern in Cretaceous Viking Formation, Alberta. Bulletin of the American Association of Petroleum Geologists, vol. 54, pp. 850-851.
- Haskett, I. 1951 Analysis of Canada's Goldens Spike reservoir. Oil and Gas Journal, vol. 49, September, pp.259-269.
- Hauquebad H. 1977. Rank of coal as an index to organic metamorphism for oil and gas in Alberta. Geological Survey of Canada Bulletin 262, 136 p.
- Hedberg, H.D. 1936. Gravitational compaction of clays and shales. American Journal of Science, vol. 31, pp. 241-287.
- Hinch, H.H. 1980. The nature of shales and the dynamics of hydrocarbon expulsion on the Gulf Coast Tertiary section. Problems in Petroleum Migration AAPG Studies in Geology #10, Roberts. W.H. and Cordell, R.J., editors, 271 p.
- Hitchon, B. 1969a. Fluid flow in the Western Canadian Sedimentary Basin. 1. Effect of topography. Water Resources Research, vol.5, no.1, pp. 186-195.
- Hitchon, B. 1969b. Fluid flow in the Western Canadian Sedimentary Basin. 2. Effect of geology. Water Resources Research, vol. 5, no. 2, pp.460-469.
- Hitchon, B., Billings, G.K., and Klovan, J.E. 1971. Geochemistry and formation waters in the Western Canada Sedimentary Basin - III Factors controlling composition. Geochimica et Cosmochimica Acta, vol. 35, pp.567-598.
- Hitchon, B. 1980. Some economic aspects of water rock interaction. Problems in Petroleum Migration, AAPG

- Studies in Geology no. 10, Roberts, W.H., and Cordell, R.J., editors, 271 p.
- Hitchon, B. 1984. Geothermal gradients, hydrodynamics, and hydrocarbon occurrences, Alberta, Canada. Bulletin of the American Association of Petroleum Geologists, vol. 68, pp. 713-743.
- Hnatiuk, J. and Martinelli, J.W. 1967. The relationship of the Westrose D-3 pool to other pools on the common aquifer. Proceedings of the 18th Annual Technical Convention of the Petroleum Society of CIM, May, 1967.
- Hopkins, J.C., Hermanson, S.W., and Lawton, D.C. 1982. Morphology of channels and channel-sand bodies in the Glauconitic Sandstone Member (Upper Mannville), Little Bow Area, Alberta. Bulletin of Canadian Petroleum Geology, vol. 30, pp. 274-285.
- Horner, D.R. 1951. Pressure buildup in wells. Proceedings of the Third World Petroleum Congress, editor E.J. Brill.
- Hubbert, M.K. 1940. Theory of groundwater motion. Journal of Geology, vol. 48, pp.785-944.
- Hubbert, M.K. 1953. Entrapment of petroleum under hydrodynamic conditions. Bulletin of the American Association of Petroleum Geologists, vol. 37, pp.1954-2026.
- Hunt, J.M. 1977. Ratio of petroleum to water during primary migration in Western Canada Basin. Bulletin of the American Association of Petroleum Geologists, vol. 61, pp. 434-435.
- Hunt, J.M. 1979. Petroleum Geochemistry and Geology. W.H. Freeman and Company, New York, 617 p.
- Kastner, M. 1984. Origin of dolomite and its spatial and chronological distribution - a new insight. CSPG Reservoir, vol. 11, no. 3, pp. 1-3.
- Jones, R.W. 1978. Some mass balance and geological restraints on migration mechanisms. In "Physical and Chemical constraints on petroleum migration", vol. 2, Notes for AAPG short course, AAPG National Meeting, Oklahoma City, April 1978.
- Labute, G.J., and Gretener, P.E. 1969. Differential compaction around a Leduc reef - Wizard Lake area,

- Alberta. Bulletin of Canadian Petroleum Geology, vol. 17, pp. 304-325.
- Magara, K. 1968. Compaction and migration of fluids in Miocene mudstones, Nagooka Plain, Japan. Bulletin of the American Association of Petroleum Geologists, vol. 52, pp. 2466-2501.
- Magara, K. 1973. Compaction and fluid migration in Cretaceous shales of western Canada. Geological Survey of Canada Paper 72-18, 82 p.
- Magara, K. 1976. Water expulsion from clastic sediments during compaction - directions and volumes. Bulletin of the American Association of Petroleum Geologists, vol. 60, pp. 543-553.
- Marine, I.W. and Fritz, S.G. 1981. Osmotic model to explain anomalous hydraulic heads. Water Resources Research, vol. 17, no. 1, pp. 73-82.
- Mattes, B.W., and Mountjoy, E.W. 1980. Burial dolomitization of the Upper Devonian Miette buildup, Jasper National Park, Alberta. Society of Economic Paleontologists and Mineralogists Special Publication no. 28, pp.259-297.
- Maxey, G.B. 1964. Hydrostratigraphic units. Journal of Hydrology, vol. 2, pp. 124-129.
- McCrossan R., and Glaister, P., editors. 1964. Geological History of Western Canada. Alberta Society of Petroleum Geologists, Calgary, Alberta.
- McCrossan, R.G., editor. 1973. The future petroleum provinces of Canada - their geology and potential. Canadian Society of Petroleum Geologists Memoir #1, 720 p.
- McGillivray, J.G., and Mountjoy, E.W. 1975. Facies and related reservoir characteristics, Golden Spike reef complex, Alberta. Bulletin of Canadian Petroleum Geology, vol. 23, pp. 753-809.
- Moshier, S.D., and Waples, D.W. 1985. Quantitative evaluation of Lower Cretaceous Mannville Group as source rocks for Alberta's oil sands. Bulletin of the American Association of Petroleum Geologists, vol. 69, pp. 161-172.
- Mossop, G.D. 1972. Origin of the peripheral reef rim,

- Redwater reef, Alberta. Bulletin of Canadian Petroleum Geology, vol. 20, pp. 238-280.
- O'Connor, M.J. and Gretener, P.E. 1974. Differential compaction within the Woodbend Group of central Alberta. Bulletin of Canadian Petroleum Geology, vol. 22, pp. 269-304.
- O'Connor, M.J. 1972. Differential Compaction, Central Alberta. M.Sc Thesis, The University of Calgary, 160p.
- Oliver, T.A. and Cowper, N.W. 1965. Depositional Environments of the Ireton Formation, central Alberta. Bulletin of the American Association of Petroleum Geologists, vol. 49, pp. 1410-1425.
- Perrier R., and Quiblier, J. 1974. Thickness changes in sedimentary layers during compaction history; methods for quantitative evaluation. Bulletin of the American Association of Petroleum Geologists, vol. 58, pp. 507-520.
- Powers, M.C. 1967. Fluid release mechanisms in compacting marine mudrocks and their importance in oil exploration. Bulletin of the American Association of Petroleum Geologists, vol. 51, pp. 1240-1254.
- Price, L.C. 1976. Aqueous solubility of petroleum as applied to its origin and primary migration. Bulletin of the American Association of Petroleum Geologists, vol. 60, pp. 213-244.
- Pugh, P.C. 1971. Subsurface Cambrian stratigraphy in southern and central Alberta. Geological Survey of Canada Paper 70-10, 31 p.
- Putnam, P.E. and Pedskalny, M.A. 1983. Provenance of Clearwater Formation reservoir sandstones, Cold Lake, Alberta. Bulletin of Canadian Petroleum Geology, vol. 31, pp. 148-160.
- Reiss, L.H. 1980. The Reservoir Engineering Aspects of Fractured Formations. Gulf Publishing, Houston, Texas, 108 p.
- Reitzel, G.A., and Callow, G.O. 1977. Pool description and performance analysis leads to understanding of Golden Spike's miscible flood. Journal of Petroleum Technology, July, 1977, pp. 867-872.
- Smith, J.E. 1971. The dynamics of shale compaction and

- evolution of pore fluid pressures. *Mathematical Geology*, vol. 3, pp. 239-263.
- Smith, J.E., 1973. Shale compaction. *Society of Petroleum Engineers Journal*, February, 1973, pp. 12-25.
- Stoakes, F.A., 1979. Sea level control of carbonate - shale deposition during progradational basin - filling: the Upper Devonian Duvernay and Ireton formations of Alberta Canada. Ph.D. thesis, The University of Calgary, 346 p.
- Stoakes, F.A., 1980. Nature and control of shale basin fill and its effect on reef growth and termination: Upper Devonian Duvernay and Ireton formations of Alberta, Canada. *Bulletin of Canadian Petroleum Geology*, vol. 28, pp. 345-410.
- Stoakes, F.A., and Creaney, S., 1984. Sedimentology of a carbonate source rock: The Duvernay Formation of central Alberta. *Carbonates in Subsurface and Outcrop*, CSPG Core Conference Guidebook, pp. 132-147.
- Toth, J., 1963. A theoretical analysis of groundwater flow in small drainage basins. *Journal of Geophysical Research*, vol. 68, pp. 4795-4812.
- Toth, J., 1978. Gravity induced cross - formational flow of formation fluids in the Red Earth Region, northern Alberta. *Water Resources Research*, vol. 14, pp. 805-843.
- van Everdingen, R.O., 1968. Studies of formation waters in Western Canada: Geochemistry and hydrodynamics. *Canadian Journal of Earth Sciences*, vol. 5, pp. 523-543.
- Weller, J.M., 1959. Compaction of sediments. *Bulletin of the American Association of Petroleum Geologists*, vol. 43, pp. 273-310.
- Westoll, T.S., 1962. The standard model cyclotherm of the Visean and Namurian sequence of Northern England. *Compte rendu, quatrieme Congres pour l'avancement des etudes de stratigraphie et de geologie du Carbonifere*, tome III, pp. 767-773.
- Zienkiewicz, O.C., 1977. *The Finite Element Method*, 3rd edition. McGraw - Hill, United Kingdom, 787p.

## Appendix 1

The finite element algorithm on which program CAPFEA is based upon was originally written by L. Kiraly of the University of Neuchatel in Switzerland. CAPFEA was expanded by adding plotting routines in 1976 and 1977 by K.U. Weyer and H.K. Pearse of the Inland Waters Branch of Environment Canada. The program was modified to work on either the Honeywell Multics computer at the University of Calgary or an IBM computer. The structure of the program was taken from the text by O.C. Zienkiewicz, The Finite Element Method In Engineering Science (3rd edition, 1977).

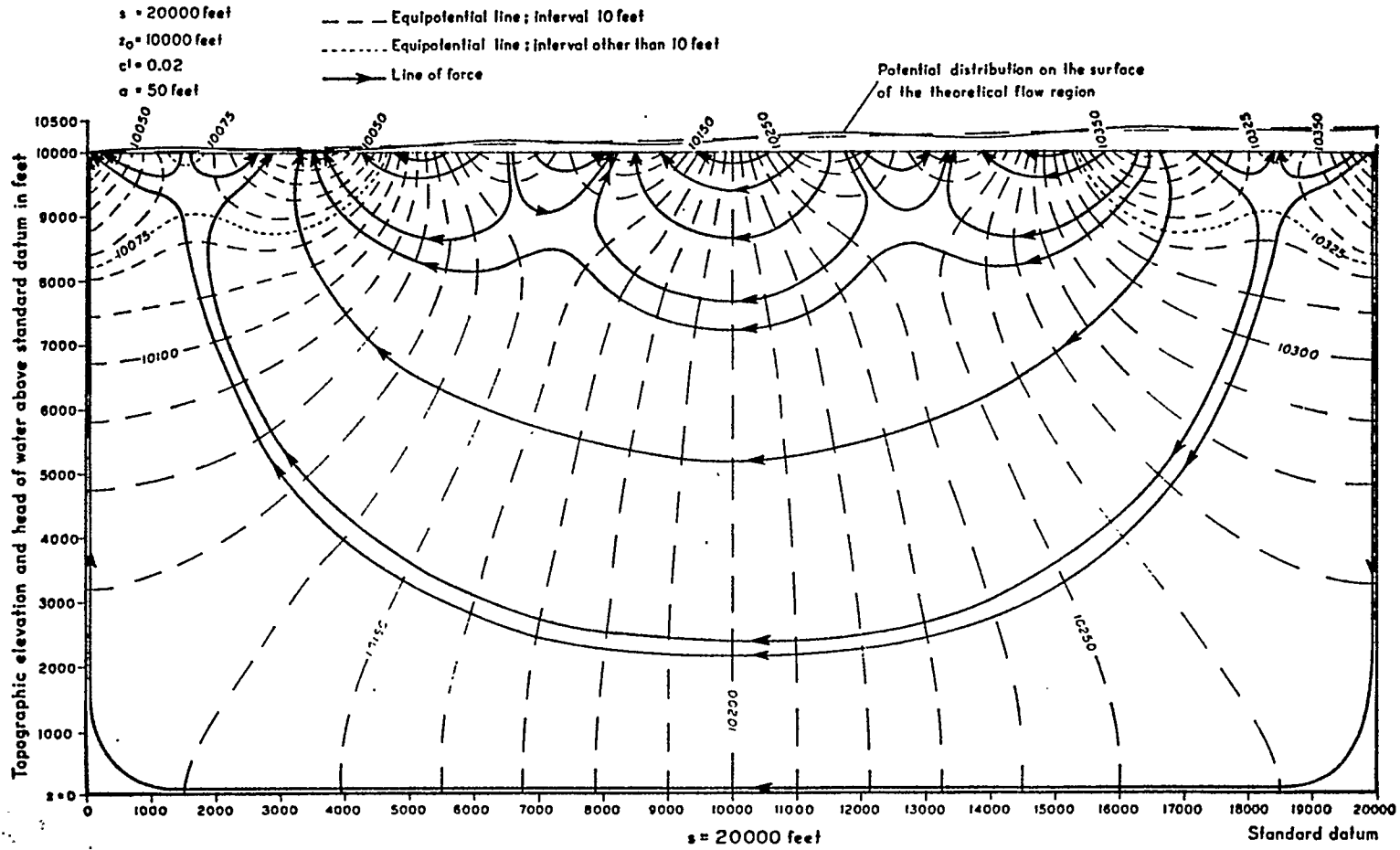
Program CAPFEA is a priority program, written for the Inland Waters Branch of Environment Canada, and lent to the author for the exclusive use in this thesis. Arrangements to examine or utilize CAPFEA must be made with the offices of Environment Canada.

The CAPFEA program provides a finite element solution to the continuity equation which describes groundwater flow through an anisotropic heterogeneous medium. The procedure involves a general discretization of the continuously varying hydraulic head. This discretization involves subdividing the flow area into discrete domains (triangular elements), and, by matrix manipulation, solving for the head distribution at the vertices (nodes) of each triangular element.

In order to assess the accuracy and reliability of the CAPFEA program a comparison was made between an exact mathematical solution to a flow problem and the CAPFEA finite element approximation to the same problem. Toth (1963) derived an exact mathematical solution to a groundwater flow system in a theoretical small drainage basin. The solution to the continuity equation of this flow system, given the particular boundary conditions, involved an infinite trigonometric series. The results of his solution are presented in Figure A1, reproduced from Toth (1963).

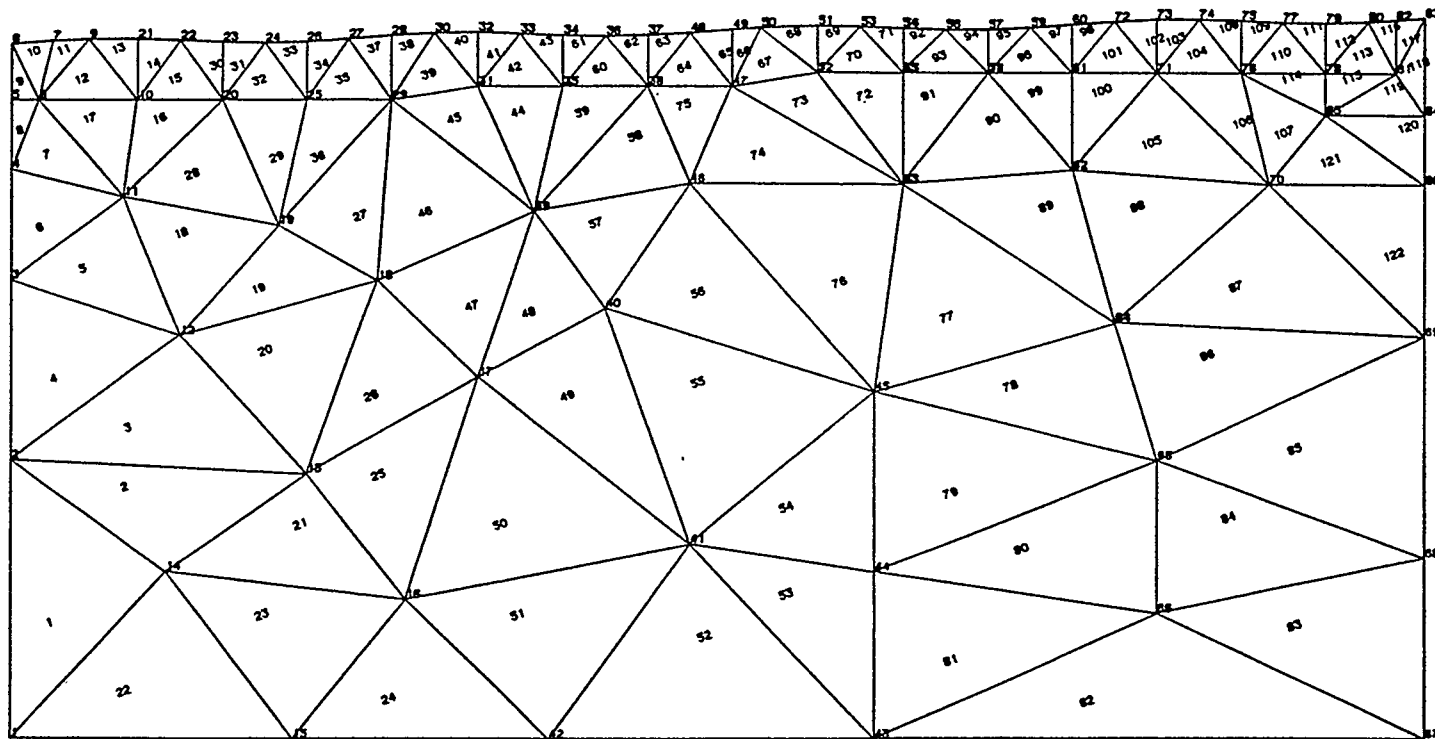
The boundary conditions and dimensions Figure A1 were exactly duplicated for the finite element simulation. The finite element mesh (Figure A2) used in this simulation is representative of the type of grid pattern used in this thesis. The density of nodes is similar to the density of nodes used in the various models throughout the thesis. The increase in the number of nodes near the top of the section is necessary in order to describe the upper boundary properly, and to give sufficient nodal points where the equipotential gradients are most variable.

Results of the finite element simulation are presented in Figure A3. The solution to the continuity equation by the finite element method corresponds almost exactly with the exact mathematical solution of Toth's (1963). This suggests that, given a reasonable number of nodes in a



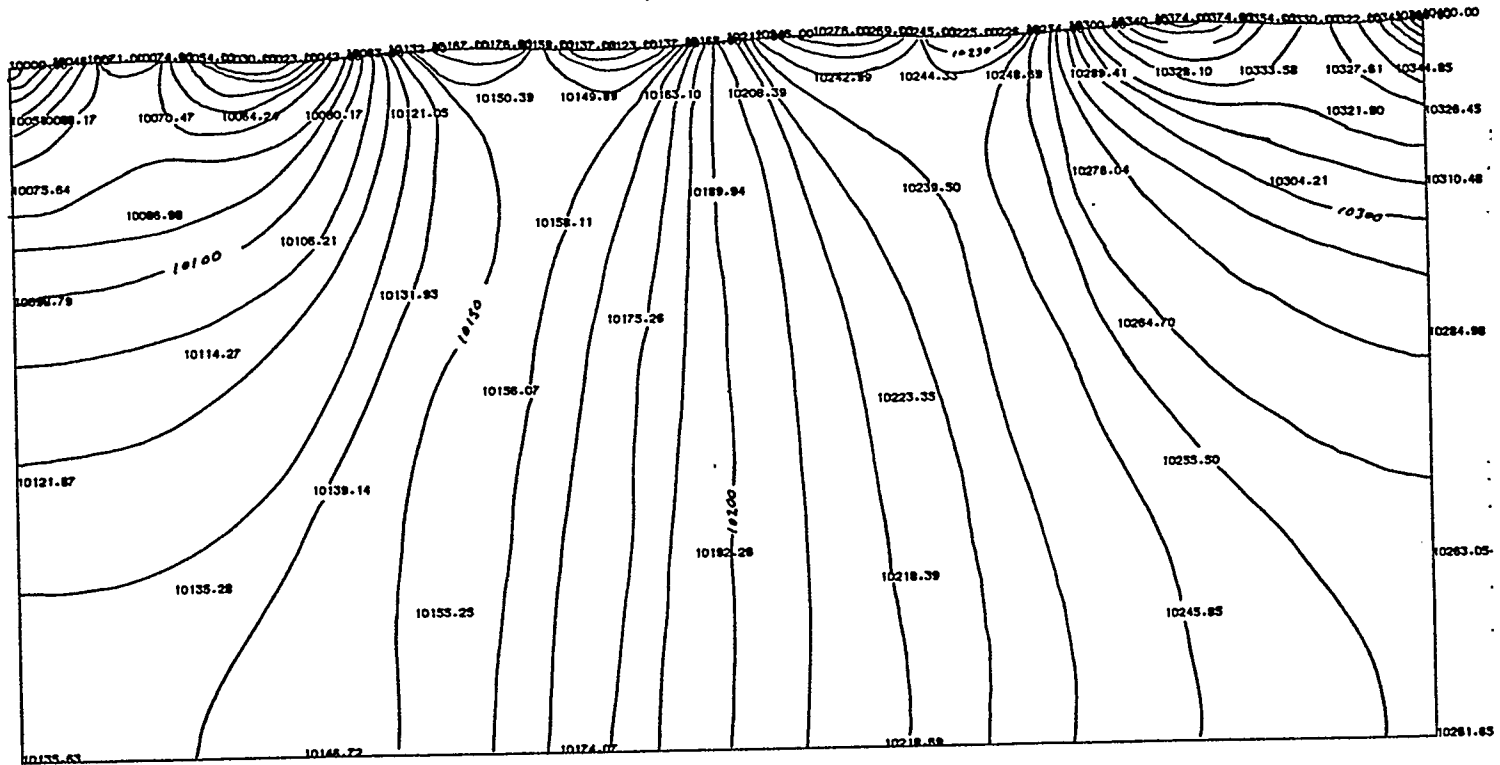
A1 Groundwater flow in a small drainage basin (from Toth 1963)

86 node mesh - Toth Model



A2 86 node mesh for finite element simulation

86 node mesh - loth model



A3 Basin flow based on 86 node simulation

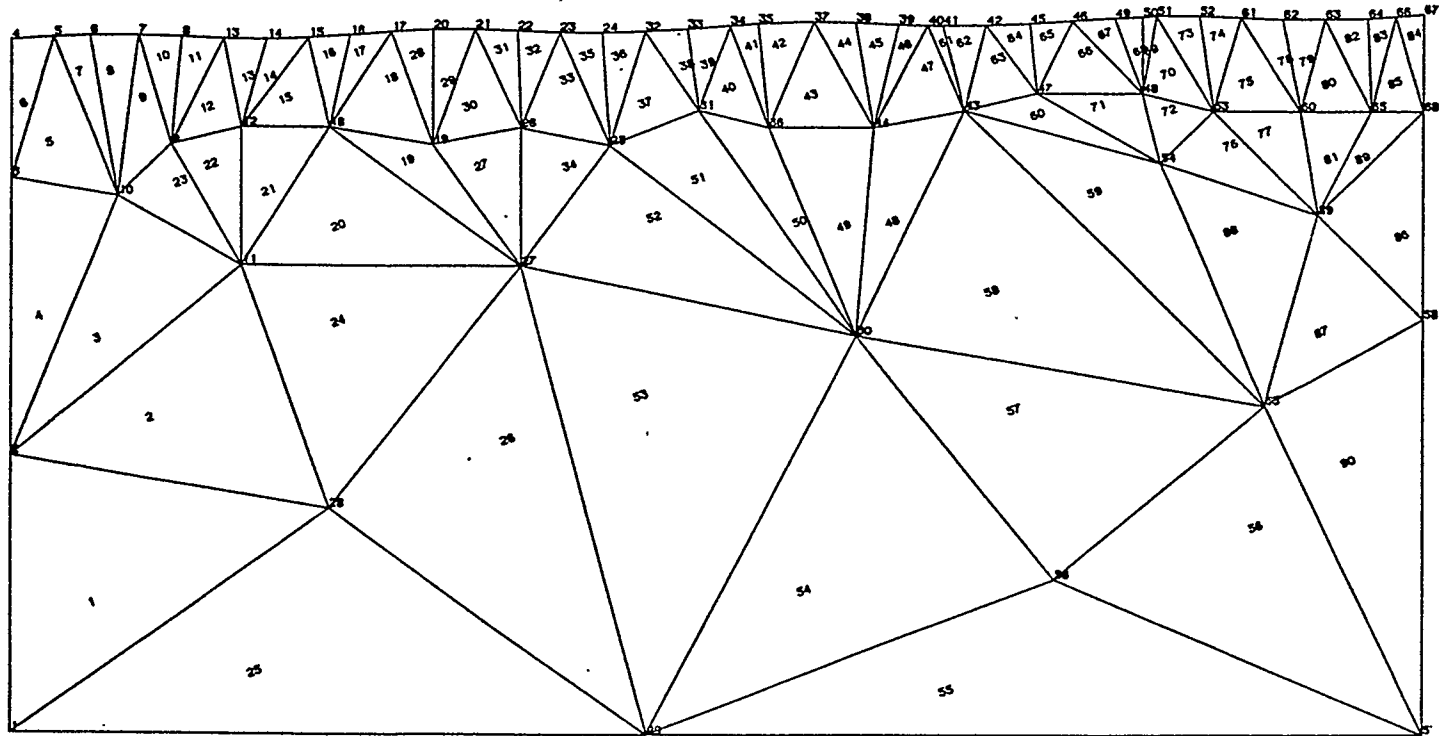
model, the finite element method will provide an adequate solution to the continuity equation for a groundwater flow system.

In order to ascertain how the form of the model (i.e. mesh pattern) affects the solution to the flow system, a sensitivity analysis of the finite element method was undertaken. This analysis involves construction of another mesh with the same boundary conditions as previously presented. A comparison of the results of these two models with identical dimensions, boundary and internal conditions, but of different mesh patterns, allows for an analysis of the sensitivity of the solution to the modelling process.

Figure A4 shows the finite element mesh for this final model. Considerably less nodes were used in this model than in the previous one (68 nodes versus 86 nodes). The result of the simulation, Figure A5, shows that the coarser grid spacing leads to small errors in the hydraulic head values at the base of the section (maximum of 5 m of hydraulic head difference, or 1/2 contour interval spacing). As well, accurate determination of the exact position of the near surface contours is impossible, as the coarse node spacing did not provide sufficient control for accurate contouring.

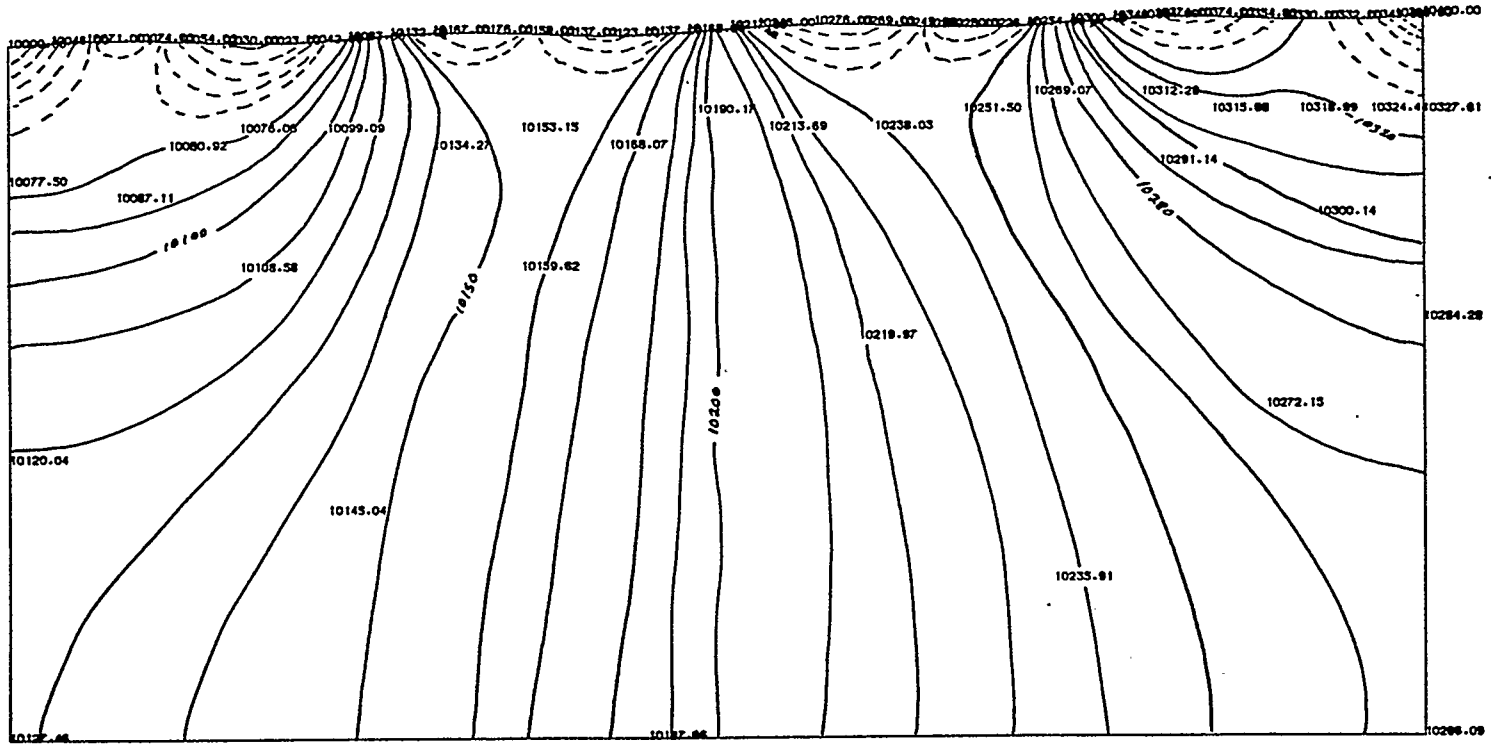
Since the grid spacing in the finite element method can be easily varied, models should have sufficient node

Toth model - 68 node mesh



A4 68 node mesh for finite element simulation

Toth model 68 node mesh



A5 Basin flow based on 68 node simulation

points in areas that show rapidly changing hydraulic head. Too coarse a grid spacing (i.e. individual elements too large) can also lead to errors in the approximation to the head values.

In summary, given sufficient detail in the mesh pattern of a model, the finite element method provides an acceptable solution to the continuity equation. With this method the theoretical flow distribution through the subsurface can be simulated.